Identifying the role of TALK-1 channels in islet hormone secretion, mitochondrial function, and the ER stress response.

By

Sarah Milian Graff

Dissertation

Submitted to the Faculty of the

Graduate School of Vanderbilt University

in partial fulfillment of the requirements

for the degree of

DOCTOR OF PHILOSOPHY

in

Molecular Physiology and Biophysics

June 30th, 2021

Nashville, TN

Approved:

David Jacobson, PhD

Richard O'Brien, PhD

Marcela Brissova, PhD

Wenbiao Chen, PhD

Eric Delpire, PhD.

Acknowledgements

First and foremost, I would like to thank both past and present members of the Jacobson Lab, including Prasanna Dadi, Dr. Nicholas Vierra, Dr. Matthew Dickerson, Arya Nakhe, Kelli Jordan, Dr. Molly Altman, Dr. Karolina Zaborska, and Dr. Charles Schaub. Over the years they have provided me with un-failing support, help, and friendship. Prasanna Dadi in particular taught me the ways of the lab, showed me how to be a better scientist, was patient with me when I was learning, and was always there to lend a helping hand. For that I will be forever grateful. As my mentor, Dr. David Jacobson taught me to never give up, to ask interesting questions, and to think critically. Most importantly he pushed me to always be my best and provided me with multiple opportunities to succeed. I am grateful for everything David has taught me.

Secondly, I would like to thank the members of my committee: Dr. Richard O'Brien (chair), Dr. Marcela Brissova, Dr. Wenbiao Chen, and Dr. Eric Delpire. They gave me invaluable guidance that helped make this dissertation work possible. I would especially like to thank Dr. Richard O'Brien. He provided me with a great deal of support and went above and beyond his duty as the chair of my committee.

I would also like to thank the faculty, staff, and students of the Molecular Physiology and Biophysics Department. This department made my graduate school years very memorable. I would especially like to thank Karen Gieg and Kandi Granberry for helping me stay organized and for answering every administrative question I came up with.

The work presented here would not be possible without the Vanderbilt Core Facilities. Therefore, I would like to thank Dr. Mark Magnuson and Jennifer Skelton in the Vanderbilt

Genome Editing Resource, Dr. Jenny Schafer and Dr. Robert Matthews in the Cell Imaging Shared Resource, Dr. Paige Vinson and Debbi Mi of the High Throughput Screening core, Dr. Dale Edgerton and Susan Hajizadeh in the Hormone Core, as well as Dr. David Wasserman and Dr. Louise Lantier in the Mouse Metabolic Phenotyping Core.

I would also like to acknowledge the funding sources that enabled both my work and my studies: The Molecular Endocrinology Training Program, The Ruth L. Kirschstein NRSA Individual Predoctoral Fellowship (F31DK118855), and support provided to Dr. David Jacobson through the grants (R01 DK-081666, R01 DK115620) from the National Institutes of Health, the American Diabetes Association (Grant 1-17-IBS-024), and a Vanderbilt University Diabetes Research Training Center Pilot and Feasibility Grant (P60-DK-20593).

Importantly, I would also like to thank my family and friends. To my parents, Karen Milian and Ricardo Milian, thank you for your unwavering love and support over the past 28 years. You have believed in me, supported my goals, and been there to comfort me when I was my own worst critic. To my siblings, Kyle Milian and Lauren Fosselman, thank you for being a source of laughter and support. I will always be grateful that I am able to call you both my best friends as well as my siblings. To all of my grandparents, thank you for always having a kind word for me, constantly keeping me in your prayers, and reminding me that you are my biggest fans. Your love and support are cherished. To my friend Melissa Weil, thank you for being the best listener and friend I could ask for. Your friendship has helped me become the person I am today. To my parents-in-law, Jeremy and Teresa Graff, thank you for your guidance, your advice, and your love.

Lastly, I would like to thank my husband, Nate Graff. You celebrated every one of my victories (no matter how small), you picked me up when I felt like I had fallen, and you always believed in me. Your loving support helped get me through graduate school and I know it will help me through any other endeavor I undertake.

Table of Contents

List of Figures

List of Tables

List of Abbreviations

ADP	Adenosine Diphosphate
ATP	Adenosine Triphosphate
$[Ca^{2+}]_c$	Cytosolic Calcium
$[Ca^{2+}]_{ER}$	Endoplasmic Reticulum Calcium
$[Ca^{2+}]_{mito}$	Mitochondrial Calcium
VDCC	Voltage-Dependent Calcium Channels
cAMP	Cyclic adenosine monophosphate
CICR	Calcium-induced calcium release
GSIS	Glucose-stimulated insulin secretion
ER	Endoplasmic Reticulum
GIRK	G protein-coupled inwardly-rectifying potassium channel
GTT	Glucose Tolerance Test
ITT	Insulin Tolerance Test
KCNK16	Potassium channel subfamily K member 16
K2P	Two Pore Domain Potassium Channel
K_{ATP}	ATP-sensitive potassium channel
β-TALK1-KO	β-cell specific TALK-1 knock-out mouse model
δ-TALK1-KO	δ-cell specific TALK-1 knock-out mouse model
T2DM	Type-2 Diabetes Mellitus
MODY	Mature-Onset Diabetes of the Young
WT	Wild-Type
V_m	Membrane Potential
GLP-1	Glucagon-like peptide-1
K_v	Voltage gated potassium channels
SERCA	The sarcoendoplasmic reticulum calcium transport ATPase
MCU	Mitochondrial calcium uniporter
NCLX	Sodium/Lithium/Calcium exchanger
PMCA	Plasma membrane Ca^{2+} ATPase
MAM	Mitochondrial-associated membrane
K_{Ca}	Calcium gated potassium channel
CPA	Cyclopiazonic Acid
TEA	Tetraethylammonium
PKA	Protein Kinase A
PKC	Protein Kinase C
ROS	Reactive Oxygen Species
UPR	Unfolded-Protein Response

Chapter I
Introduction

Preface

Glucose Homeostasis

Glucose is the primary energy source for nearly all living organisms. In humans, glucose metabolism utilizes glycolysis, production of pyruvate that enters the citric acid cycle, and oxidative phosphorylation to produce ATP. Precise regulation of glucose levels in the blood (between 4.0-6.0 mM[1]) is critical to maintaining normal cellular ATP production and thus function. For example, glucose is the primary energy source of the brain; therefore, if blood glucose drops below 4.0 mM then neuronal function in the central nervous system becomes impaired. Alternatively, hyperglycemia (above 6.0 mM) results in glucose toxicity which causes cellular dysfunction through changes such as advanced protein glycation[2; 3], activation of protein kinase C-dependent (PKC) pathways resulting in gene expression changes[4; 5], and the initiation of oxidative stress[6; 7]. Dr. Michael Brownlee proposed a model in which increased glycation end products and PKC activation is due to hyperglycemia-induced increases in reactive oxygen species (ROS)[8]. In this model, ROS activates poly(ADP-ribose) polymerase, thereby reducing GAPDH, and activating both protein glycation and PKC. Therefore, proper maintenance of blood glucose homeostasis is critical for cellular energy utilization and function.

The Pancreas

The pancreas is an organ that functions in both the digestive and endocrine systems. As a part of the digestive system, the pancreas uses acinar cells to secrete digestive enzymes into the duodenum through the pancreatic duct. The endocrine component of the pancreas is made up of pancreatic islets (Islets of Langerhan[9]) which are dispersed throughout the pancreas and make up 1-2% of the pancreatic mass. Islets are clusters of β-cells, α-cells, and δ-cells which regulate blood glucose levels through the secretion of the hormones insulin, glucagon, and somatostatin, respectively.

Insulin is released when blood glucose levels rise above 6 mM, both suppressing hepatic glucose production (HGP) and initiating glucose uptake by peripheral muscular tissues. Insulin directly reduces HGP by binding to the hepatic insulin receptor thereby signaling a reduction in glycogenolysis[10-12]. Insulin mediates muscle tissue glucose uptake by binding to insulin receptors and initiating a phosphorylation cascade that activates insulin responsive substrates (IRS)[13]. Phosphorylated IRS1 then activates PI3K which promotes the translocation of the glucose transporter GLUT4 to the plasma membrane thereby initiating glucose uptake[13; 14]. Insulin also functions as a paracrine regulator of glucagon release **(Figure 1.1)**. Specifically, insulin receptor signaling modulates the glucose signal that is required for glucagon secretion to be suppressed by high glucose levels[15].

In contrast to insulin, glucagon is released when blood glucose levels are low (typically below 4 mM); stimulating hepatic glucose production and output, specifically glycogenolysis, thereby raising blood glucose levels[11]. Glucagon binds to G-protein coupled glucagon receptors (G_s-coupled glucagon receptor) on the plasma membrane of liver cells. This initiates a phosphorylation cascade that activates glycogen phosphorylase

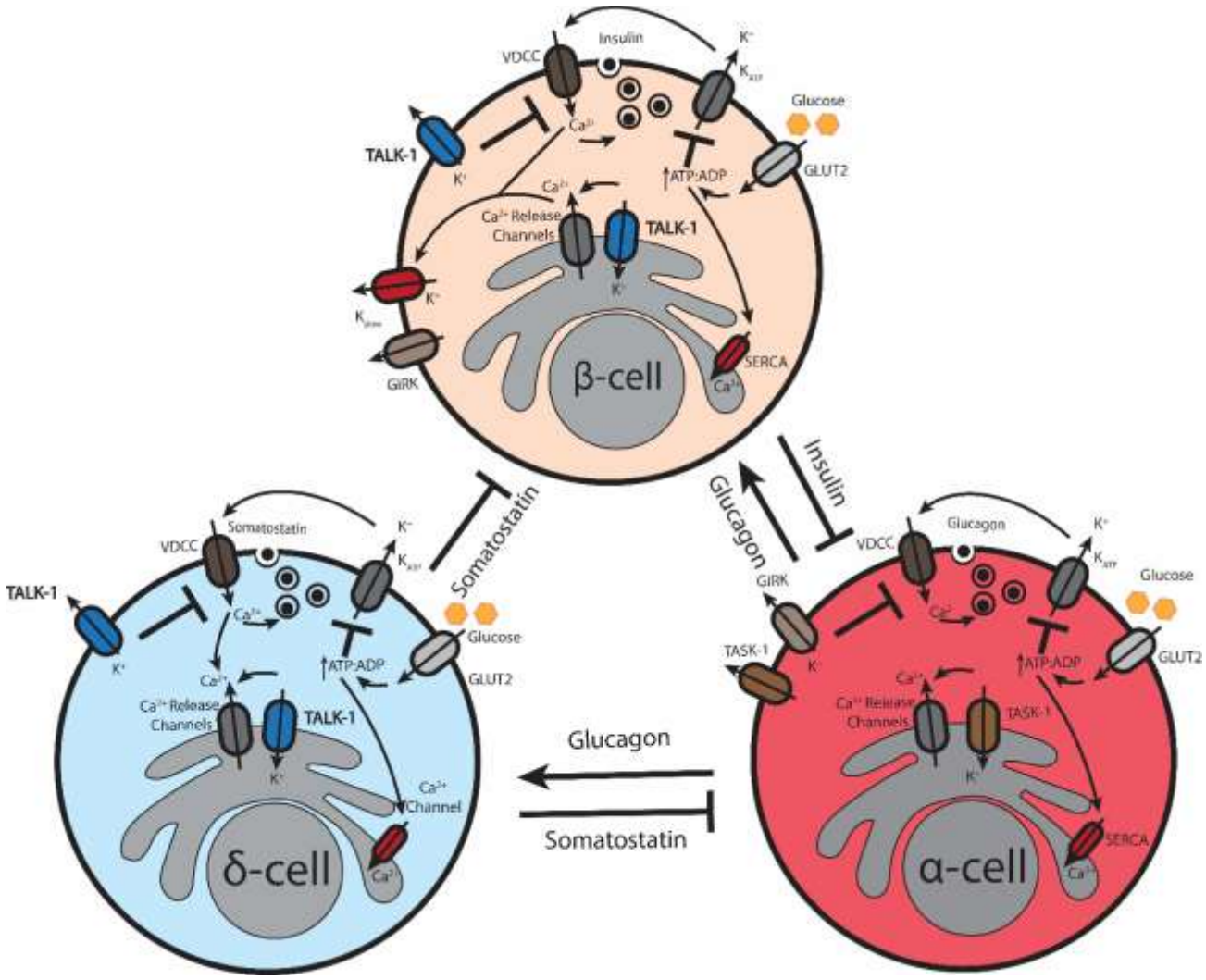

Figure 1.1: Islet paracrine regulation.

Insulin secretion from β-cells inhibits glucagon secretion from α-cells while glucagon secretion increases both somatostatin and insulin secretion. Somatostatin secretion from δ-cells inhibits both glucagon and insulin secretion.

to catalyze the breakdown of stored glycogen into glucose[11; 16; 17]. Furthermore, studies have shown that glucagon acts as a paracrine regulator to stimulate insulin secretion by activating glucagon and GLP-1 receptors on β-cells[18; 19] **(Figure 1.1)**. Recent studies have also shown that glucagon can increase somatostatin secretion in a dose dependent manner **(Figure 1.1)**[20].

Somatostatin functions as a local paracrine regulator of β-cell and α-cell function **(Figure 1.1)**[21]. Somatostatin functions locally at the islet, as opposed to systemically, as it is quickly degraded by systemic peptidase enzymes. Somatostatin binds to somatostatin receptors on the membranes of β-cells and α-cells, initiating $G_{\alpha i}$ cascades that inhibit insulin and glucagon release. Somatostatin receptor signaling in β-cells inhibits insulin secretion by hyperpolarizing the β-cell membrane through the activation of G-protein-coupled inward rectifying K^+ channels (GIRK) and inhibition of Ca^{2+} entry through L-type Ca^{2+} channels (detailed below)[22; 23]. Through capacitance measurements done by Kailey et al., somatostatin has also been shown to directly inhibit exocytosis of insulin granules downstream of Ca^{2+} influx[23].

In α-cells, somatostatin receptor signaling inhibits glucagon release by reducing cAMP levels[24], activating hyperpolarizing GIRK channels[25], inhibiting Ca^{2+} entry, and suppressing exocytosis of secretory granules[26]. The ability of δ-cells to function as paracrine regulators lies, in part, in their unique morphology. These δ-cells contain neuron-like processes that extend up to 20 μm allowing the δ-cell to make contact with, and therefore regulate, β- and α-cells throughout the islet[27]. Together this indicates that local paracrine signaling between the different islet cell-types is critical for normal function.

As paracrine regulation is local, the architectural makeup of an islet would be predicted to affect paracrine regulation of cells within an islet. There are significant differences in the architecture of mouse and human islets. Mouse islets are made up of approximately 75% β-cells, 19% α-cells and 6% δ-cells while adult human islets are made up of approximately 54% β-cells, 34% α-cells, and 10% δ-cells[28]. Additionally, mouse islets contain a core that is made up of β-cells surrounded by α- and δ-cells while human islets contain these three cell types evenly dispersed throughout the islet[28] **(Figure 1.3)**. Interestingly, the architecture of juvenile human islets tend to closely resemble that of mouse islets. This suggests that the islet architecture seen in adult human pancreata evolves during human development[29]. Islet architecture has been shown to be critical for the islets proper function. Stress, such as over nutrition, has been shown to alter islet architecture[30] and dispersion of mouse and human islets results in a loss of physiological function[28].

In addition to the three main hormone secreting cells described above, islets also contain other cell-types such as PP-cells, ε-cells, neurons, vasculature, and macrophages. PP-cells secrete pancreatic polypeptide while ε-cells secrete ghrelin. Pancreatic islets are innervated by both the parasympathetic and sympathetic nervous system. While human islets have much less innervation compared to mouse islets, the autonomic effects seem to be similar between the two[31; 32]. Parasympathetic innervation of the islets potentiates glucose-stimulated insulin secretion (GSIS) through the through the release of acetylcholine which binds to β-cell muscarinic receptors[33]. The sympathetic nervous system affects both α- and *β*-cell function.

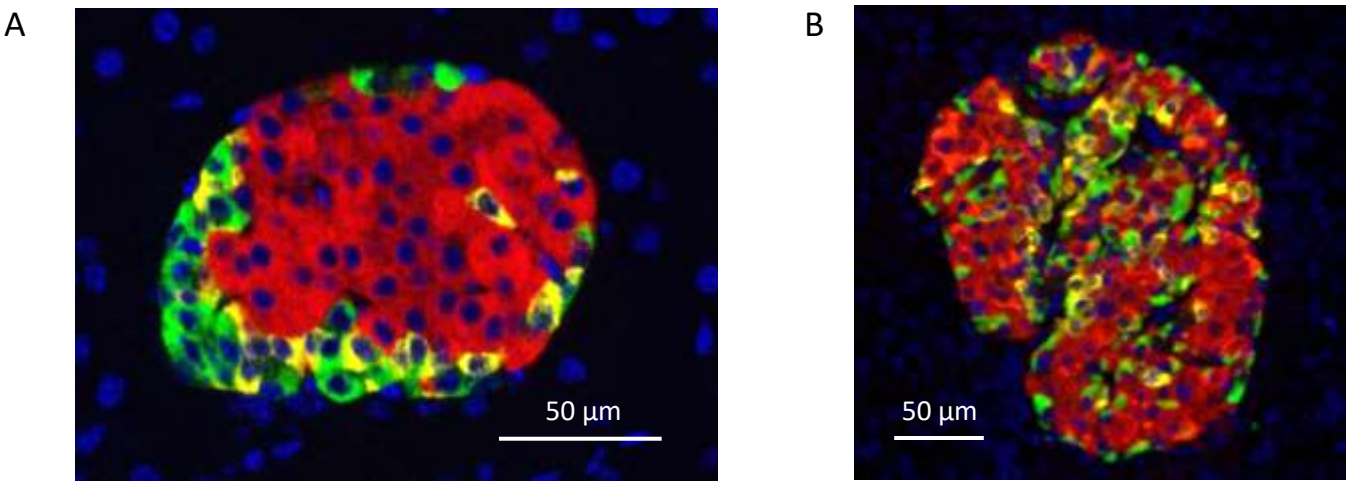

Figure 1.3: Mouse islet architecture.

Immunofluorescence from a mouse pancreata (A) and human pancreata (B) stained with insulin (red), somatostatin (yellow), glucagon (green), and nuclei (blue).

Noradrenaline stimulates glucagon secretion by binding to α-cell β2-adrenergic receptor, whereas it inhibits insulin secretion by binding to the β-cell α2-adrenergic receptors[34]. The islets are also highly vascularized (receiving approximately 10-fold the blood supply of the exocrine tissue by volume)[35; 36]. This allows the islets to quickly sense and respond to changes in blood glucose levels. Macrophages within the islet contribute to proper islet function and are key contributors to β-cell proliferation and death[37]. While all of these cell types are critical for proper islet function, in this thesis we will focus on the pancreatic β-cell.

The roles of Ca^{2+} in regulating β-cell insulin secretion

Ca^{2+} influx

GSIS is dependent on β-cell membrane potential (V_m) depolarization. β-cells are electrically excitable and express multiple ion channels that regulate V_m. Resting β-cell V_m is primarily regulated by current through the ATP-sensitive K^+ channel (K_{ATP})[38]. K_{ATP} is active under low glucose conditions where it shifts the β-cell V_m towards the equilibrium potential of K^+. Glucose is transported into the β-cell where it is metabolized to increase the intracellular ATP levels. This along with decreased ADP levels increases the ATP:ADP ratio. Increased ATP:ADP ratio under high glucose conditions inhibits K_{ATP} channels thereby allowing a background depolarizing current to depolarize the β-cell V_m to an excitatory potential known as the plateau potential. When this depolarization reaches the threshold for the activation of voltage-dependent Ca^{2+} channels (VDCCs), Ca^{2+} influx occurs and the β-cell fires action potentials from a depolarized plateau V_m.

In mouse β-cells, the opening of VDCC's and subsequent Ca^{2+} influx stimulates each action potential depolarization phase. Two types of VDCC channels have been identified in these β-cells, low-threshold voltage activated current and high-threshold voltage activated current. These currents are carried by T-type and L-type Ca^{2+} channels, respectively. While T-type Ca^{2+} channels are important for initial depolarization, the L-type channels have been shown to be the major voltage-dependent depolarizing current in both mouse and human β-cells[39; 40].

Glucose-stimulated Ca^{2+} influx results in GSIS. Ca^{2+} controls GSIS by binding to the primary Ca^{2+} sensor for exocytosis, synaptotagmin, which is expressed on the insulin granule membrane. Binding of Ca^{2+} to synaptotagmin initiates an interaction of the granule with the SNARE proteins, such as, syntaxin and SNAP25 on the plasma membrane near the L-type Ca^{2+} channels[41-43] A mechanical force is then produced to pull the granule and plasma membranes together until exocytosis occurs[44]. It has also been shown that Ca^{2+} activated protein kinase C stimulates insulin release. This is likely caused by reorganizing the actin network and phosphorylating the SNARE proteins, munc18 and SNAP25[45]. Thus, tight regulation of Ca^{2+} homeostasis has been shown to play a critical role in insulin exocytosis.

Insulin secretion from the β-cell is not continuous, instead it is pulsatile. This is due to the β-cell displaying waves of depolarization separated by silent phases, thereby resulting in $[Ca^{2+}]_c$ oscillations and pulsatile insulin secretion. These insulin pulses are critical for glycemic control. Under diabetic conditions (described in more detail below) Ca^{2+} oscillations are lost thereby terminating insulin pulsatility and resulting in hyperglycemia. Interestingly, at super-physiological glucose levels, β-cells display sustained $[Ca^{2+}]_c$

increases instead of displaying $[Ca^{2+}]_c$ oscillations, indicating that insulin pulsatility is affected by glucose levels and diabetic conditions[46]. Indeed, low grade inflammation seen under diabetic conditions initiates increased $[Ca^{2+}]_c$ oscillations thereby enhancing insulin secretion as an acute protective effect[47].

Intracellular Ca^{2+} stores

Endoplasmic reticulum (ER) Ca^{2+} ($[Ca^{2+}]_{ER}$)

In pancreatic β-cells, the ability of the ER to store Ca^{2+} is a key contributor to both basal cytosolic Ca^{2+} as well as glucose-stimulated Ca^{2+} oscillations. High $[Ca^{2+}]_{ER}$ is maintained by sarco-endoplasmic Ca^{2+} ATPases (SERCA) pumps, which pump Ca^{2+} against its concentration gradient and into the ER. However, the ER has ion channels which allow Ca^{2+} efflux, such as $InsP_3$ receptors, ryanodine receptors, and currently unknown Ca^{2+} leak channels[48; 49]. Therefore, when SERCA pumps are inhibited, $[Ca^{2+}]_{ER}$ stores are quickly released into the cytosol through ER Ca^{2+} leak channels **(Figure 1.4)**. When the β-cell depolarizes, the ER buffers $[Ca^{2+}]_c$ influx by taking up Ca^{2+} through SERCA pumps. The ER then releases it again through $InsP_3$ receptors and ryanodine receptors (ryanodine receptors are expressed at extremely low levels in the β-cells) in a mechanism known as Ca^{2+}-induced Ca^{2+} release (CICR). Some of the Ca^{2+} that contributes to CICR enters the cell through store-operated Ca^{2+} channels where it is then taken up by the ER[50]. ER Ca^{2+} release during the oscillation activates a V_m repolarizing current, K_{slow} (discussed in more detail below)[46] which terminates $[Ca^{2+}]_c$ oscillations. Increased $[Ca^{2+}]_{ER}$ leak during repolarization also provides a tail to the Ca^{2+} oscillation between silent phases. Therefore, eliminating $[Ca^{2+}]_{ER}$ handling by inhibiting or limiting the SERCA

pump[51] results in a loss of K_{slow} current as well as increases both the frequency and amplitude of β-cell $[Ca^{2+}]_c$ oscillations[52]. In some cases this leads to increases in second-phase insulin secretion[51], but prolonged loss of SERCA can lead to ER stress and therefore reduced insulin secretion[53]

Additionally, $[Ca^{2+}]_{ER}$ is a critical regulator of β-cell health. During stressful conditions, such as diabetes, β-cell $[Ca^{2+}]_{ER}$ drops as a result of increased $[Ca^{2+}]_{ER}$ leak through IP_3 receptors[49]. In addition, SERCA expression is also reduced under diabetic conditions, further reducing $[Ca^{2+}]_{ER}$[53]. As the ER is responsible for protein folding and quality control, if $[Ca^{2+}]_{ER}$ drops too low, Ca^{2+}-dependent protein folding chaperones will fail, resulting in misfolded proteins, and ER stress[49; 54]. In response to this stress, the β-cell will prompt the activation of the unfolded-protein response; however, if the stress is not remedied, the β-cell will initiate apoptosis. This is a main contributor to β-cell failure in diabetes which will be discussed in detail below. As the ER and mitochondria are closely linked, stress-induced drops in $[Ca^{2+}]_{ER}$ results in large increases in mitochondrial Ca^{2+} uptake and apoptotic signaling.

A

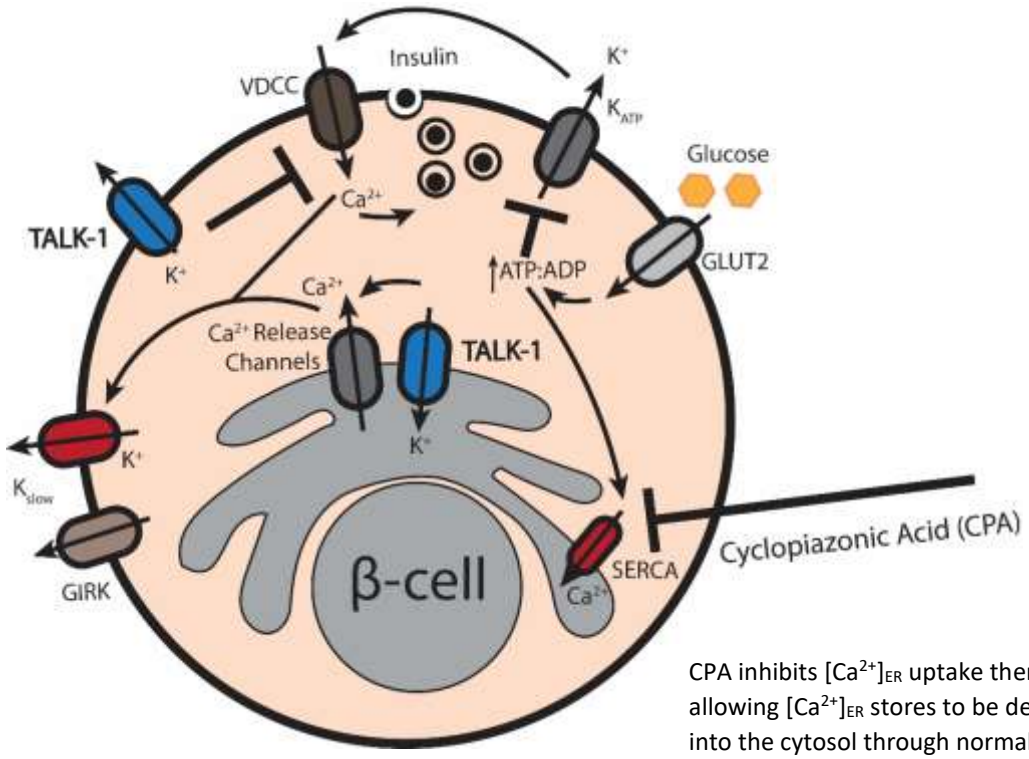

CPA inhibits $[Ca^{2+}]_{ER}$ uptake thereby allowing $[Ca^{2+}]_{ER}$ stores to be depleted into the cytosol through normal $[Ca^{2+}]_{ER}$ release.

B

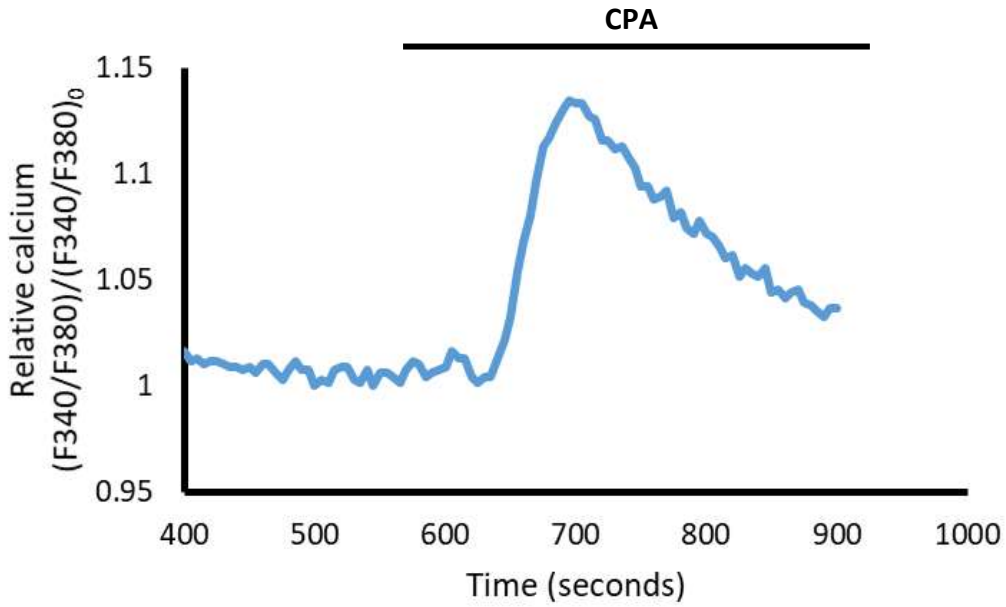

Figure 1.4: CPA induced $[Ca^{2+}]_{ER}$ release.

CPA induces $[Ca^{2+}]_{ER}$ release by inhibiting $[Ca^{2+}]_{ER}$ uptake through SERCA channels (A). Fura2am $[Ca^{2+}]_c$ measurements of a representative control mouse islet upon CPA-induced SERCA inhibition (B).

Mitochondrial Ca^{2+} ($[Ca^{2+}]_{mito}$)

In addition to the ER, mitochondria also function in β-cell Ca^{2+} storage. Mitochondria are double-membrane-bound organelles which supply the cell with energy while also modulating cellular Ca^{2+} signaling and apoptosis[55]. The double membrane organization of mitochondria results in each mitochondrion containing five parts: the outer mitochondrial membrane, the intermembrane space, the inner mitochondrial membrane, the cristae space, and the matrix. The inner membrane maintains a membrane potential due to the electron transport chain shuffling H^+ ions back and forth across the inner mitochondrial membrane to produce ATP through the ATP synthase in the matrix. Ca^{2+} regulates respiration by activating mitochondrial dehydrogenases, thereby increasing respiration, and by modulating the mitochondrial membrane potential. In addition to Ca^{2+} being a critical regulator of ATP production through respiration, Ca^{2+} also regulates cellular ATP hydrolysis by modulating the activity of SERCA and PMCA pumps.

Under basal conditions, $[Ca^{2+}]_{mito}$ is similar to $[Ca^{2+}]_c$, but upon depolarization $[Ca^{2+}]_{mito}$ increases up to 70 μM[56]. This $[Ca^{2+}]_{mito}$ influx occurs through the mitochondrial Ca^{2+} uniporter (MCU) and is critical for dehydrogenase activation and subsequent mitochondrial respiration. Indeed, β-cell mitochondrial ATP levels have been shown to be dependent on $[Ca^{2+}]_c$ levels and to oscillate out-of-phase with electrical oscillations[57; 58]. $[Ca^{2+}]_{mito}$ uptake through the MCU is balanced by the mitochondrial Na^+/ Ca^{2+} exchanger (NCLX) which becomes activated after cell depolarization resulting in mitochondrial Na^+ uptake and $[Ca^{2+}]_{mito}$ release. Mitigating $[Ca^{2+}]_{mito}$ uptake is critical as too much $[Ca^{2+}]_{mito}$ results in apoptosis.

While $[Ca^{2+}]_c$ is a major source of $[Ca^{2+}]_{mito}$ uptake, $[Ca^{2+}]_{ER}$ has also been shown to contribute to $[Ca^{2+}]_{mito}$ uptake through Ca^{2+} "hotspots" located at the mitochondrial associated membrane (MAM)[59]. The MCU has a fairly low affinity for Ca^{2+}, so it is predicted that the high Ca^{2+} concentration found at the MAM is critical for MCU function. Furthermore, as $[Ca^{2+}]_{mito}$ has been shown to reach 70 μM[56], the low $[Ca^{2+}]_c$ would not provide the concentration driving force needed for $[Ca^{2+}]_{mito}$ uptake. $[Ca^{2+}]_{ER}$ however is much higher and would be able to provide the needed driving force at the MAM for $[Ca^{2+}]_{mito}$ uptake. Taken together, this shows that, $[Ca^{2+}]_c$, $[Ca^{2+}]_{ER}$, and $[Ca^{2+}]_{mito}$ function together to regulate β-cell membrane potential and function.

K^+ channel regulation of β-cell membrane potential and Ca^{2+} handling

Ca^{2+} activated and voltage gated K^+ channels

Each glucose-induced β-cell action potential repolarization phase is regulated by VDCC inactivation, as well as Na^+ channel inactivation in human β-cells, and the opening of K^+ channels. These K^+ channels are characterized as either ligand gated K^+ (K_{Ca}) channels or voltage gated K^+ channels (K_v).

K_{Ca} channels consist of big conductance (BK), small (SK)[60] or intermediate conductance (IK), and a slowly activated K^+ conductance (K_{slow})[61; 62]. Blockade of β-cell BK channels results in increased action potential height[63; 64] while inhibition of SK channels results in increased action potential duration when the voltage-dependent K^+ channel, Kv2.1, is also inhibited or ablated[64]. This indicates that both BK and SK current are important contributors to β-cell action potential repolarization. The molecular identity of K_{slow} has yet

to be discovered; however, it is sensitive to the SK channel blocker, UCL1684, indicating that it might be part of the SK channel family[62]. Current through K_{slow} is responsible for the termination of the action potential slow wave and the start of the silent phase thereby contributing to insulin secretion pulsatility[61]. K_{slow} is unique in that it has been shown to be activated by $[Ca^{2+}]_{ER}$ release[65]. The current through K_{slow} inactivates during the action potential silent phase in a time course that is similar to the restarting of the action potential slow wave[61] indicating that termination of K_{slow} conductance may allow for the reactivation of action potential firing. Together, K_{Ca} channels function to polarize the β-cell V_m after depolarization-induced $[Ca^{2+}]_c$ influx and $[Ca^{2+}]_{ER}$ release.

K_v currents are classified by the biophysical and pharmacological properties: delayed-rectification, sensitivity to 4-AP or TEA, and V_m sensitivity. In mouse β-cells, the K_v channel that is most responsible for voltage-dependent V_m repolarization is Kv2.1. This was established in-part through adenovirus-mediated expression of a truncated Kv2.1 subunit that reduced delayed rectifier currents by 60-70% and enhanced β-cell insulin secretion by 60%[66]. Human β-cells express two types of voltage-gated K^+, K_v2.1 and K_v2.2. These studies indicate that K_v current regulates β-cell $[Ca^{2+}]_c$ influx and insulin secretion by repolarizing the β-cell V_m[66-68]

ER K^+ channels

In addition to being functional on the plasma membrane, K^+ channels also function on the ER membrane where they allow K^+ to move from the cytosol into the ER. Movement of K^+ into the ER is critical to maintain the ER membrane potential away from the equilibrium potential of Ca^{2+} so that $[Ca^{2+}]_{ER}$ efflux can be maintained across the ER membrane[69]. Knockout of the K^+ channels, TRIC-A or TRIC-B, results in increased $[Ca^{2+}]_{ER}$,

presumably due to the loss of a K^+ countercurrent which regulates the $[Ca^{2+}]_{ER}$ efflux described above[70; 71]. Studies have also shown that both SK channels and the potassium–proton exchanger leucine zipper-EF-hand-containing transmembrane protein 1 (LETM1) are present on the ER membrane[72]. Importantly, inhibiting SK channels affects the ability of the ER to take up Ca^{2+}[72].

Two-Pore Domain K^+ channels

In addition to K_{Ca} and K_v channels, two-pore domain K^+ (K2P) channels also regulate V_m repolarization. K2P channels are open at resting V_m and their current results in an outward leak of K^+ ions that drives a slight polarizing influence on the V_m. There are 15 genes in the mammalian K2P channel family and they are categorized into 6 subfamilies based on amino acid sequence and functional properties[73]. K2P current can be regulated by a variety of stimuli such as membrane stretch, pH, neurotransmitters, heat, phosphorylation, voltage, and in some cases Ca^{2+} [74-76]. These regulation differences allow K2P channels to play very diverse roles despite their similar structures.

All K2P channel structures consist of two-pore domains in each subunit and the subunits then dimerize to form a single functional pore, containing four pore domains, in the membrane **(Figure 1.5)** [73; 77; 78]. In the center of the pore is a K^+ selectivity filter (G-Y-G) which allows only dehydrated K^+ ions to pass. Each subunit also consists of four transmembrane domains which results in both the short NH_2 and long COOH-termini being positioned in the cytosol. After the first trans-membrane domain is a large extracellular “cap”. This cap is positioned above the K^+ selectivity filter and renders K2P

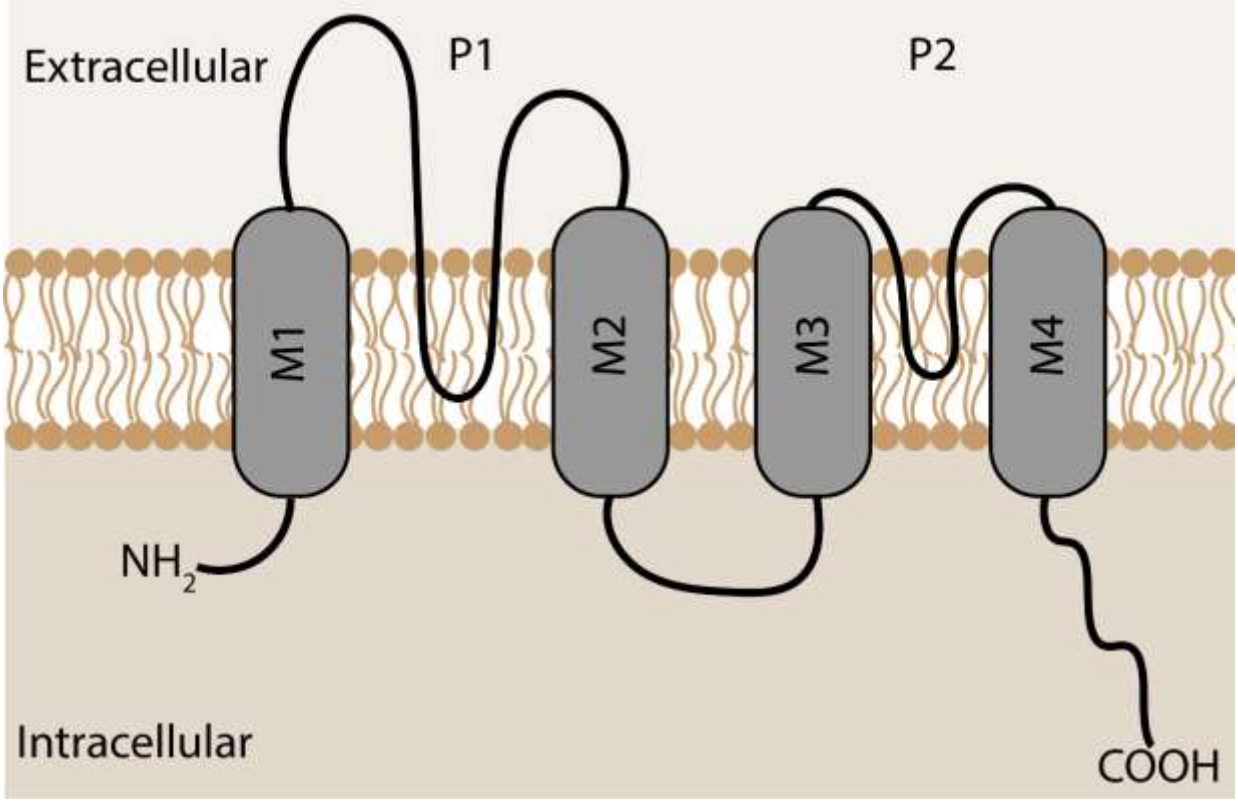

Figure 1.5: General structure of a K2P subunit.

K2P channels contain 2 pore domains and 4 transmembrane domains, resulting in intracellular N- and C-termini. The first pore domain (P1) contains a large extracellular "cap".

channels insensitive to toxins and molecules that successfully inhibit other K^+ channels. This characteristic is useful for experimentally recording K2P current, as other endogenous K^+ channels can be blocked with inhibitors such as TEA so that the remaining K^+ current is that of K2P channels[79]. The open and closed structures of K2P channels have yet to be clarified,[80] but it is clear that they are regulated by a "C-Type" gate[81; 82]. "C-Type" gates, which are also found in K_v channels[83], inhibit ion conductance by inducing a conformational change within the pore. Members of this functionally diverse K2P channel family are expressed in the brain, peripheral nervous system, muscles, heart, and pancreas. Here, we will focus on K2P channels expressed in the pancreas: this includes TWIK-1, TASK-1, and TALK-1.

TWIK-1

TWIK-1 was first identified by Dr. Florian Lesage in 1996 through a Gen Bank search for sequences related to the pore domains of previously cloned K^+ channels[84]. TWIK-1 contains 336 amino acids and has the typical K2P channel structure of 2 pore and 4 transmembrane domains[84]. It is expressed at significant levels kidney, heart, brain, lung, placenta, and both the endocrine and exocrine pancreas[84; 85].TWIK-1 K^+ currents expressed in *Xenopus laevis* oocytes were weakly inward rectifying and were activated by protein kinase C but inhibited by acidification[84]. TWIK-1 is a unique K2P channel in that at acidic pHs when TWIK-1 K^+ current is inhibited, it can conduct Na^+[86]. TWIK-1 K^+ current was found to be active at all membrane potentials and to exhibit time-independent gating, indicating that it was probably a background K^+ conductance channel[84]. It also exhibits low K^+ channel activity at the plasma membrane, most likely due to its

predominant localization to endosomes. Interestingly, the acidic pH of endosomes (~pH 6.0) changes the ionic preference of TWIK-1, causing it to conduct Na^+ instead of K^+. This results in a depolarizing Na^+ current at the plasma membrane. Indeed, TWIK-/- β-cells are hyperpolarized compared to WT cells and this is exaggerated when K_{ATP} channels are closed, indicating the TWIK-1 regulates β-cell V_m during glucose stimulation[86].

TASK-1

TASK-1 is a part of the TWIK K^+ channel family and was first identified a year after TWIK-1 by searching the GenBank database for sequences related to TWIK-1[87]. TASK-1 contains 395 amino acids and has the typical K2P channel structure of 2 pore domains and 4 transmembrane domains[87]. The electrophysiological properties of TASK-1 were determined after expression in *Xenopus laevis* oocytes and COS cells. At low extracellular K^+ concentrations, TASK-1 displays outward rectification of a K^+ selective, instantaneous, non-inactivating, and voltage-insensitive current[87]. TASK-1 is sensitive to extracellular pH, with 90% of the maximum current at pH 7.7 and only 10% at pH 6.7[87]. The lack of inactivation kinetics, as well as the lack of voltage sensitivity indicates that TASK-1 possesses all of the characteristics of a background “leak” channel. Indeed, it has been shown to function as a background leak channel in both pancreatic β-cells and α-cells[88; 89].

In both human and rodent β-cells, TASK-1 is highly expressed and localizes to the plasma membrane[88]. Both pharmacological inhibition (A1899) and genetic ablation of TASK-1 significantly depolarizes the glucose-stimulated β-cell V_m thereby resulting in greater

glucose-stimulated Ca^{2+} influx[88]. This increased Ca^{2+} influx resulted in increased glucose-stimulated insulin secretion as well as improved glucose tolerance[88]. Interestingly, insulin secretion in low glucose, and fasting blood glucose levels were not changed, indicating that TASK-1 can only affect β-cell function under glucose-stimulated conditions when K_{ATP} would be closed. Together, this indicates that TASK-1 limits glucose-stimulated insulin secretion by limiting β-cell electrical excitability and Ca^{2+} influx.

TASK-1 is also expressed on the plasma membrane of pancreatic α-cells[89]. Similarly, to TASK-1 in β-cells, A1899 inhibition of TASK-1 increases α-cell electrical excitability in high glucose resulting in increased glucose-stimulated Ca^{2+} influx and glucagon secretion[89]. Inhibition of TASK-1 also reduces glucose-inhibition of glucagon secretion. Studies shave also shown that TASK-1 is activated by ATP. This could contribute to the glucose-sensitivity of TASK-1 in alpha-cells. In contrast to inhibition with A1899, genetic ablation of α-cell TASK-1 reduced glucagon secretion thereby resulting in improved glucose tolerance[88]. This contrast could be explained by the fact that TASK-1 is also expressed on the ER membrane where it modulates ER Ca^{2+} handling[65; 90; 91]. Acute inhibition with A1899 would be expected to primarily affect plasmalemmal TASK-1 while genetic ablation would be expected to affect both plasmalemmal and ER TASK-1. This indicates that TASK-1 on the ER membrane may play a more important role in modulating glucagon secretion than plasmalemmal TASK-1.

TALK-1

The focus of this dissertation will be on the K2P channel, TALK-1. TALK-1 was identified in 2001 by the Lesage group when they searched for homologs of known K2P channels[92]. In this study, they identified three novel K2P channels, TALK-1, TALK-2, and THIK-2[92].

All three of these K2P channels showed expression in the pancreas; however, TALK-1 was the only one that seemed to be restricted to the pancreas. Studies on mRNA expression showed that *KCNK16*, the gene that encodes TALK-1, was highly expressed in pancreatic tissue, but low or undetectable in most other tissues[93-95], with the only exception being δ-cells in the gut which express TALK-1. While TALK-1 mRNA is found in pancreatic β-, δ-, and α-cells, TALK-1 protein is only expressed in pancreatic β-cells and δ-cells and is absent from α-cells and the surrounding exocrine tissue[79]. Not only is TALK-1 expressed in β-cells, TALK-1 is the most highly expressed K^+ channel transcript within β-cells[93; 96] . Additionally, a study in 2003 verified that all four TALK-1 splice-variants were expressed in the pancreas[97]. This expression pattern, along with the evidence that a non-synonymous polymorphism in *KCNK16* is associated with T2DM[98; 99] (discussed in more detail below), makes TALK-1 an interesting candidate for diabetic therapeutics.

As mentioned above, TALK-1 has four splice variants, TALK1a (the original variant identified by the Lesage group in 2001[77]) , TALK1b, TALK1c, and TALK1d[97]. TALK1a and TALK1b contain all 4 transmembrane domains that are typical to K2P channels and form functional channels in the membrane[97]. TALK1c and TALK1d; however, lack the fourth transmembrane domain and therefore do not have the ability to form functional channels in the membrane[97]. Once formed in the plasma membrane, TALK1a and TALK1b allow K^+ to move down it's concentration gradient and out of the cell, resulting in cell membrane polarization[79; 92]. Regulation of this TALK-1 K^+ flux thereby modulates β-cell membrane potential.

Recent studies indicate that TALK-1 contains two phosphorylation sites for protein kinase C (PKC) and a phosphorylation site for the cAMP-dependent protein kinase (PKA) in the

C-terminus, two N-linked glycosylation sites after the first transmembrane domain, and a leucine zipper motif in the fourth trans-membrane domain[92]. In addition to regulation at these sites, TALK-1 is also regulated by pH[92]. As pH increases, the TALK-1 channels become more activated. This function could be important in intestinal d-cells that express TALK-1; however, as the pH of the pancreas remains rather stable, it does not seem to affect TALK-1 in the pancreas. Instead, TALK-1 functions as more of a background leak channel in the pancreas, thereby regulating membrane potential and excitability.

Mechanisms of TALK-1 islet cell regulation.

In β-cells, when glucose metabolism closes K_{ATP} channels, the outward rectifying, non-inactivating K^+ current of TALK hyperpolarizes the β-cell membrane, thereby limiting VDCC channel activation and subsequent insulin secretion[79]. This was shown in the β-cell tissue culture line, EndoC-βH1. The EndoC-βH1 cell line were generated from human fetal pancreas, and they express numerous beta-cell markers as well as responding to elevated glucose with stimulation of insulin secretion[100; 101]. They also show a very similar electrophysiological profile as human β-cells[102]. Knockdown of *KCNK16* in EndoC-βH1 cells via siRNA resulted in increased GSIS[103]. More importantly, this effect of TALK-1 current on insulin secretion was also shown in a global TALK-1 KO mouse model. In this model, TALK-1 KO causes the β-cell membrane potential to depolarize thereby increasing action-potential firing frequency[79]. This increased action potential frequency results in increased Ca^{2+} oscillations, and therefore increased first-phase pulsatile-insulin secretion[79].

Interestingly, TALK-1 not only forms functional channels on the β-cell plasma membrane, it can also form function channels on the ER memrane[65]. Indeed, many of the proteins that have been found to interact with TALK-1 are ER resident proteins[104; 105]. At the ER membrane, TALK-1 allows K^+ to move down its concentration gradient and into the ER thereby providing a counter-current for $[Ca^{2+}]_{ER}$ release[65]. This was established with studies that showed increased $[Ca^{2+}]_{ER}$ in global TALK-1 KO cells and reduced $[Ca^{2+}]_{ER}$ in cells expressing TALK-1 with a gain-of-function polymorphism[65; 79]. Reduced $[Ca^{2+}]_{ER}$ results in ER stress and reduced insulin secretion[49; 65] This suggests that polymorphisms or mutations in TALK-1 that result in a gain-of-function would result in ER stress, reduced insulin secretion, and diabetes (discussed in more detail below).

Within δ-cells, glucose metabolism also results in K_{ATP} channel closure and VDCC activation. However, in contrast to insulin secretion, Ca^{2+} influx through the VDCC is not the most critical contributor to somatostatin secretion. Instead, due to high expression of RyRs[106], somatostatin secretion is dependent on CICR from the ER[107]. Therefore, TALK-1 activity on the δ-cell ER membrane reduces CICR, which reduces somatostatin secretion[108]. Indeed, a global TALK-1 KO mouse demonstrated increased $[Ca^{2+}]_{ER}$ and reduced somatostatin secretion[108].

Due to the high level of islet cell paracrine regulation described above **(Figure 1.1)**; TALK-1 regulation of insulin and somatostatin secretion was hypothesized to affect glucagon secretion. Indeed, even though TALK-1 protein is not expressed in α-cells, TALK-1 KO islets showed increased glucagon secretion[108]. Binding of somatostatin to somatostatin receptors on α-cells activates GIRK channels thereby polarizing the membrane, limiting VDCC activity, and reducing glucagon secretion. Therefore, increased glucagon

secretion in global TALK-1 KO islets was hypothesized to be caused by reduced somatostatin-induced α-cell inhibition[108]. Indeed, an SSTR inhibitor eliminated the impact of TALK-1 ablation on glucagon secretion. As these TALK-1 studies were completed with a global TALK-1 KO, it is difficult to distinguish what effects are due to changes in somatostatin secretion and what are due to insulin secretion. Therefore; a β-cell specific TALK-1 KO mouse model is needed to identify the exact contributions of TALK-1 in the development of diabetes.

Diabetes

Type-2 Diabetes Mellitus (T2DM)

Type 2 diabetes mellitus (T2DM) is characterized by chronic hyperglycemia, resulting from β-cell dysfunction induced insulin deficiency and tissue insulin resistance[109]. If left untreated, T2DM causes several severe complications including diabetic retinopathy[110], diabetic ketoacidosis[111], peripheral neuropathies[112], and an increased risk for cardiovascular and kidney disease[109; 113-116]. Worldwide, 422 million people have diabetes mellitus, with 1.6 million deaths directly attributed to it[117]. T2DM is the most common form of diabetes mellitus, and with the prevalence of T2DM continually rising, defining the mechanisms which cause this disease is critical for improving its worldwide diagnosis and treatment.

Islet cell K^+ channels have been identified as major contributors to the development of diabetes. Genome-wide association studies (GWAS), which analyze the genomes of large populations to identify genetic markers associated with disease, have identified

candidate loci which regulate islet cell function and contribute to diabetes risk. To date, this approach has identified four K^+ channel GWAS signals associated with T2DM susceptibility, including *KCNJ11*[118-121], *KCNJ15*[122], *KCNQ1*[123], and the TALK-1 gene, *KCNK16*[98; 99; 124; 125]. Specifically, the studies on *KCNK16* established that *KCNK16* contains a single nucleotide, non-synonymous, polymorphism (rs1535500) associated with an increased risk for T2DM in Pima-American Indians as well as individuals of East Asian ancestry[98; 124; 126]. These findings, as well as the above studies[65; 79; 104; 108] that highlight the mechanisms of TALK-1- mediated islet cell regulation make TALK-1 a viable candidate for diabetic therapies.

As mentioned above, insulin resistance is a major contributor to hyperglycemia. Insulin resistance occurs when peripheral tissues, such as the muscle and the liver, stop responding normally to insulin signaling; therefore, reducing glucose uptake from the blood[127; 128]. The development of insulin resistance is the result of multiple perturbations to cellular signaling[129; 130]. One mechanism of insulin resistance is impaired phosphorylation of insulin receptor substrate, IRS1. IRS1 is a scaffolding protein and its phosphorylation is one of the first events in insulin signaling. Studies reveal that insulin-stimulated tyrosine phosphorylation of IRS-1 is impaired in non-obese and obese Type 2 diabetic patients[131-133].

Other studies show that increased serine phosphorylation of IRS-1 (specifically of serine 312[134] and 636[131]) can also result in insulin resistance. Interestingly, one proposed mechanism of increased IRS-1 serine phosphorylation is through the accumulation of lipids in the liver and muscle. Accumulated lipids can activate stress-induced protein

kinases such as the novel protein kinase C (nPKCs) and the c-Jun N-terminal kinases (JNKs)[135; 136]. These kinases then go on to phosphorylate IRS-1.

Another proposed mechanism of insulin resistance is NF-κB activated pro-inflammatory cytokines. Activation of these cytokines results in inflammation, insulin signaling inhibition, and insulin resistance through the accumulation of macrophages[137-140]. Furthermore, PKCε can also be activated through the accumulation of the lipid, diacylglycerol[141].

One way in which hyperglycemia results in β-cell failure is through ER stress. Hyperglycemia results in an increased demand for insulin which leads to β-cell ER stress, the UPR, and eventual β-cell dysfunction. As described above, in addition to limiting both glucose-stimulated insulin and somatostatin secretion by hyperpolarizing the membrane, TALK-1 also enhances $[Ca^{2+}]_{ER}$ release and ER stress[65]. Therefore, limiting TALK-1 current on the ER membrane is predicted to reduce β-cell ER stress during diabetes. Indeed, a global TALK-1 KO mouse model shows reduced expression of ER stress markers while on a high fat diet (HFD) compared to control[65].

In addition to ER stress, mitochondrial dysfunction also leads to β-cell failure through the production of reactive oxygen species (ROS) and the initiation of apoptosis. As described above, the ER and the mitochondria are closely linked at the MAM. Furthermore, defects in the MAM are suggested to play a role in the pathogenesis of diabetes[142]. Tubbs et al. showed that knockdown of IP3R1 to reduce MAM integrity triggers mitochondrial dysfunction and glucose intolerance in obese mice[143]. Additionally, treatment with metformin reinforced MAM integrity thereby improving glucose homeostasis[143]. As TALK-1 regulates $[Ca^{2+}]_{ER}$ and ER stress, it is predicted that it would also regulate diabetic-

induced mitochondrial dysfunction. This makes TALK-1 a possible target for improving β-cell mitochondrial function, reducing ROS production, and preventing β-cell dysfunction.

Another contributor to β-cell dysfunction during diabetes is the presence of elevated cytokines, reflection a state of low-grade inflammation. Conditions of over-nutrition result in low-grade systemic inflammation during which pro-inflammatory cytokine concentrations increase dramatically[144; 145]. These cytokines contribute to insulin resistance and diminished β-cell function[146]. Interestingly, cytokine exposure has been shown to decrease *KCNK16* transcript abundance as well as the associated TALK-1 protein expression, thereby increasing $[Ca^{2+}]_{ER}$ storage and glucose-stimulated insulin secretion[47]. These findings indicate that TALK-1 plays an important role in altered β-cell function during low-grade inflammation and suggests that cytokines may reduce TALK-1 expression to acutely protect β-cells from dysfunction. This highlights yet another reason why TALK-1 makes an interesting target to reduce β-cell dysfunction during the pathogenesis of diabetes.

Mature-onset Diabetes of the Young (MODY)

Maturity-onset diabetes of the young (MODY) is a rare monogenic form of familial diabetes. To date, 13 genes have been predicted to cause MODY, all involved in pancreatic β-cell function and all with autosomal dominant transmission[147]. The most common types are HNF1A-MODY (also known as MODY3)[148], which accounts for 50-70% of cases, and GCK-MODY (MODY2)[149], accounting for 30-50% of cases. GCK-MODY is caused by mutation in the gene that encodes glucokinase. Glucokinase is an

enzyme that facilitates the phosphorylation of glucose into glucose-6-phosphate, allowing glycolysis to occur. As glucokinase mutations prevent glucose metabolism, these mutations impact glucose-stimulated elevations in the ATP/ADP levels and thus closure of K_{ATP}. This results in blunted glucose-stimulated insulin secretion.

MODY-related mutations have also been shown to cause β-cell ER stress. For example, mutations in glucokinase have been shown to result in improper protein folding thereby activating the unfolded protein response[149]. Furthermore, mutations in *WFS-1* have also been shown to cause MODY through the initiation of β-cell ER stress[150].

Up to 2-2.5% of pediatric diabetes cases carry pathogenic/likely pathogenic variants in MODY genes[151; 152]; however, MODY is often undiagnosed, either because the diagnosis is not considered[153] or because genetic screening is limited. There are also cases with compelling clinical histories in whom, despite comprehensive screening of known MODY genes, a genetic diagnosis cannot be made[152], suggesting as-yet-unidentified genetic cause(s).

As TALK-1 function reduces insulin secretion and reduces ER Ca^{2+}, TALK-1 gain-of-function mutations would be predicted to cause ER stress and diabetes similarly to mutations in GCK and K_{ATP}. This makes *KCNK16*, the gene that encodes TALK-1 an interesting candidate for a possible unknown MODY gene. Indeed, in this dissertation, we will describe a significant gain-of-function mutation (Leu114Pro) in *KCNK16* that is associated with exogenous insulin-specific MODY.

Neonatal Diabetes

Neonatal diabetes is a rare form of monogenic diabetes that presents within the first 6 months of life. Half of neonatal diabetic cases are transient, meaning they resolve within the first 12 weeks of life; however, the other half are permanent. A large international cohort study found that 80% of neonatal diabetics had a known genetic diagnosis[154]. Interestingly, 40% of these cases are due to mutations in the genes encoding the K_{ATP} channel subunits, *ABCC8*[155; 156] and *KCNJ11*[156], showing that β-cell K^+ channel activity is a critical contributor to neonatal diabetes.

We have identified a novel recessive mutation in *KCNK16* (TALK-1 R13Q) that has been associated with neonatal diabetes in a consanguineous family. This mutation ablates TALK-1 current at the plasma membrane but maintains current on the ER membrane. This is presumably due to altered palmitoylation-mediated TALK-1 trafficking and results in abnormal β-cell Ca^{2+} handling and reduced GSIS.

ER stress is a major contributor to neonatal diabetes. Mutations in *WFS1*[157] and *INS1*[158] result in the unfolded protein response, β-cell ER stress, and neonatal diabetes. As TALK-1 functions on the ER membrane and has been shown to regulate β-cell ER stress[65], the TALK-1 R13Q mutation might also increase β-cell ER stress.

As there are still many neonates with diabetes and unknown genetic etiology, it is important to consider other β-cell K^+ channels as possible causes. Indeed, this dissertation will discuss the possibility that the novel recessive mutation (R13Q) in *KCNK16* is a new neonatal diabetic mutation.

Goals of this Dissertation

Diabetes affects 422 million people worldwide, including almost 10% of the American population, and it is caused in-part by pancreatic β-cell failure. TALK-1 is the most highly expressed K^+ channel transcript in β-cells and is also restricted to the islet. This, along with the association of TALK-1 with T2DM, makes TALK-1 an interesting candidate for a novel therapeutic target. The goal of this thesis was to determine the mechanisms by which TALK-1 modulates β-cell ER stress and mitochondrial dysfunction, and therefore the risk of β-cell failure during the pathogenesis of diabetes. These findings are expected to significantly contribute to our understanding of how β-cells become impaired during diabetes and illuminate a new, islet-specific, target for the treatment of metabolic diseases. In the following chapters, I describe how changes in TALK-1 current regulates intracellular β-cell Ca^{2+} handling to modulate ER stress, mitochondrial function, and insulin secretion under physiological conditions, as well as T2DM, MODY, and neonatal diabetic conditions.

First, we utilized β-cell specific TALK-1 KO mice (β-TALK1-KO) to identify the specific role of β-cell TALK-1 in regulating β-cell function, whole islet function, and therefore whole-body glycemic control. We found that ablating TALK-1 current specifically in β-cells increases β-cell $[Ca^{2+}]_c$ oscillations and increases $[Ca^{2+}]_{ER}$ storage. The increase in $[Ca^{2+}]_c$ and $[Ca^{2+}]_{ER}$ also resulted in increased mitochondrial Ca^{2+} ($[Ca^{2+}]_{mito}$). This is predicted to depolarize the mitochondrial V_m and indeed, β-TALK1-KO islets have reduced glucose-induced mitochondrial hyperpolarization which interestingly leads to increased ATP production. Finally, we showed that under diabetic conditions (60% HFD) β-TALK1-KO mice have improved glucose tolerance but show reduced GSIS compared to controls.

This suggests that TALK-1 regulating the β-cell function may affect insulin resistance under diabetic conditions or altered pulsatile insulin secretion.

The association between TALK-1 current and T2DM made us want to investigate the role of TALK-1 in other diabetic conditions. We investigated the effects of two TALK-1 mutations, TALK-1 L114P and TALK-1 R13Q that were associated with MODY and neonatal diabetes, respectively. We first assessed how TALK-1 L114P affects channel activity. Interestingly, this mutation results in a drastic gain-of-function, leading to an over 300-fold increase in current. This TALK-1 current increase leads to β-cell hyperpolarization, a loss of glucose-stimulated Ca^{2+} influx, reduced $[Ca^{2+}]_{ER}$, and a reduction in GSIS.

We next assessed how TALK-1 R13Q impacts TALK-1 channel activity and Ca^{2+} handling. Interestingly, in contrast to the gain-of-function seen with TALK-1 L114P, TALK-1 R13Q results in a complete loss of function on the plasma membrane. It does however maintain function on the ER membrane leading to reduced β-cell $[Ca^{2+}]_{ER}$ and a complete inhibition of GSIS. This unique TALK-1 activity profile is hypothesized to be due to improper trafficking of the TALK-1 protein. The TALK-1 R13Q mutation is adjacent to palmitoylation sites on TALK-1 that we have shown regulate TALK-1 R13Q trafficking from the ER membrane to the plasma membrane. Together, this suggests that TALK-1 R13Q causes β-cell dysfunction through an intracellular, opposed to plasmalemmal, mechanism. Therefore, as we have shown TALK-1 regulates mitochondrial function, it we investigated whether TALK-1 R13Q is causing mitochondrial dysfunction, thereby inhibiting GSIS.

Together the findings in this dissertation suggest that TALK-1 controls the β-cell response to ER stress leading to β-cell dysfunction under diabetic phenotypes. Specially, by modulating β-cell $[Ca^{2+}]_c$, $[Ca^{2+}]_{ER}$, $[Ca^{2+}]_{mito}$, and therefore mitochondrial function. Furthermore, mutations in TALK-1 that increase either plasmalemmal or intracellular TALK-1 current, can result in β-cell dysfunction and diabetes. Overall, these studies have enhanced our understanding of the most highly expressed β-cell K^+ channel transcript and have nominated TALK-1 as a possible therapeutic target for treatment of T2DM, MODY, and neonatal diabetes.

Chapter II
β-cell TALK-1 ablation increases cytoplasmic and mitochondrial Ca^{2+} leading to increased insulin secretion and improved glucose homeostasis.

Abstract

The two-pore domain K^+ channel, TALK-1 modulates islet Ca^{2+} handling and hormone secretion. However, the exact role(s) that TALK-1 plays in modulating β-cell function is still unknown. Therefore, we generated a β-cell specific TALK-1 KO mouse model (β-TALK1-KO) which shows increased β-cell $[Ca^{2+}]_c$ oscillation frequency and $[Ca^{2+}]_{ER}$ storage. The increase in $[Ca^{2+}]_c$ and $[Ca^{2+}]_{ER}$ also resulted in increased mitochondrial Ca^{2+} ($[Ca^{2+}]_{mito}$). This is predicted to depolarize the mitochondrial membrane potential (V_m) and indeed, β-TALK1-KO islets have reduced glucose-induced mitochondrial hyperpolarization. We next determined how these changes in β-cell Ca^{2+} handling influence respiration and found that β-TALK1-KO increases ATP production. Finally, we tested how β-TALK1-KO mice respond to diabetic conditions. β-TALK1-KO mice have improved glucose tolerance on a high-fat diet but interestingly show reduced GSIS compared to controls. This suggests that, instead of increased insulin secretion, the kinetics of GSIS from the β-cell TALK-1 could be responsible for the improved glucose tolerance. These data suggest that TALK-1 modulation of β-cell mitochondrial function may tune GSIS pulsatility in a manner that controls peripheral tissue insulin action under diabetic conditions.

Introduction

Pancreatic β-cell insulin secretion is a key regulator of blood glucose homeostasis. Glucose-stimulated insulin secretion (GSIS) is coupled to β-cell $[Ca^{2+}]_c$ influx through voltage-dependent Ca^{2+} channels (VDCCs), which are active at depolarized β-cell membrane potentials (V_m). Under low glucose conditions K_{ATP} hyperpolarizes the β-cell V_m limiting $[Ca^{2+}]_c$ influx through VDCCs and following glucose stimulation closure of K_{ATP} channels depolarizes V_m activating VDCCs, $[Ca^{2+}]_c$ influx, and insulin secretion. During glucose-stimulated K_{ATP} channel inhibition, the β-cell V_m is modulated by two-pore domain K^+ (K2P) channels such as the TWIK-related alkaline pH-activated K2P-1 (TALK-1)[79] channel. In human islets the *KCNK16* gene that encodes TALK-1 is the most abundant K^+ channel transcript and is also functionally expressed in β- and δ-cells. Importantly, a non-synonymous, gain-of-function (GOF), polymorphism in *KCNK16* (rs1535500) has been associated with an increased risk for T2DM[98; 99] and may increase the risk of developing T2DM by reducing β-cell insulin secretion[79]. TALK-1 is also expressed in δ-cells where it limits glucose-stimulated $[Ca^{2+}]_c$ elevations, somatostatin secretion, and controls paracrine regulation of α-cell glucagon secretion[108]. Therefore, TALK-1 and/or changes to the activity of TALK-1 (e.g. rs1535500 non-synonymous polymorphism) could be affecting both β-cell and δ-cell function to control glucose homeostasis. Furthermore, when on a high-fat diet (HFD), global TALK-1 KO mice did not gain as much weight as WT mice. It is important to examine if TALK-1 loss in β-cells is responsible for the reduced weight, and if not, if the changes in weight are responsible for the alterations in fasting glucose seen in global TALK-1 KO animals. Therefore, it important to identify the β-cell specific role(s) of TALK-1 function in the context of β-cell function or dysfunction.

β-cell insulin secretion occurs in a pulsatile manner from the pancreas due to oscillations in electrical excitability and $[Ca^{2+}]_c$ influx[46]. In addition to $[Ca^{2+}]_c$ influx, intracellular endoplasmic reticulum (ER) Ca^{2+} stores ($[Ca^{2+}]_{ER}$) contribute to controlling β-cell $[Ca^{2+}]_c$ oscillations. The kinetics and amplitude of $[Ca^{2+}]_{ER}$ release is regulated by TALK-1 which provides a K^+ countercurrent across the ER membrane that promotes $[Ca^{2+}]_{ER}$ release by enhancing the electrical driving force for $[Ca^{2+}]_{ER}$ efflux[65]. TALK-1 augmentation of $[Ca^{2+}]_{ER}$ release during glucose-stimulation activates the Ca^{2+} sensitive K^+ current, K_{slow}, which increases the inter-burst interval between $[Ca^{2+}]_c$ oscillations and reduces $[Ca^{2+}]_c$ oscillation frequency. In δ-cells, TALK-1 current has also been shown to limit somatostatin secretion by modulating Ca^{2+} induced Ca^{2+} release (CICR) from the ER[108]. TALK-1 control of $[Ca^{2+}]_{ER}$ is also important for controlling the ER stress response under diabetic conditions and may also contribute to the impact of a TALK-1 GOF polymorphism (rs1535500) on β-cell dysfunction.

Mitochondria are very sensitive to $[Ca^{2+}]_{ER}$ as well as $[Ca^{2+}]_c$ levels and undergo dynamic Ca^{2+} changes that regulate β-cell respiration. Under basal conditions mitochondrial Ca^{2+} ($[Ca^{2+}]_{mito}$) is similar to $[Ca^{2+}]_c$, but glucose-stimulation can increase β-cell $[Ca^{2+}]_{mito}$ to approximately 12 μm[159]. Other groups have shown that that β-cell V_m depolarization can increase $[Ca^{2+}]_{mito}$ all the way up to 70 μM[56; 160]. While $[Ca^{2+}]_c$ is a major source of $[Ca^{2+}]_{mito}$ uptake, $[Ca^{2+}]_{ER}$ has also been shown to contribute to $[Ca^{2+}]_{mito}$ handling through Ca^{2+} “hotspots” located at junctions between ER and mitochondria, termed mitochondrial associated membrane (MAM)[59]. The high $[Ca^{2+}]_c$ at the MAM is critical for $[Ca^{2+}]_{mito}$ uptake for two reasons: the mitochondrial Ca^{2+} uniporter has a low affinity to Ca^{2+} and glucose-stimulated $[Ca^{2+}]_{mito}$ levels reach much higher levels (approximately 12 μm[159]) than that

of $[Ca^{2+}]_c$ (approximately 1 μm). TALK-1 control of the driving force for $[Ca^{2+}]_{ER}$ release is thus likely to regulate $[Ca^{2+}]_{mito}$. Furthermore, TALK-1 regulation of $[Ca^{2+}]_c$ is also predicted to modulate $[Ca^{2+}]_{mito}$. As elevations in β-cell $[Ca^{2+}]_{mito}$ are critical for dehydrogenase activation and mitochondrial respiration, TALK-1 may play an important role in regulating β-cell mitochondrial function and ATP production.

Here we tested how TALK-1 control of β-cell Ca^{2+} handling affects β-cell function and glucose homeostasis. This was accomplished by creating a β-cell specific TALK-1 KO (β-TALK1-KO) mouse model. β-TALK1-KO mice have increased β-cell Ca^{2+} oscillation frequency, increased $[Ca^{2+}]_{ER}$ storage, increased ATP production, and improved glucose tolerance. Furthermore, we find that β-TALK1-KO mice have increased β-cell $[Ca^{2+}]_{mito}$, depolarized mitochondrial membrane potential, and elevated mitochondrial respiration. Interestingly, under diabetic conditions β-TALK1-KO mice show improved glucose tolerance with reduced GSIS. This suggests that, instead of increased insulin secretion, the kinetics of GSIS from the β-cell TALK-1 could be responsible for the improved glucose tolerance. Together, these data indicate that TALK-1 regulates glucose tolerance and insulin sensitivity in a β-cell specific manner and therefore suggests that TALK-1 could be a β-cell specific target for treating insulin resistance and T2DM.

Results

Development of a β-cell specific TALK-1 KO mouse model

The β-cell specific TALK-1 KO mouse model was created by the Vanderbilt Genome Editing Resource via microinjection of genetically modified mouse ESCs into 3.5-day old mouse embryos. Within the *KCNK16* gene, loxP sites were placed on either side of exons

2 and 3. Mice expressing the floxed *KCNK16* gene were then crossed with mice expressing the *Ins1*^{cre} to allow for the removal of the floxed exons specifically in β-cells. These mice will here on be referred to as β-TALK1-KO mice[161].

Immunofluorescence staining on isolated pancreata was used to confirm that β-TALK1-KO mice had β-cell specific TALK-1 ablation. We found that, in contrast to WT C57Bl/6J islets, β-TALK1-KO islets lacked TALK-1 protein expression in insulin-positive β-cells, but maintained TALK-1 protein expression in somatostatin-positive δ-cells (Figure 2.1 A). We next used patch clamp electrophysiology to determine whether TALK-1 currents were successfully ablated in β-cells from β-TALK1-KO islets. For specific examination of K2P channels, K_{ATP} channels were blocked with tolbutamide (100 µmol/L), voltage-gated K^+ channels were blocked with tetraethylammonium (10 mmol/L), and Ca^{2+} was removed from the extracellular buffer to prevent activation of Ca^{2+}-activated K^+ (K_{Ca}) channels. Indeed, compared to β-cells from control islets (fl/fl), β-cells from β-TALK1-KO islets demonstrated significantly reduced K2P current, indicating successful loss of functional TALK-1 channels (Figure 2.1 B and C).

<u>β-cell specific TALK-1 regulates whole-islet cytosolic Ca^{2+} handling</u>

To investigate whether the previously shown TALK-1 regulation of islet $[Ca^{2+}]_c$ handling[79] was a result of TALK-1 function specifically in β-cells, we measured glucose-stimulated islet $[Ca^{2+}]_c$ oscillations in β-TALK1-KO islets compared to control islets (fl/fl). In response to an increase from 1 mM to 11 mM glucose, $[Ca^{2+}]_c$ oscillation frequency was increased in the β-TALK1-KO islets compared to control (fl/fl), indicating that β-cell TALK-1 is able to modulate whole islet $[Ca^{2+}]_c$ handling (Figure 2.2).

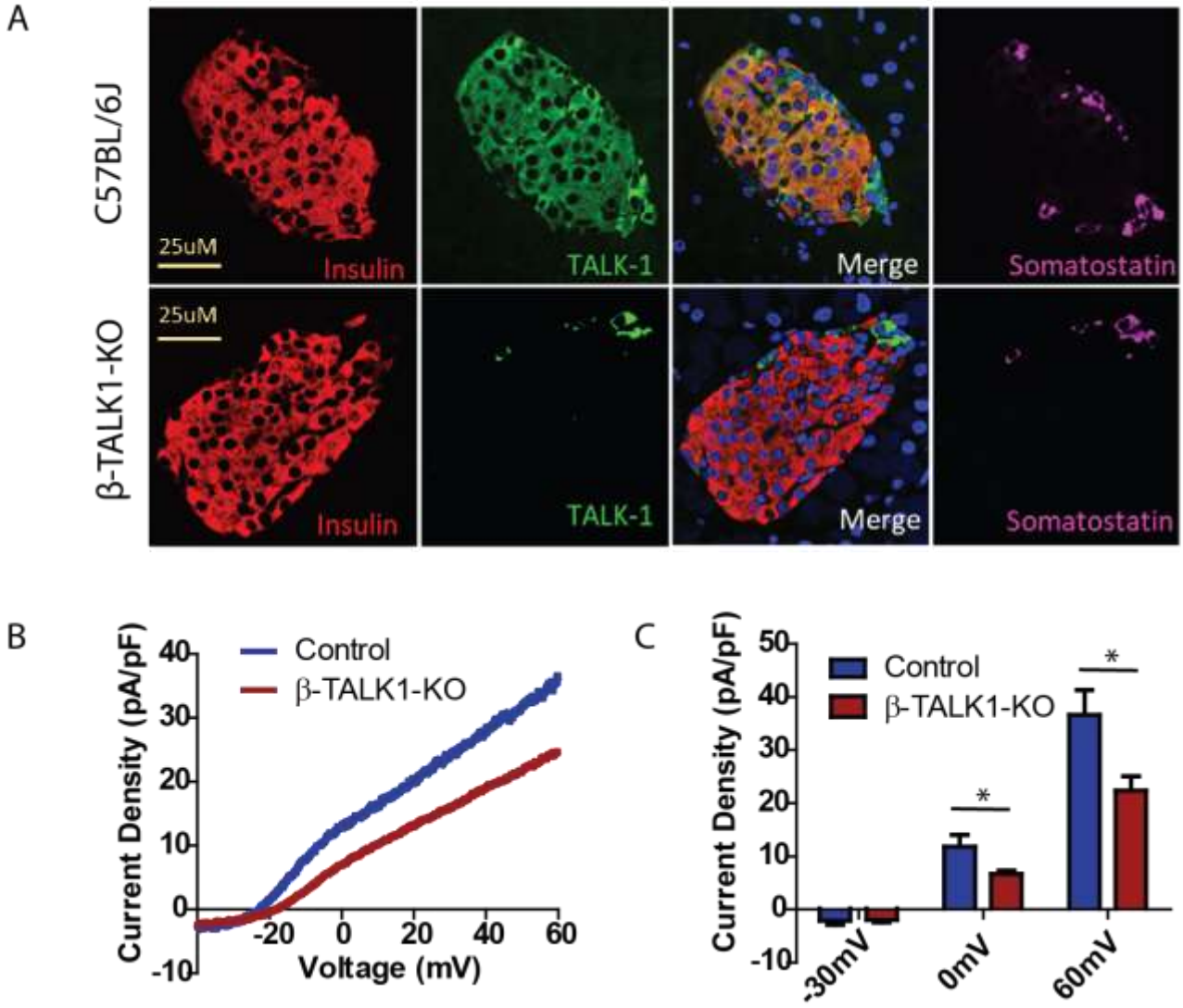

Figure 2.1. β-TALK-1-KO islets show loss of β-cell TALK-1 protein and current.

Representative immunofluorescent staining of control and β-TALK-1-KO islets for insulin, somatostatin, and TALK-1 (nuclei in blue labeled with Hoechst) **(A)**. β-cells from either control mice or β-TALK-1-KO mice were recorded for TALK-1 currents by voltage clamp, in response to a ramp from -120 mV to 60 mV. Representative control cell and β-TALK-1-KO cell **(B)** as well as average responses **(C)**. Mean ± SEM, N = 4 control and 5 β-TALK-1-KO. P < 0.05.

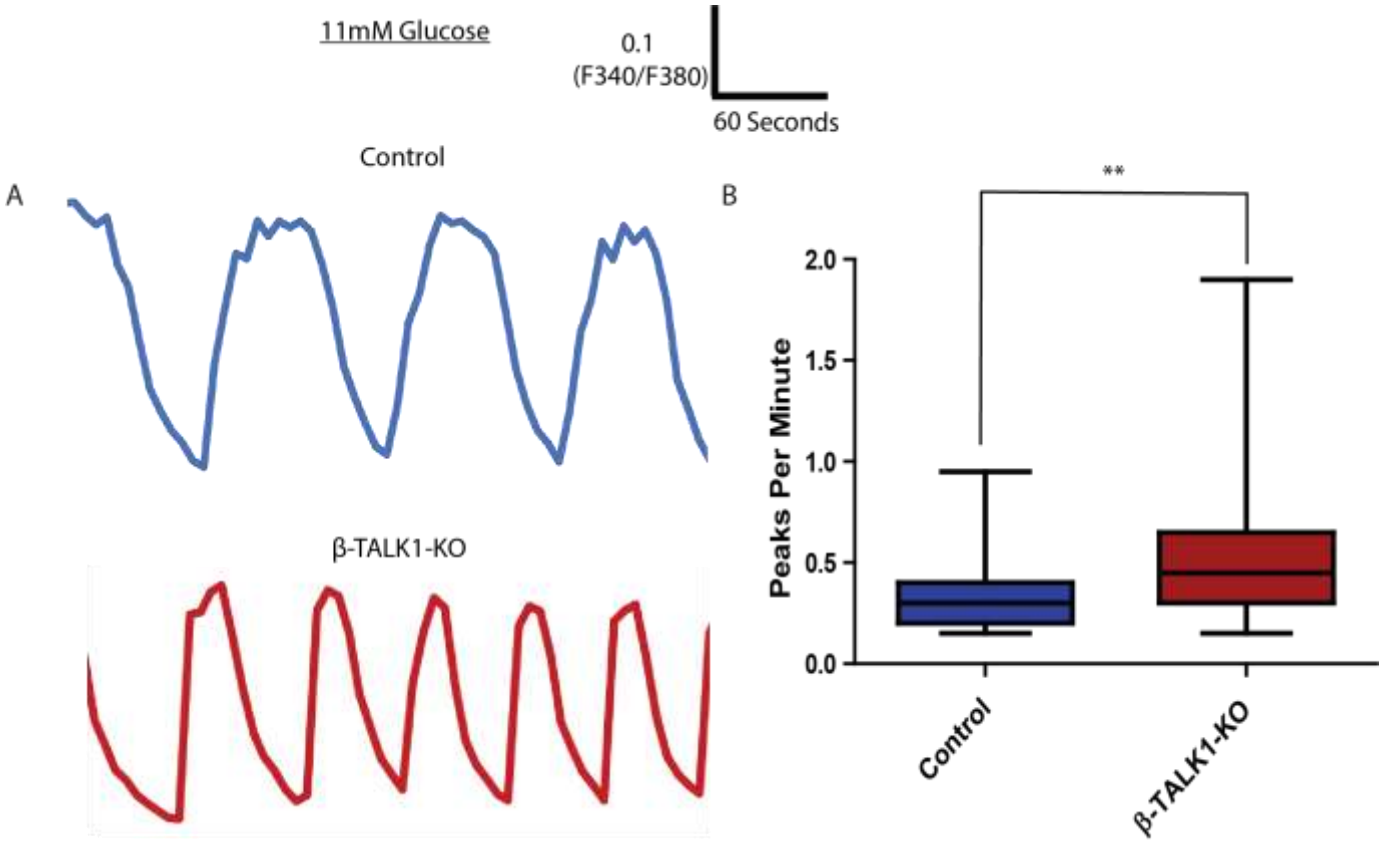

Figure 2.2: β-cell TALK-1 ablation increases glucose-stimulated Ca^{2+} oscillation frequency.

β-cells from either control or β-TALK1-KO mice were stimulated with 11 mM glucose and cytosolic Ca^{2+} was measured with Fura2am. Representative traces **(A)** and average oscillation peaks per minute **(B)**; mean ± SEM; N=44 Control islets from 3 animals; N = 44 β-TALK1-KO islets from 3 animals. **P < 0.01

β-cell specific TALK-1 regulates mitochondrial Ca^{2+} handling

To determine the intracellular effects of β-cell TALK-1 $[Ca^{2+}]_c$ regulation, we investigated $[Ca^{2+}]_{mito}$ handling in β-cells within β-TALK1-KO islets and compared them to β-cells within control islets (fl/fl). To measure $[Ca^{2+}]_{mito}$, we utilized the $[Ca^{2+}]_{mito}$ indicator, Cepia2mt[162]. We created a lentivirus that utilized a rat-insulin promoter expressing Cepia2mt so that we could measure $[Ca^{2+}]_{mito}$ specifically in β-cells. Islets from β-TALK1-KO and control (fl/fl) mice were transduced with the virus and imaged on a Zeiss LSM780 confocal with a 20X objective. β-cells within both β-TALK1-KO and control (fl/fl) islets $[Ca^{2+}]_{mito}$ decreased upon glucose stimulation, presumably due to the activation of the mitochondrial Na/Ca^{2+} exchanger (NCLX) which becomes activated after cell depolarization resulting in mitochondrial Na^+ uptake and $[Ca^{2+}]_{mito}$ release[163] (Figure 2.3A). Interestingly, β-cells within β-TALK1-KO islets showed increased $[Ca^{2+}]_{mito}$ compared to control (fl/fl) in both low (1mM) and high (11mM) glucose (Figure 2.3A) . NCLX-mediated $[Ca^{2+}]_{mito}$ efflux is triggered by depolarization-mediated Na^+ influx that occurs alongside depolarization-induced $[Ca^{2+}]_{mito}$ influx through the MCU. Therefore, a glucose-stimulated $[Ca^{2+}]_{mito}$ influx is expected to be seen with cepia2mt prior to the glucose-stimulated decrease. Increasing line scan resolution by raising the number of pixels per cell, increased the data generated per field and allowed for more dynamic cepia2mt measurements to be recorded. Under these measurement conditions, cells displayed the expected glucose-stimulated $[Ca^{2+}]_{mito}$ influx followed by an overall $[Ca^{2+}]_{mito}$ efflux (Figure 2.3B and C). These measurements showed the same increased β-TALK1-KO basal $[Ca^{2+}]_{mito}$ but interestingly showed that β-cells within β-TALK-1 KO islets do not

have as large of a glucose-stimulated $[Ca^{2+}]_{mito}$ increase as control (fl/fl) (Figure 2.3D). This is presumably due to the finding that β-cells within β-TALK-1 KO islets have increased basal $[Ca^{2+}]_{mito}$, thereby reducing the driving force of Ca^{2+} through the MCU. Similarly, the overall glucose-stimulated $[Ca^{2+}]_{mito}$ decrease was enhanced in β-cells within β-TALK-1 KO islets compared to control, presumably due to the increased driving force for $[Ca^{2+}]_{mito}$ efflux in the β-TALK-1 KO islets (Figure 2.3E).

As cepia2mt is not a ratiometric indicator, it is possible that the increased basal $[Ca^{2+}]_{mito}$ seen in β-TALK-1 KO islets is only due to increased cepia2mt expression. To test this, we created a lentivirus expressing a mitochondrial calcium fret-based indicator[164] on the β-cell specific rat-insulin promoter. Following transduction with this virus, β-cells within β-TALK1-KO showed increased basal $[Ca^{2+}]_{mito}$ compared to control (fl/fl), supporting the finding that β-TALK1-KO β-cells do indeed have increased $[Ca^{2+}]_{mito}$ compared to control and it is not just a difference in cepia2mt expression (Figure 2.4).

<u>β-cell specific TALK-1 mitochondrial Ca^{2+} regulation modulates mitochondrial membrane potential</u>

Mitochondria have been shown to hyperpolarize during metabolism[165]; however, the increased $[Ca^{2+}]_{mito}$ seen in in β-TALK-1 KO islets is predicted to depolarize the mitochondrial V_m. Therefore, we utilized the mitochondrial V_m indicator dye, TMRE to measure glucose-stimulated mitochondrial V_m in β-TALK-1 KO and control (fl/fl) islets. Interestingly, β-TALK-1 KO islets do not hyperpolarize in response to glucose as much as control (fl/fl) islets do, presumably due to increased $[Ca^{2+}]_{mito}$ (Figure 2.5).

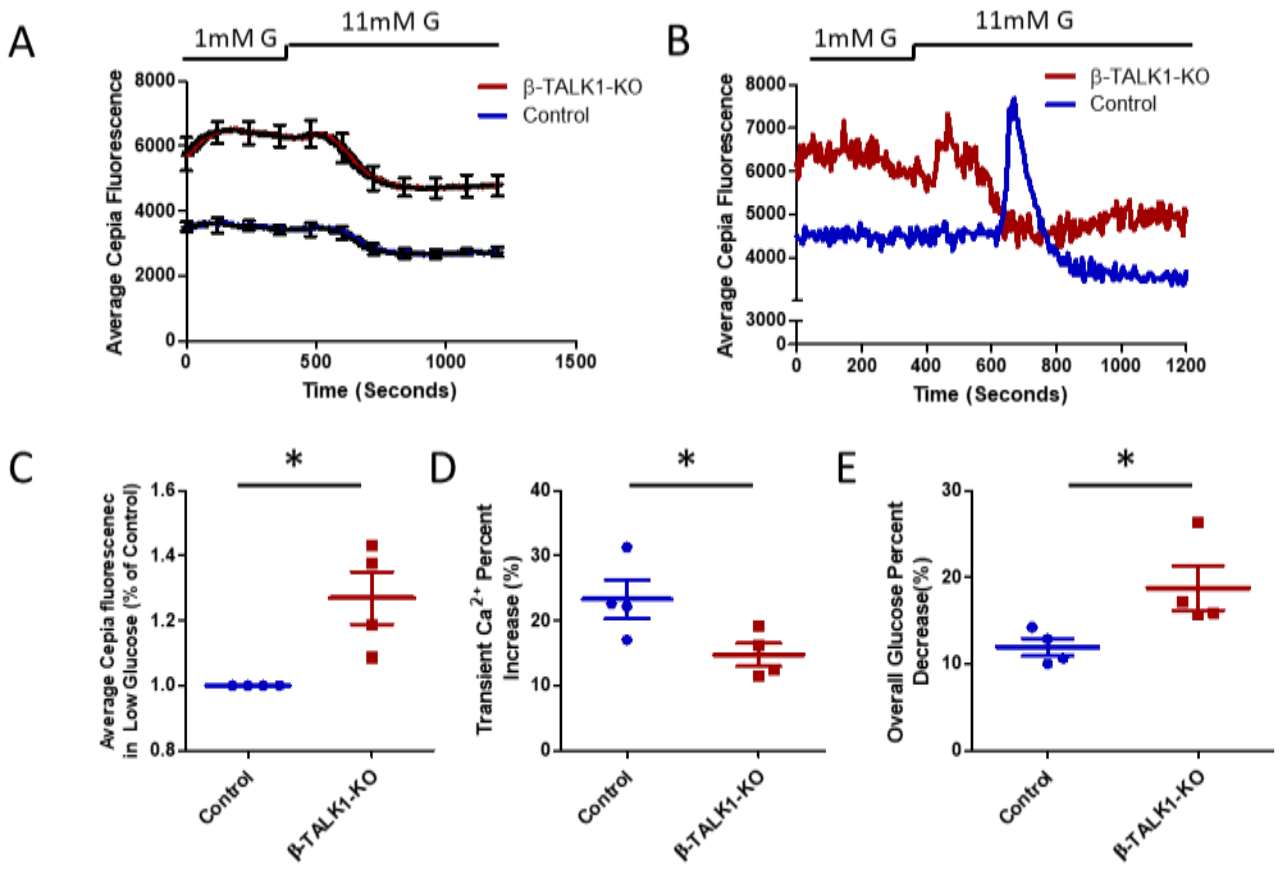

Figure 2.3. β-cells in β-TALK1-KO islets have increased basal mitochondrial Ca^{2+}, a smaller transient increase in glucose-stimulated mitochondrial Ca^{2+}, and an increased overall glucose-stimulated mitochondrial Ca^{2+} decrease.

β-TALK1-KO and Control (fl/fl) islets were transduced with a lentivirus expressing Cepia2mt on a RIP promoter and imaged on the LSM 780. Representative traces at 0.5X magnification **(A)** and 1X magnification **(B)** with markers for what regions were quantified. Average Cepia2mt fluorescence in 1mM glucose **(C)**, the transient percent increase due to glucose **(D)** and the prolonged overall glucose stimulated decrease in mitochondrial Ca^{2+} were all quantified **(E)**. Mean ± SEM; N = 3 control mice and N = 3 β-TALK1-KO mice **(A)**. Mean ± SEM; N = 4 control mice and N = 4 β-TALK1-KO mice **(B-E)**.

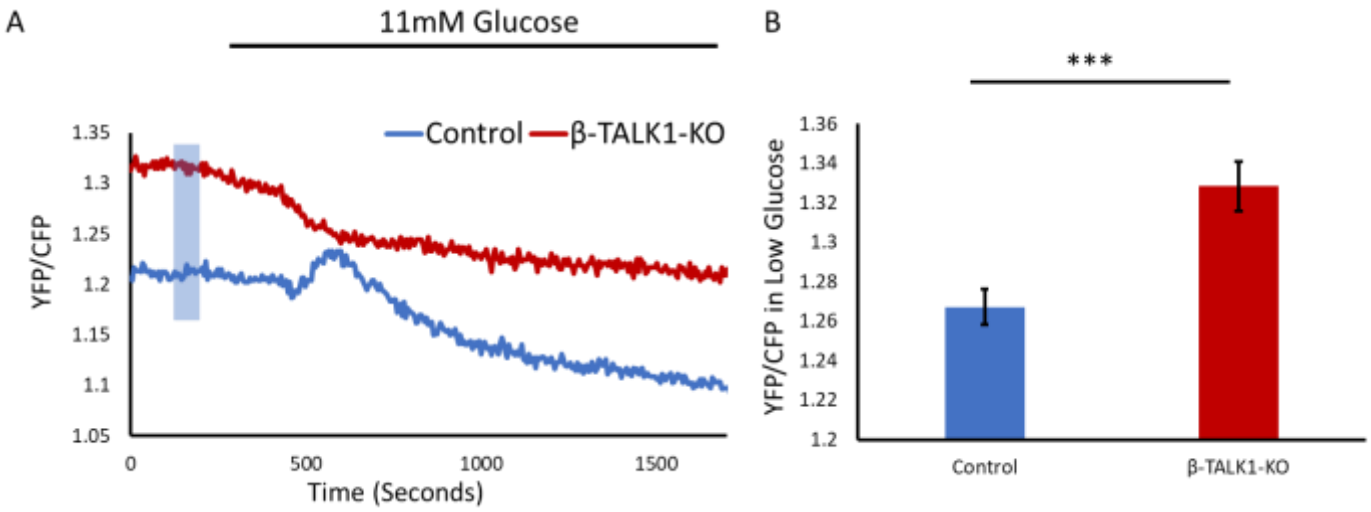

Figure 2.4. A lentivirus expressing a FRET-based mitochondrial Ca^{2+} indicator also shows increased basal mitochondrial Ca^{2+} in β-cells from β-TALK1-KO islets.

β-TALK1-KO and Control (fl/fl) islets were transduced with a lentivirus expressing a Fret based mitochondrial Ca^{2+} indicator expressed on a RIP promoter. Representative traces **(A)** and average responses from the highlighted portion **(B)**. Mean ± SEM; N = 51 control islet cells and N = 41 β-TALK1-KO islet cells.

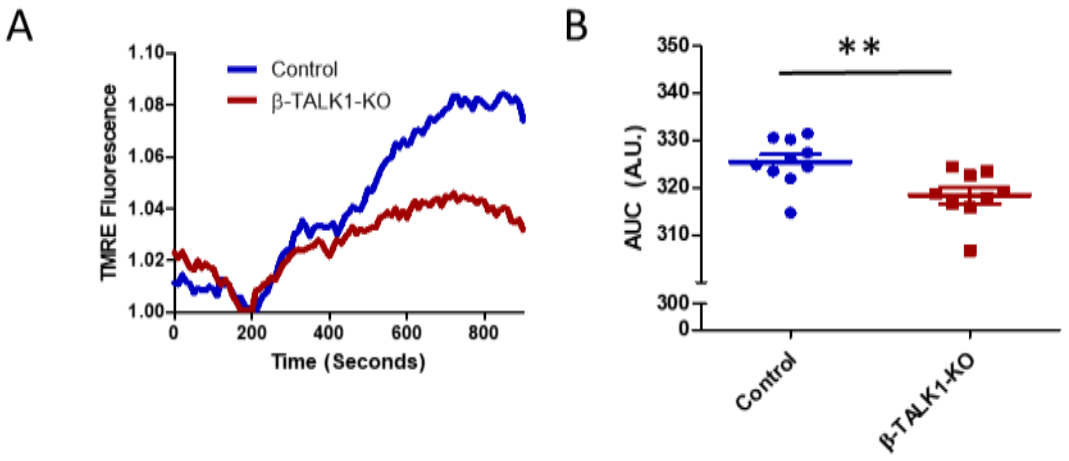

Figure 2.5. β-TALK1-KO mitochondria do not hyperpolarize in response to glucose as much as control.

β-TALK1-KO and control islets were loaded with TMRE and incubated in low glucose (3 mM). TMRE fluorescence was recorded while the islets were perfused with low glucose (3 mM) followed by high glucose (17mM). TMRE fluorescence was normalized to minimum fluorescence. Mean ± SEM. N = 10 β-TALK1-KO islets from 5 animals; N = 10 Control (fl/fl) islets from 5 animals. *P < 0.05

ATP production is increased with β-cell specific TALK-1 ablation

Glucose-stimulated $[Ca^{2+}]_{mito}$ influx activates mitochondrial dehydrogenases[166; 167] thereby stimulating mitochondrial respiration and ATP synthesis[166; 168; 169]. Therefore, we wanted to investigate whether the increased $[Ca^{2+}]_{mito}$ seen in β-TALK-1 KO islets affected mitochondrial metabolism. To accomplish this, we utilized a Seahorse XFE96 with an Agilent Seahorse XFe96 Spheroid Microplate[170] to measure oxygen consumption rate (OCR) in β-TALK-1 KO islets compared to control (fl/fl) islets on either a chow or HFD diet (Figure 2.6A and B). The Agilent Seahorse Cell Mito Stress Test kit, which is a well-accepted standard for measuring mitochondrial function, was used to add glucose (20mM), oligomycin (4.5 μM), FCCP (1 μM), and Rotenone/AA (2.5 μM) at different assay timepoints. On a regular chow diet, β-TALK1-KO islets showed increased ATP production compared to control islets (fl/fl) (Figure 2.6C). Interestingly, there was no difference in β-TALK1-KO and control (fl/fl) on a HFD, presumably because the control (fl/fl) islets had to increase their ATP production in response to the HFD while the β-TALK1-KO islets already had increased ATP production. (Figure 2.6C). Therefore, β-TALK1-KO islets produce just as much ATP on a chow diet as control (fl/fl) islets do on a HFD diet. This could indicate that mitochondria in the β-TALK1-KO islet are protected from the stress of the HFD initiation. There was no difference in glucose response, basal respiration, spare respiratory capacity, proton leak, or coupling efficiency between β-TALK1-KO and control (fl/fl) islets (Figure 2.6 D-H)

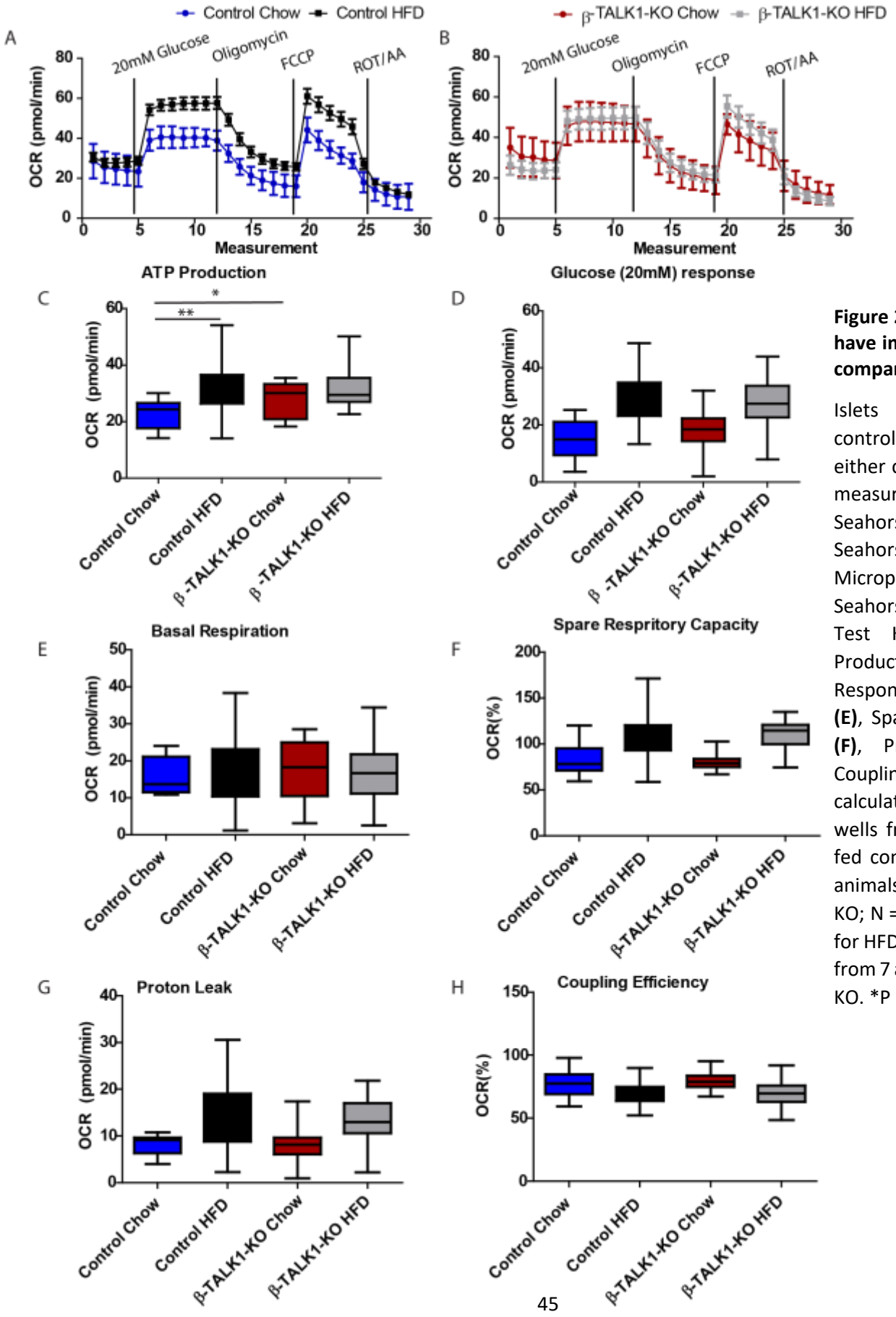

Figure 2.6. β-TALK1-KO animals have improved ATP production compared to control.

Islets from β-TALK1-KO and control mice that had been on either chow diet or a HFD were measured for OCR on a Seahorse XFE96 with an Agilent Seahorse XFe96 Spheroid Microplate and Agilent Seahorse XF Cell Mito Stress Test Kit **(A and B)**. ATP Production **(C)**, Glucose Response **(D)**, Basal Respiration **(E)**, Spare Respiratory Capacity **(F)**, Proton Leak **(G)**, and Coupling Efficiency **(H)** were all calculated. Mean ± SEM. N = 12 wells from 3 animals for chow fed control, N=16 wells from 3 animals for chow fed β-TALK1-KO; N = 38 wells from 4 animals for HFD fed control; N = 44 wells from 7 animals for HFD β-TALK1-KO. *P < 0.05 **P < 0.01

TALK-1 ablation specifically in β-cells regulates whole-body physiology

As β-TALK1-KO islets showed altered β-cell Ca^{2+} handling and mitochondrial function, we were interested in whether or not the whole-body glucose response was affected. Male β-TALK1-KO mice show improved glucose tolerance on a chow diet and an even further improvement when put on a HFD for only 2-weeks, (Figure 2.7A-D). Female β-TALK1-KO mice had improved glucose tolerance on both a chow diet and a HFD as well (Figure 2.7E-H). This indicates that TALK-1 regulation of β-cell Ca^{2+} handling and mitochondrial function improves whole-body glucose tolerance; especially under conditions of increased insulin demand such as a HFD.

As indicated with the GTT zero timepoints (Figure 2.7A,C,E,G), there was no difference in fasting blood glucose between the β-TALK1-KO and control mice. This is in contrast to the global TALK-1 KO mice which showed improved fasting blood glucose levels. This indicates that TALK-1 regulation of fasting blood glucose is not a β-cell intrinsic mechanism and instead could be due to another islet cell, such as the α-cell. The reduced glucagon secretion seen in the global TALK-1 KO mice[171] may be responsible for regulation of fasting blood glucose (described in more detail in chapter V)[79].

Furthermore, β-TALK1-KO mice showed no difference in weight gain on a HFD compared to control (Figure 2.8). This is again in contrast to the global TALK-1 KO mouse which showed reduced weight gain compared to WT. This indicates that TLAK-1 regulation of weight gain is not a β-cell intrinsic mechanism and instead could be due to another cell type that expresses TALK-1, such as the d-cells in the gut.

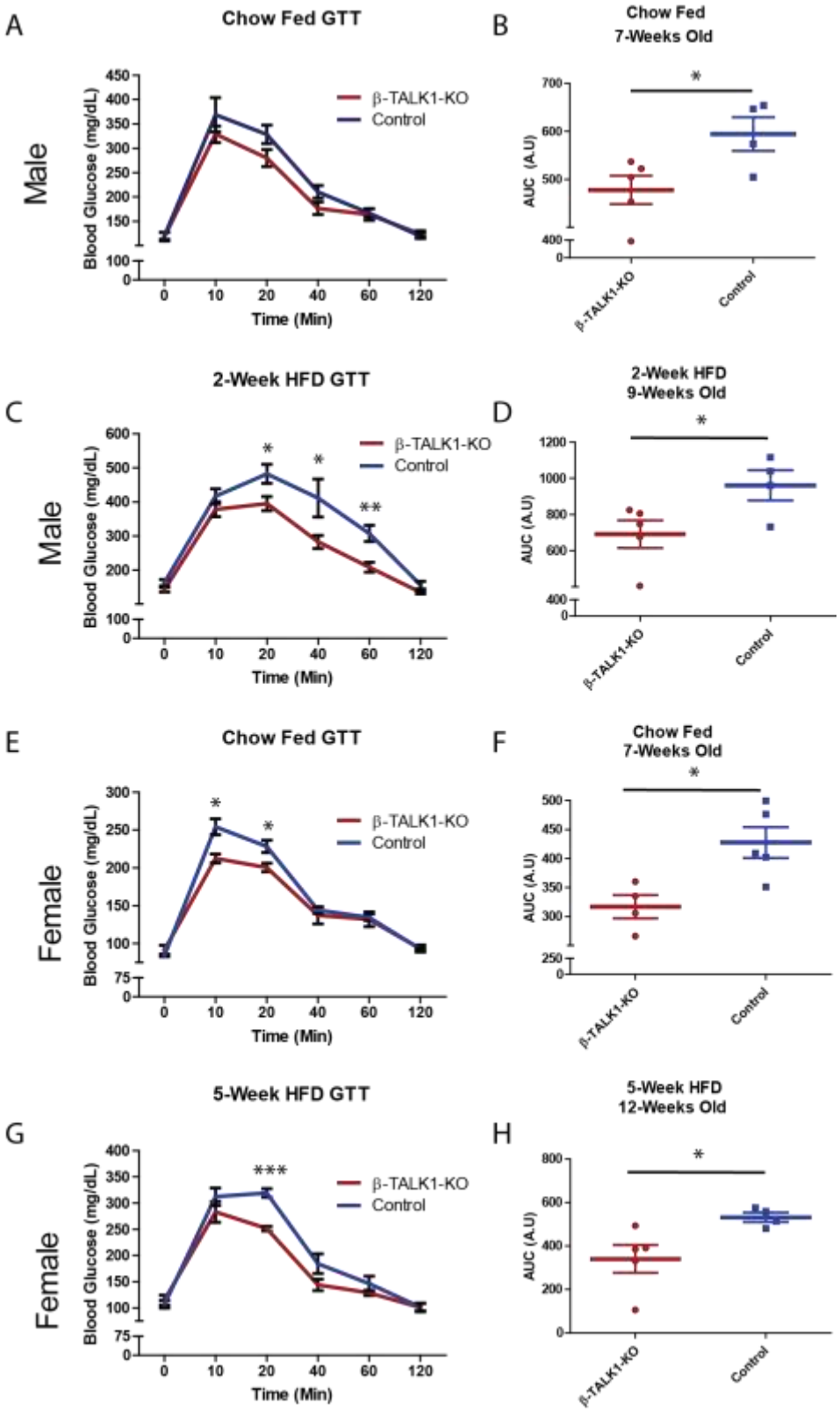

Figure 2.7. β-TALK1-KO animals have improved glucose tolerance compared to control.

β-TALK1-KO mice and control mice (fl/fl) were given an IP GTT (2mg of glucose per gram of body weight) both pre and post high fat diet (HFD). Pre- HFD male β-TALK1-KO mice showed a trend towards an increase in glucose tolerance **(A and B)** and significantly improved glucose tolerance 2-weeks post HFD **(C and D)**. Pre- HFD female β-TALK1-KO mice showed improved glucose tolerance both pre and post-HFD **(E-H)**. Mean ± SEM N = 5 male β-TALK1-KO mice; N = 4 male Control (fl/fl); N = 4 female β-TALK1-KO mice; N = 5 female Control (fl/fl) mice on chow and N = 5 female β-TALK1-KO mice; N = 4 female Control (fl/fl) mice on HFD mice. *P < 0.05 **P < 0.01 ***P < 0.001

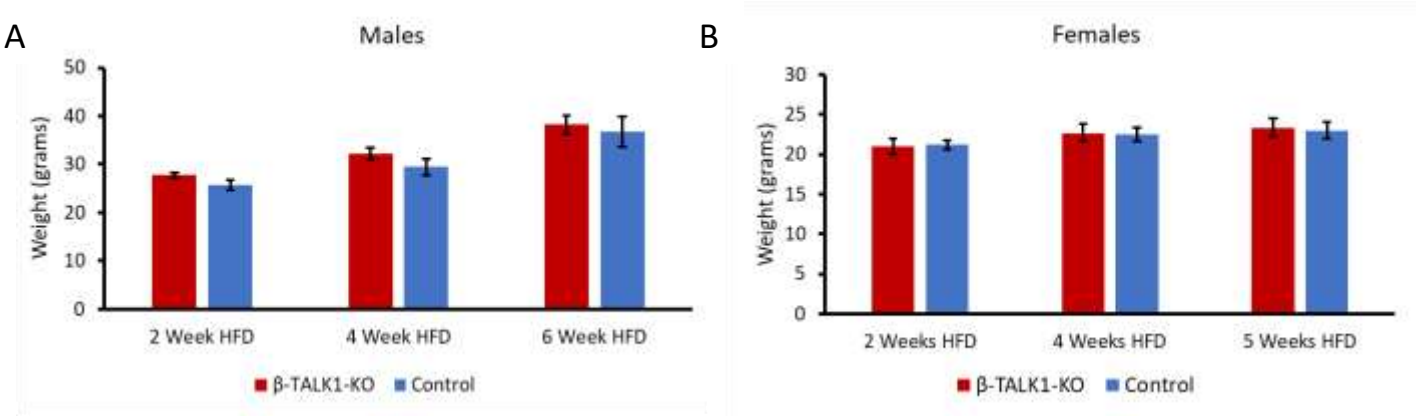

Figure 2.8. There is no difference in weight between the β-TALK1-KO and control animals on a HFD.

Male (A) and female (B) β-TALK1-KO and control mice (fl/fl) were weighed after the indicated amount of time on a HFD. Mean ± SEM N = 5 male β-TALK1-KO mice; N = 5 male Control (fl/fl); N = 5 female β-TALK1-KO mice; N = 5 female Control (fl/fl) mice.

Despite improving glucose tolerance, β-cell specific TALK-1 ablation reduces insulin secretion on a HFD

We next wanted to investigate whether or not this improved glucose tolerance was due to increased insulin secretion. Interestingly, after a HFD, β-TALK1-KO islets showed reduced insulin secretion compared to control (fl/fl) (Figure 2.9A). Further, both global TALK-1 KO mice (data generated by Dr. Nicholas Vierra) and β-TALK1-KO mice showed reduced serum insulin compared to control after an IP injection of 2 mg/g dextrose in PBS (Figure 2.9B and D). This interesting finding led us to investigate whether this could be explained by changes in insulin sensitivity upon a HFD with TALK-1 ablation. Interestingly there was no difference in insulin tolerance in either global TALK-1 KO mice (data generated by Dr. Nicholas Vierra) or β-TALK1-KO mice compared to control (Figure 2.9C and E). This indicates that even though insulin secretion is reduced, and insulin sensitivity is unchanged, somehow TALK-1 ablation still improves glucose tolerance on a HFD. One possible explanation for this is a change in insulin pulsatility. Dr. Peter Butler's group showed that β-TALK1-KO mice show increased we decided to look at liver insulin sensitivity with TALK-1 ablation. Global TALK-1 KO (data generated by Dr. Nicholas Vierra) islets have increased levels of pAKT in response to insulin compared to control (Figure 2.9F), indicating that TALK-1 is somehow regulating liver insulin sensitivity

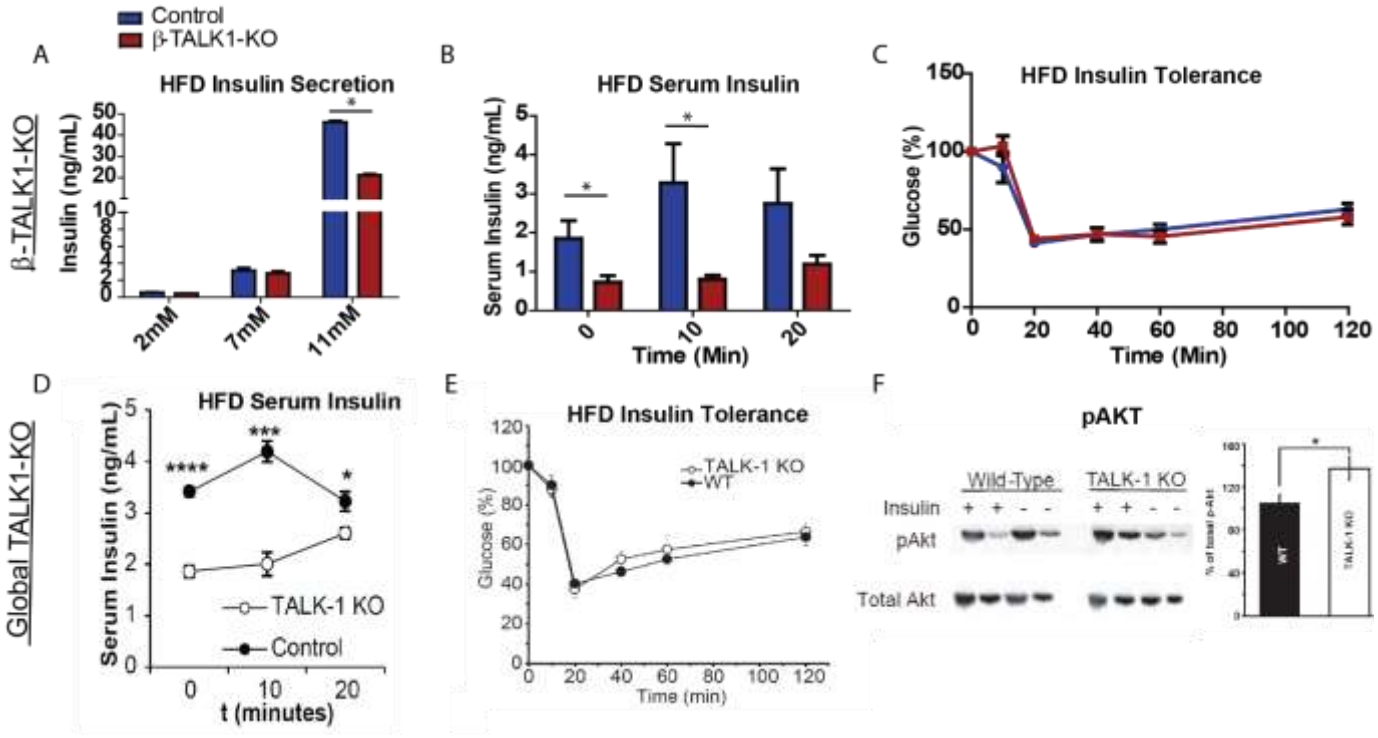

Figure 2.9. Global TALK-1 KO and β-TALK1-KO animals have reduced serum insulin compare to control.

β-TALK1-KO mice **(A)** or global TALK-1 KO mice **(D)** were given an IP GTT (2mg of glucose per gram of body weight) and then serum insulin was measured at the indicated time points. Islets from β-TALK1-KO mice were isolated and insulin was measured in response to differing glucose levels **(B)**. β-TALK1-KO **(C)** or global TALK-1 KO mice **(E)** were given an IP ITT (0.75U/kg body weight) and blood glucose was measured at the indicated time points. Phosphorylated and total AKT were measured by western blow in global TALK-1 KO mice **(F)**. Mean ± SEM. *P < 0.05 **P < 0.01 ***P < 0.001

Discussion

The K2P channel TALK-1 hyperpolarizes the β-cell V_m and limits GSIS[79]. In addition to being expressed in β-cells, TALK-1 is also expressed in δ-cells where it regulates somatostatin secretion and therefore α-cell glucagon secretion[108]. The results presented here demonstrate the role of β-cell TALK-1 in regulating mitochondrial function and peripheral insulin delivery.

Glucose stimulation causes β-cell V_m depolarization and action potential firing. Action potentials are not continuous, instead the β-cell displays bursts of electrical excitability separated by hyperpolarized silent phases[46] that are initiated by K^+ current through K_{ATP}, K_{slow}[61; 62], and TALK-1[61; 62; 65; 79]. Electrical oscillations result in $[Ca^{2+}]_c$ oscillations and pulsatile insulin secretion[173]. Glucose-stimulated $[Ca^{2+}]_c$ oscillations are also modulated by $[Ca^{2+}]_{ER}$ handling. SERCA pumps Ca^{2+} across its concentration gradient and into the ER thereby increasing $[Ca^{2+}]_{ER}$ stores. When the β-cell depolarizes, the ER buffers $[Ca^{2+}]_c$ influx by taking up Ca^{2+} through SERCA pumps. At the end of each Ca^{2+} oscillation, the ER releases Ca^{2+} [46]. This Ca^{2+} release modulates $[Ca^{2+}]_c$ oscillations and stimulates the Ca^{2+} activated K_{slow} current that contributes to the termination of β-cell action potentials. In human islets, KCNK16, the gene that encodes TALK-1 is the most highly expressed K^+ channel transcript. A global TALK-1 KO model showed that TALK-1 regulates $[Ca^{2+}]_c$ through the release of $[Ca^{2+}]_{ER}$ and the subsequent regulation of K_{slow}[65; 79]. However, the Global TALK-1 KO also demonstrated increased somatostatin secretion. As somatostatin is known to regulate insulin pulsatility, a β-cell specific TALK-1 KO was required. Here we show that β-cell specific TALK-1 KO (β-TALK1-KO) islets have increased $[Ca^{2+}]_c$

oscillation frequency, indicating that β-cell TALK-1 current provides a hyperpolarizing influence that can control whole islet $[Ca^{2+}]_c$ oscillations.

Mitochondrial Ca^{2+} handling is critical for respiration and ATP production. Under basal conditions, $[Ca^{2+}]_{mito}$ is similar to $[Ca^{2+}]_c$, but upon depolarization $[Ca^{2+}]_{mito}$ increases up to 70 μM[56]. This $[Ca^{2+}]_{mito}$ influx occurs through the mitochondrial Ca^{2+} uniporter (MCU) and is critical for dehydrogenase activation and subsequent mitochondrial respiration. Indeed, β-cell mitochondrial ATP levels have been shown to be dependent on $[Ca^{2+}]_c$ levels and to oscillate out-of-phase with electrical oscillations[57; 58]. $[Ca^{2+}]_{mito}$ uptake through the MCU is balanced by the mitochondrial Na^+/ Ca^{2+} exchanger (NCLX) which becomes activated after cell depolarization resulting in mitochondrial Na^+ uptake and $[Ca^{2+}]_{mito}$ release[163]. Indeed, after the initial $[Ca^{2+}]_{mito}$ increase, we show that β-cell depolarization results in a subsequent $[Ca^{2+}]_{mito}$ drop (Figure 2.3), presumably due to the activation NCLX. Importantly, the frequency of β-cell $[Ca^{2+}]_c$ oscillations can control the amplitude of glucose-stimulated $[Ca^{2+}]_{mito}$ influx[56]. Indeed, as described above, β-TALK1-KO islets have increased $[Ca^{2+}]_c$ oscillation frequency and we show that β-TALK1-KO islets also have increased $[Ca^{2+}]_{mito}$. This suggests that TALK-1 regulation of $[Ca^{2+}]_c$ also regulates $[Ca^{2+}]_{mito}$ dynamics.

In addition to being regulated by $[Ca^{2+}]_c$, $[Ca^{2+}]_{mito}$ is also tightly associated with $[Ca^{2+}]_{ER}$. A close contact, known as the mitochondrial associated membrane (MAM), occurs between the membranes of the ER and the mitochondria and is crucial to Ca^{2+} transmission between the two. At the MAM, Ca^{2+} is released at high concentrations from the ER through IP_3R and then immediately taken up by MCU on the mitochondrial membrane. The MCU has a low affinity for Ca^{2+}, so it is predicted that the high

concentration of Ca^{2+} found at the MAM is critical for MCU Ca^{2+} uptake[59]. As previously described, TALK-1 KO islets have increased $[Ca^{2+}]_{ER}$ presumably due to a reduced K^+ counter-current[65]. Increased $[Ca^{2+}]_{ER}$ would be predicted to provide more Ca^{2+} for Ca^{2+} release at the MAM. As $[Ca^{2+}]_{ER}$ is kept relatively high at all glucose concentrations, this could explain why we see increased $[Ca^{2+}]_{mito}$ in β-TALK1-KO islets at both high and low glucose.

β-TALK1-KO islets, which show increased basal $[Ca^{2+}]_{mito}$, also show increased ATP production in high-glucose. This indicates that TALK-1 regulation of β-cell $[Ca^{2+}]_{mito}$ regulates mitochondrial function and islet ATP synthesis. It has also been shown that cytosolic ATP levels drop during β-cell activation, possibly due to increased ATP hydrolysis by SERCA and PMCA[58]. As β-TALK1-KO islets have increased $[Ca^{2+}]_c$ oscillations, it is possible that they also have increased PMCA and SERCA activity thereby requiring more ATP production.

Increased $[Ca^{2+}]_c$ oscillations, increased $[Ca^{2+}]_{ER}$ stores, and increased ATP production are all predicted to increase β-cell insulin secretion and improve glucose tolerance. Indeed, on a HFD, β-TALK1-KO mice have improved glucose tolerance. However, β-TALK1-KO islets show reduced insulin secretion while maintaining improved glucose tolerance. One explanation for this is altered insulin action.

In fact, before being delivered to the peripheral tissues, insulin first reaches the liver where 40-80% of secreted insulin is cleared[174]. The mass of the insulin pulse that signals at the liver can determine the amount of hepatic insulin clearance that occurs[175]. Furthermore, Dr. Peter Butler's group showed that Specifically, when the pulsatile pattern of insulin secretion is disrupted, hepatic insulin receptor substrate (IRS)-1 and IRS-2 signaling is

delayed, along with activation of downstream insulin signaling effector molecules[172]. This also results in decreased expression of glucokinase[172]. β-TALK1-KO mice show increased we decided to look at the effect of TALK-1 ablation on liver insulin sensitivity. Indeed, TALK-1 ablation increases liver pAKT in response to insulin (Figure 2.9F), suggesting that TALK-1 may regulate liver insulin signaling.

Therefore, it is possible that TALK-1 regulation of β-cell $[Ca^{2+}]_c$ oscillations and pulsatile insulin secretion modulates the amount of insulin being cleared by the liver thereby lowering the amount of insulin that β-cells need to secrete. Furthermore, an adequate insulin pulse frequency is required for inhibition of endogenous glucose production[176]. Therefore, it is possible that TALK-1 regulation of pulsatile insulin secretion results in β-TALK1-KO mice having reduced hepatic glucose production. Together, this can lead to improved β-cell health and improved glucose tolerance.

In summary, our findings demonstrate that β-cell TALK-1 current slows $[Ca^{2+}]_c$ oscillation frequency, reduces β-cell $[Ca^{2+}]_{ER}$ storage and β-cell $[Ca^{2+}]_{mito}$ leading to reduced mitochondrial ATP production. Together this modulates β-cell insulin secretion and glucose tolerance. Importantly, this chapter also identifies for the first time that β-cell TALK-1 channels may regulate peripheral insulin action under diabetic conditions. Thus, these findings have implications for how the GOF single nucleotide polymorphism in *KCNK16* (rs1535500) results in an increased risk for developing T2DM. Furthermore, these findings suggest that TALK-1 could be an important, β-cell specific, target for treating β-cell dysfunction and improving insulin sensitivity in T2DM.

Chapter III

A *KCNK16* mutation causing TALK-1 gain-of-function is associated with maturity-onset diabetes of the Young

Abstract

Maturity-onset diabetes of the young (MODY) is a heterogeneous group of monogenic disorders of impaired glucose-stimulated insulin secretion (GSIS). Mechanisms include β-cell K_{ATP} channel dysfunction (e.g., *KCNJ11* (MODY13) or *ABCC8* (MODY12) mutations); however, no other β-cell channelopathies have been identified in MODY. Our collaborators identified a novel non-synonymous genetic mutation in *KCNK16* (NM_001135105: c.341T>C, p.Leu114Pro) segregating with MODY. *KCNK16* is the most abundant and β-cell-restricted K^+ channel transcript and encodes the two-pore-domain K^+ channel TALK-1. Whole-cell K^+ currents in transfected HEK293 cells demonstrated drastic (312-fold increase) gain-of-function with TALK-1 Leu114Pro vs. WT, due to greater single channel activity. Glucose-stimulated cytosolic Ca^{2+} influx was inhibited in mouse islets expressing TALK-1 Leu114Pro (area under the curve [AUC] at 20 mM glucose: Leu114Pro 60.1 vs. WT 89.1; $P = 0.030$) and less endoplasmic reticulum calcium storage (cyclopiazonic acid-induced release AUC: Leu114Pro 17.5 vs. WT 46.8; $P = 0.008$). TALK-1 Leu114Pro significantly blunted GSIS compared to TALK-1 WT in both mouse (52% decrease, $P = 0.039$) and human (38% decrease, $P = 0.019$) islets. Our data identify a novel MODY-associated gene, *KCNK16*; with a gain-of-function mutation limiting Ca^{2+} influx and GSIS. A gain-of-function common polymorphism in *KCNK16* is associated with type 2 diabetes (T2DM); thus, our findings have therapeutic implications not only for *KCNK16*-associated MODY but also for T2DM.

Introduction

Maturity-onset diabetes of the young (MODY) is a rare monogenic cause of familial diabetes. To date, 13 possible MODY genes have been identified, all involved in pancreatic β-cell insulin secretion and with autosomal dominant transmission[147]. 2-2.5% of pediatric diabetes cases carry pathogenic/likely pathogenic variants in MODY genes[151; 152]; however, MODY is often undiagnosed, either because the diagnosis is not considered[153] or because genetic screening is limited. There are also cases with compelling clinical histories in whom, despite comprehensive screening of known MODY genes, a genetic diagnosis cannot be made[152], suggesting as-yet-unidentified genetic cause(s).

β-cell glucose-stimulated insulin secretion (GSIS) is dependent on Ca^{2+} influx, through voltage-dependent calcium channels (VDCC)[177; 178]. Reduced Ca^{2+} influx decreases GSIS; thus, mutations that disrupt β-cell Ca^{2+} entry can cause MODY or the closely-related condition neonatal diabetes[179; 180]. For example, gain-of-function mutations in KATP channel subunits hyperpolarize the β-cell membrane potential, reducing VDCC activity, Ca2+ influx and GSIS[179; 181]. Other β-cell K^+ channels, including two-pore domain K^+ channels (K2P), also affect VDCC activity[79]. Expression of *KCNK16*, which encodes TWIK-related alkaline pH-activated K2P-1 (TALK-1)[92], is the most abundant and β-cell-selective of all human K^+ channel transcripts[182; 183]; and TALK-1 gain-of-function mutations would be predicted to cause diabetes similarly[79].

Here we have used exome sequencing to identify the first family with MODY likely due to a mutation in *KCNK16*. The Leu114Pro substitution in TALK-1 sits near the K^+ selectivity filter, causing a profound increase in K^+ current, altering β-cell Ca^{2+} flux, and decreasing GSIS in both human and mouse islet cells.

Results

Exome sequencing in a family with MODY identifies a novel variant in KCNK16

Exome sequencing and analysis of known MODY genes in the proband identified a splice site mutation in *ABCC8* (NM_000352 c.1332+4 delC); however, this variant was not predicted to affect splicing[184] and did not segregate appropriately in the pedigree.

Exome sequencing and analysis of the extended pedigree identified novel good-quality coding variants (with minor allele frequency (MAF) <0.05) in two genes, *KCNK16* and *USP42*, with appropriate segregation (Fig. 3.1A and 3.1B; coverage statistics for exome sequencing, Table 3.1; exome data filtering, Table 3.2). *USP42* (*Ubiquitin-specific peptidase 42*) is involved in spermatogenesis[185] and is not expressed in the pancreas; and was considered an unlikely MODY candidate. However, *KCNK16 (Potassium channel, subfamily K, member 16)* encodes for TALK-1, with its established role in GSIS[79]. Further, the *KCNK16*-containing locus is associated with T2DM[79]

The *KCNK16* variant *(*NM_001135105: c.341T>C) has not previously been reported in ExAC (http://exac.broadinstitute.org), 1000 Genomes (http://www.1000genomes.org), or dbSNP137 (http://www.ncbi.nlm.nih.gov/projects/SNP/) databases. It affects a highly conserved base (GERP score 5.65) with the resultant amino acid change (p.Leu114Pro)

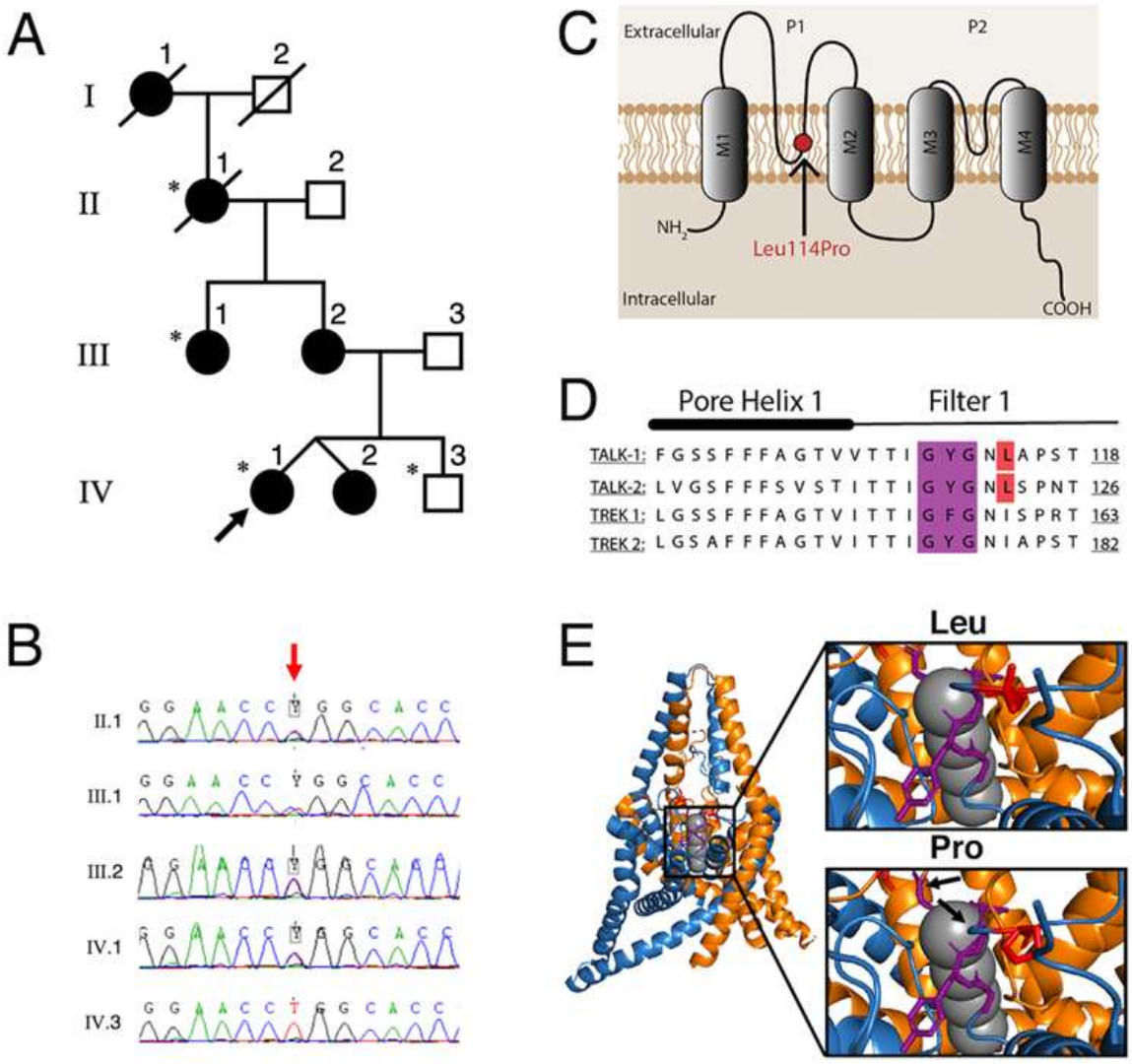

Figure 3.1: A novel *KCNK16* mutation co-segregates with MODY in a four-generation family and is predicted to affect the K^+-selectivity channel of TALK-1.

Family pedigree (Panel A: asterisks indicate individuals that underwent WES; filled-in shapes indicate individuals with diabetes; arrow indicates proband), with chromatogram of *KCNK16* variant (c.341T>C) (Panel B; red arrow indicates variant). Location of the predicted protein change (p.Leu114Pro), within the first pore domain and K^+-selectivity channel of TALK-1 (Panel C), with alignment of Pore Helix 1 and Filter 1 amino acid sequences of *KCNK16* with other KCNK channels (Panel D; mutation position indicated in red; selectivity filter indicated in purple). Predicted conformational shifts (indicated by the arrows) in the K^+ selectivity filter, modelled using TREK2 crystalline structure (Panel E).

.

Table 3.1 Coverage statistics for exome sequencing

-data generated by Dr. Emma Duncan and Dr. Stephanie Johnson at the University of Queensland

	MODY_II.1	MODY_III.1	MODY_IV.1	MODY_IV.3
Total bases	5835073129	5386986408	5187196181	1824158333
% bases on target exons	38.4	35.9	47.9	35.8
Target exon median base coverage	52.9	44.2	32.0	12.8
Target exon mean base coverage	64.4	53.5	37.6	14.2
% target exon bases with coverage >1x	98.2	98.6	91.0	95.5
% target exon bases with coverage >5x	93.6	94.5	94.4	90.4
% target exon bases with coverage >10x	88.0	88.7	79.2	80.1
% target exon bases with coverage >30x	65.9	63.0	54.6	59.9

Table 3.2: Bioinformatic filtering of identified variants

-data generated by Dr. Emma Duncan and Dr. Stephanie Johnson at the University of Queensland

Filtering steps	MODY-II.1*	MODY-III.1*	MODY-IV.1*	MODY-IV.3
Variants identified with MAF≤0.05	7114	7389	8368	7320
Remaining variants of potentially damaging consequence** of good quality after removal of platform-related artefact	659	639	434	(NA)
Heterozygous variants remaining with MAF <0.001	343	333	213	(NA)
Remaining variants segregating appropriately with observed autosomal dominant inheritance	13			
Remaining variants with high conservation (GERP >2.5)	6			
Remaining variants predicted to be damaging[#] ; MAF reported from ExAC	*KCNK16 (*NM_001135105) c.341T>C; p.Leu114Pro; MAF = 0 *USP42* (NM_032172) c.C3569G: p.Pro1190Arg; MAF=0 *KIAA1407* (NM_020817) c.2687G>A; p.Arg89Gln; MAF 0.00007 (rs144192553)			
Remaining variants in candidate genes known to be involved in insulin secretion	*KCNK16 (*NM_001135105) c.341T>C; p.Leu114Pro			

*affected individuals

**potentially damaging consequences defined as nonsynonymous single nucleotide variants (SNVs), splice site SNVs, frameshift substitution, stopgain or stoploss SNVs.

#Using protein prediction algorithms SIFT[7], Mutation Taster Human Splicing Finder v3.0[186] and PolyPhen2[187]

MAF: minor allele frequency. ExAC: Exome Aggregation Consortium. QC: quality control. GERP: genomic evolutionary rate profiling score.

predicted to involve the pore domain one of TALK-1, immediately downstream of the GYG K^+ selectivity filter (Fig. 3.1C). The GYG motif, and leucine 114 specifically, shows strong sequence homology with other K2P channels (Fig. 3.1D). As the crystal structure of TALK-1 is unpublished, TREK-2 was used to model the p.Leu114Pro mutation which demonstrated a conformational shift in both the GYG motif and pore domain (Fig. 3.1E), strongly suggesting that TALK-1 Leu114Pro would significantly affect K^+ permeability

Extended Clinical Data

The non-obese proband (individual IV.1) was diagnosed with antibody-negative diabetes age 15 years. Now age 32 years she only requires a maximum of 1-2 units of basal insulin to maintain an HbA1c 5.7-6.5%. She has not had ketosis or other diabetes-related complications. Sanger sequencing screening for mutations *GCK, HNF1A* and *HNF4A* was negative.

The proband's identical twin sister (individual IV.2) was diagnosed with diabetes contemporaneously with the proband. This individual is managed with multiple daily injections of insulin. She has never experienced ketosis or diabetes-related complications. Other clinical information for this individual is unavailable.

The proband's mother (individual III.2) and aunt (individual III.2), both of normal weight, presented aged 15 and 13 years respectively with antibody-negative diabetes. Neither has experienced ketosis or diabetes-related complications after many decades. The proband's mother requires 8-11 units isophane insulin daily, maintaining an HbA1c of 6-7%. Her aunt requires 9-10 units of mixed insulin (Mixtard® 30/70 mane), maintaining an HbA1c <6%.

The proband's maternal grandmother (individual II.1) was diagnosed with diabetes during pregnancy, aged 30 years. She required <10 units/day of basal insulin, maintaining an HbA1c 6-6.5%. She recently died aged 82 years, without experiencing ketosis or diabetes-related complications.

The proband's maternal great-grandmother (individual I.1) also had diabetes. Further details of this individual are not available.

The proband's brother (individual IV.3), currently aged 26 years, does not have diabetes.

TALK-1 Leu114Pro results in a gain-of-function

K^+ currents were recorded using HEK293 cells transfected with either TALK-1 WT or TALK-1 Leu114Pro followed by a P2A mCherry (Figure 3.2). Expression levels of the TALK-1 WT and TALK-1 Leu114Pro constructs were similar (Figure 3.3). TALK-1 Leu114Pro caused a massive (312-fold) increase in whole-cell K^+ currents compared to TALK-1 WT (current at −40mV: TALK-1 Leu114Pro 774.16 ± 218.75 pA vs. TALK-1 WT 2.48 ± 1.86 pA; Fig. 3.4A, 3.4B). Individual TALK-1 channel activity showed a 3.6-fold increase in current amplitude and a 2.9-fold increase in open probability at 100 mV for TALK-1 Leu114Pro compared to TALK-1 WT (Fig. 3.4C, 3.4D, 3.4E, 3.4F). Thus, TALK-1 Leu114Pro is a gain-of-function mutation, predicted to cause hyperpolarization of the β-cell membrane potential. The reversal potential for TALK-1 Leu114Pro currents (-79 mV) was near the equilibrium potential of K^+ (E_K) and the single channel currents also reversed near E_K. Thus, channels containing TALK-1 Leu114Pro subunits are likely still selective for K^+.

As this TALK-1 mutation causes MODY in a dominant manner, we also measured the TALK-1 current under heterozygous conditions by creating a TALK-1-WT-P2A-TALK-1-Leu114Pro construct which allows for equivalent expression of the TALK-1 WT and TALK-1 Leu114Pro subunits. Currents from HEK cells transduced with the TALK-1-WT-P2A-TALK-1-Leu114Pro construct displayed significant increases in TALK-1 currents (Fig 3.5- data generated by Dr. Matthew Dickerson) equivalent to cells expressing the TALK-1 Leu114Pro alone (Fig. 3.4). Therefore, heterodimeric TALK-1 channels with a Leu114Pro and WT version are likely to show significant gain-of-function, predicted to cause β-cell V_m hyperpolarization.

TALK-1 Leu114Pro inhibits glucose-stimulated β-cell depolarization.

Changes to TALK-1 K^+ current is predicted to modulate β-cell membrane potential. To monitor this, the glucose-stimulated membrane potential (V_m) of β-cells transduced with either TALK-1 WT or TALK-1 Leu114Pro was recorded. Glucose was ramped from 2 mM to 14 mM and then back to 2 mM glucose. While cells expressing TALK-1 WT depolarized and fired action potentials as expected, 10% of β-cells expressing TALK-1 Leu114pro demonstrated glucose-stimulated V_m depolarization but not action potential firing while 80% of β-cells expressing TALK-1 Leu114Pro neither depolarize nor fired action potentials in response to glucose (Fig 3.6A, 3.6C, 3.6D, 3.6E, 3.6F-data generated by Dr. Matthew Dickerson). This is presumably due to the large TALK-1 Leu114Pro K^+ conductance. However, 10% of the β-cells expressing TALK-1 Leu114Pro both depolarized and fired action potentials, demonstrating that while TALK-1 Leu114Pro

prevents glucose-stimulated action-potential firing in most β-cells, some β-cells are able to still

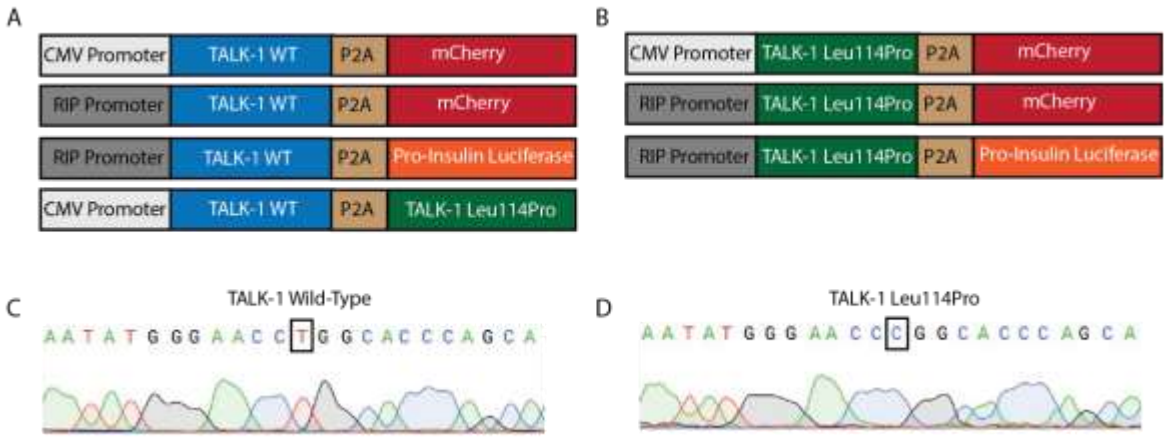

respond normally (Figure 3.6B).

Figure 3.2. Lentiviral plasmids designed for TALK-1 WT and TALK-1 Leu114Pro expression in HEK cells and β-cells.

Lentiviral Plasmids were designed with either a CMV promoter or a Rat-Insulin Promoter expressing TALK-1 followed by a P2A cleavage site and either mCherry (for electrophysiology a calcium experiments) or Pro-insulin Luciferase (For insulin secretion experiments). The TALK-1 cloned into these constructs were either Wild-Type (WT) **(Panel A)** or TALK-1 Leu114Pro **(Panel B).** Plasmids were sequenced and chromatograms show the correct TALK-1 WT **(Panel C)** and TALK-1 Leu114Pro **(Panel D)** sequences

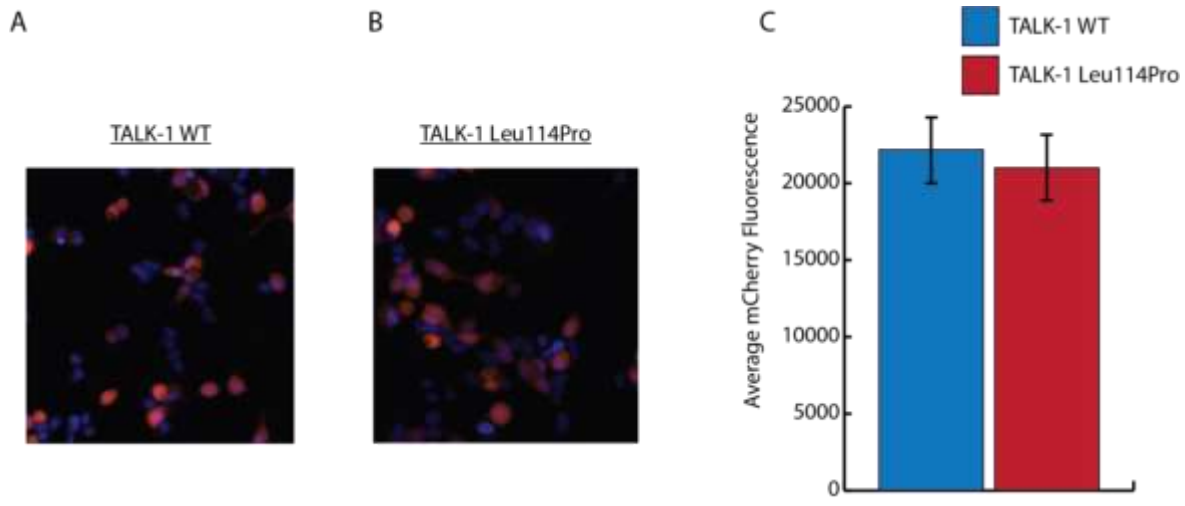

Figure 3.3. Expression of TALK-1 WT and TALK-1 Leu114Pro is similar in HEK cells for current recordings. HEK cells were transfected with constructs containing a CMV Promoter expressing TALK-1 followed by a P2A cleavage site and mCherry. TALK-1 expressing cells are represented by mCherry fluorescence (red) and all nuclei were stained with Hoescht (blue); cells expressing TALK-1 WT **(Panel A)** or TALK-1 Leu114Pro **(Panel B)** (images shown were taken at 20X magnification). Equivalent mCherry fluorescence in TALK-1 WT- and TALK-1 Leu114Pro-expressing cells indicates similar TALK-1 expression levels **(Panel C)** (N = 3 cells expressing TALK-1 WT; N = 26 cells expressing TALK-1 Leu114Pro).

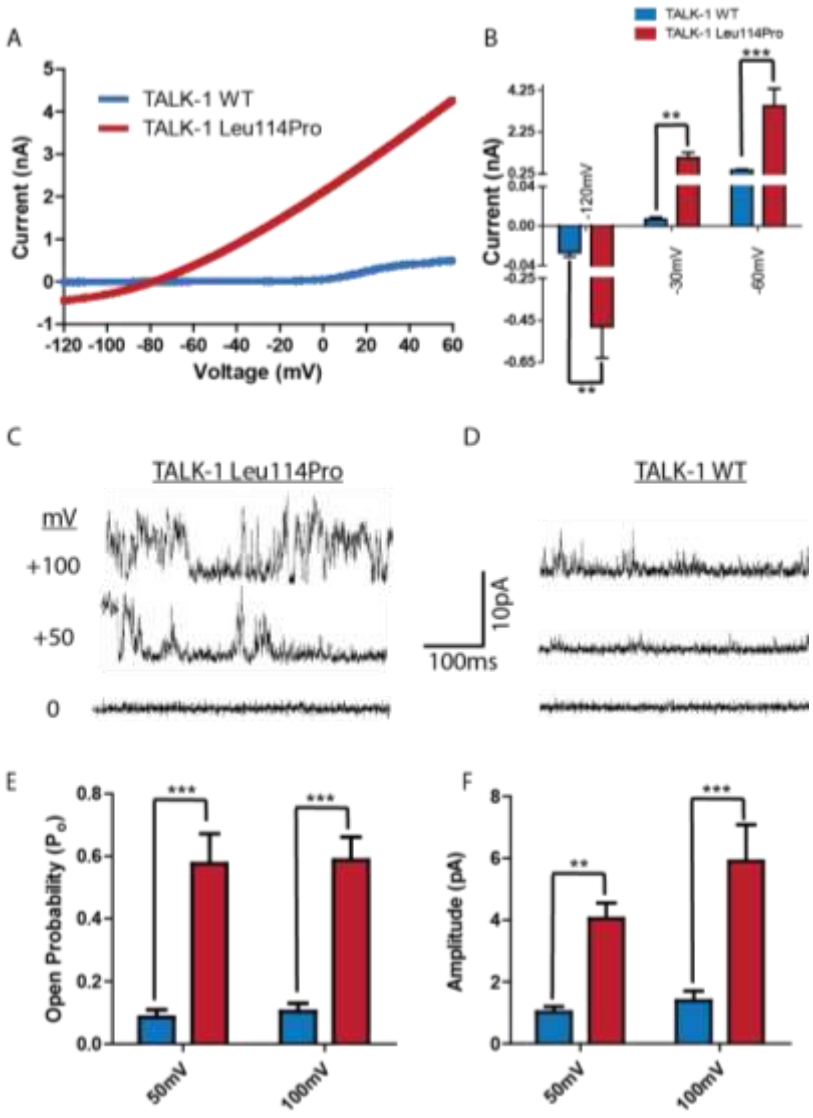

Figure 3.4: TALK-1 Leu114Pro causes a drastic gain-of-function in TALK-1 K^+ current.

K^+ currents monitored from HEK293 cells expressing TALK-1 WT or TALK-1 Leu114Pro with whole-cell voltage clamp recordings, in response to a voltage ramp from -120 mV to 60 mV (Panel A); mean ± SEM; N = 11 control cells; N = 10 TALK-1 Leu114Pro cells (Panel B). Single-channel plasma membrane K^+ currents monitored through TALK-1 Leu114Pro or TALK-1 WT with attached patch voltage clamp recordings, in response to the indicated voltage steps (Panel C and Panel D). Single channel recordings were analyzed for current amplitude (Panel E) and channel open probability (Panel F); mean ± SEM; N = 8 TALK-1 WT cells; N = 11 TALK-1 Leu114Pro cells $*P < 0.05$, $**P < 0.01$, $***P < 0.001$.

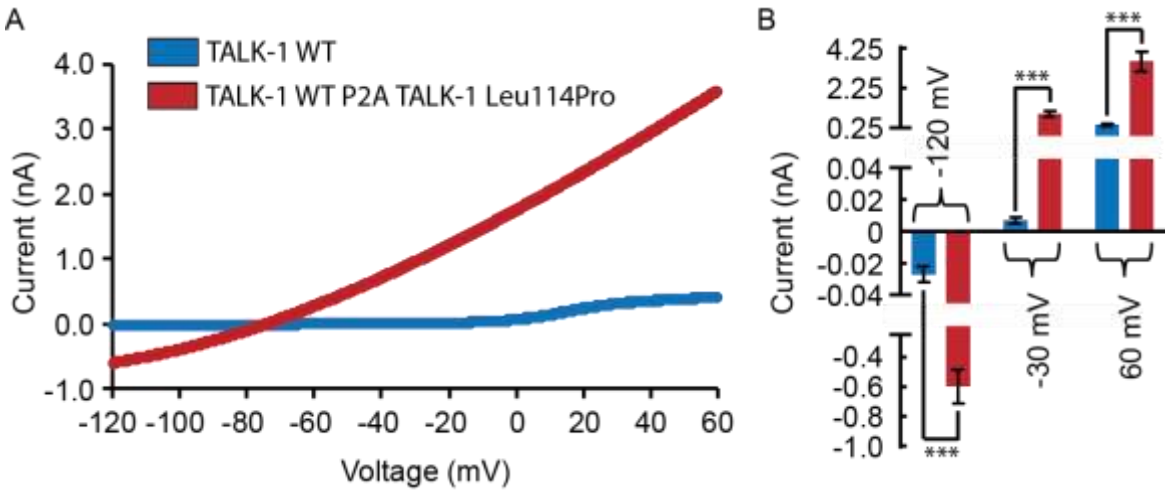

Figure 3.5: Average whole cell TALK-1 current recordings in HEK cells expressing TALK-1 WT P2A Leu114Pro construct vs. TALK-1 WT.

Average whole cell currents from TALK-1 WT P2A TALK-1 Leu114Pro expressing cells (in red) is dramatically greater than the K2P currents from cells expressing TALK-1 WT (in blue) (Panel A). The mean K2P current recorded at -120 mV, -30 mV, and 60 mV for cells expressing either TALK-1 WT (blue bars, N = 11) or TALK-1 WT P2A TALK-1 Leu114Pro (red bars, N = 15) ± SEM (Panel B).

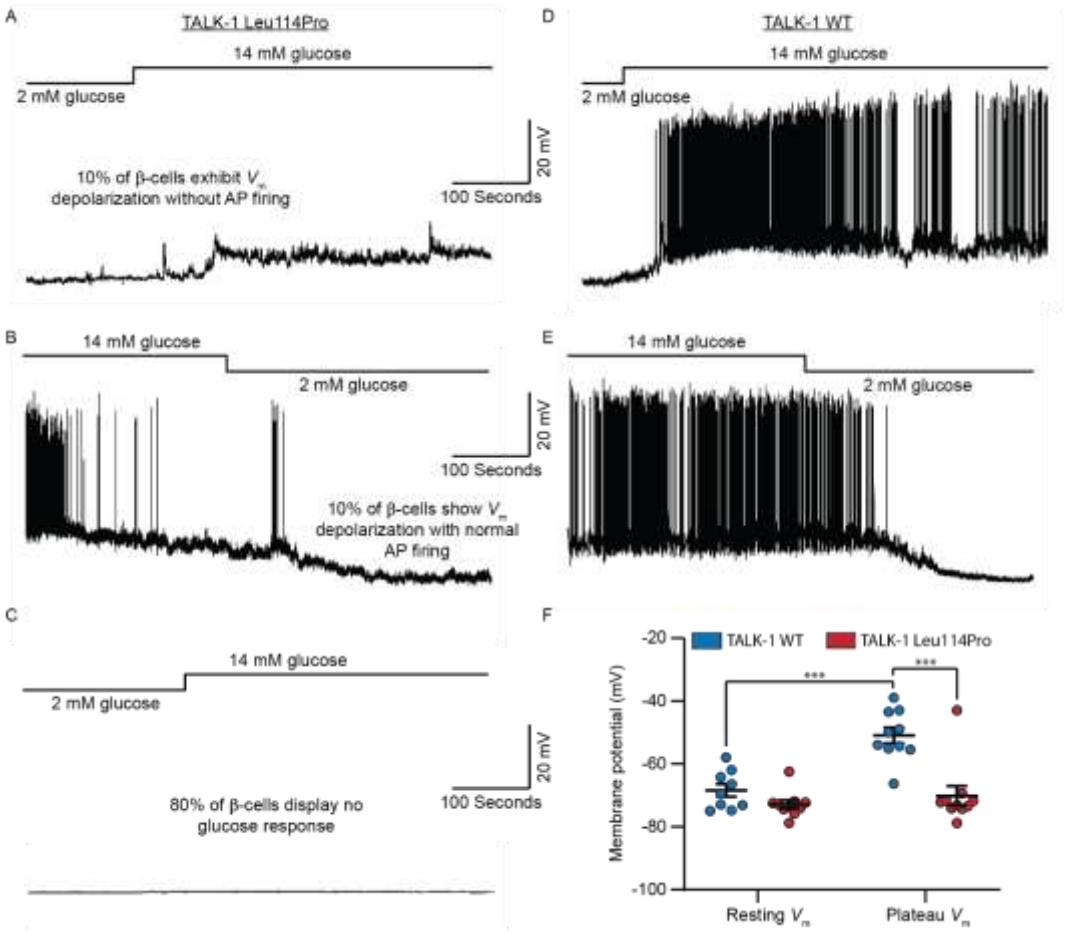

Figure 3.6: TALK-1 Leu114Pro hyperpolarizes the β-cell membrane and prevents action potential firing

V_m was monitored from β-cells transduced with either TALK-1 WT or TALK-1 Leu114Pro, in response to a 2 or 14 mM glucose as indicated in the figure. (Panel A, B, C, D). Average resting and plateau V_m were calculated for TALK-1 Leu114Pro and TALK-1 WT (Panel F) mean ± SEM; N = 15 control cells; N = 17 TALK-1 Leu114Pro cells *P < 0.05, **P < 0.01, ***P < 0.001**.**

TALK-1 Leu114Pro reduces β-cell Ca^{2+} influx and ER Ca^{2+} stores

Ca^{2+} handling was monitored in mouse β-cells following transduction of either TALK-1 WT or TALK-1 Leu114Pro followed by a P2A mCherry (Figure 3.2). Glucose-stimulated (20mM) β-cell Ca^{2+} influx was abolished by expression of TALK-1 Leu114Pro (Fig. 3.7A, 3.7C, and 3.7D). TALK-1 has been previously shown to modulate Ca^{2+}_{ER} homeostasis by providing a countercurrent for Ca^{2+}_{ER} release[65]; thus TALK-1 Leu114Pro control of Ca^{2+}_{ER} storage was also examined. Inhibition of SERCAs with CPA (50μM) resulted in significantly less Ca^{2+}_{ER} release in β-cells expressing TALK-1 Leu114Pro compared to TALK-1 WT (62.6% decrease; Fig. 3.7E, 3.7F- (data generated by Arya Nakhe) suggesting reduced Ca^{2+}_{ER} storage with TALK-1 Leu114Pro. β-cells expressing TALK-1 Leu114Pro also showed elevated basal [Ca^{2+}_{cyto}] compared to β-cells expressing TALK-1 WT (28.8% increase in AUC; Fig. 3.7A, 3.7B). Taken together, this suggests that under basal conditions, TALK-1 Leu114Pro enhances Ca^{2+}_{ER} leak, thereby increasing basal [Ca^{2+}_{cyto}]. Furthermore, the usual transient drop in β-cell [Ca^{2+}_{cyto}] following glucose stimulation of Ca^{2+}_{ER} uptake (termed phase-0) was amplified with TALK-1 Leu114Pro compared to TALK-1 WT. These changes would be predicted to diminish GSIS.

TALK-1 Leu114Pro reduces glucose-stimulated insulin secretion

To monitor insulin secretion specifically from β-cells transduced with either TALK-1 WT or TALK-1 Leu114Pro, we first employed viral constructs containing a p2A pro-insulin luciferase reporter where the insulin C-peptide has been replaced with luciferase (Figure 3.2), β-cells expressing TALK-1 Leu114Pro showed comparable basal (5 mM glucose)

insulin secretion but reduced GSIS (14 mM glucose) compared to TALK-1 WT, in both mouse (52% decrease in GSIS) and human (38% decrease in GSIS) islets (Figure 3.7). This reduction cannot be attributed to difference in construct expression, as expression levels were identical between the TALK-1 WT and TALK-1 Leu114Pro constructs (Figure 3.8). Transduction efficiency was also similar between the two constructs, approxixmately 55% for TALK-1 WT and 61% for TALK1 Leu114Pro.

However, this pro-insulin luciferase plasmid is not the standard for measuring insulin secretion; therefore, we also measured insulin secretion from mouse islets using a standard radioimmunoassay. Similar to the pro-insulin luciferase assay, islets expressing TALK-1 Leu114Pro had reduced GSIS compared to TALK-1 WT (Figure 3.9A). These changes in insulin secretion were not due to changes in total β-cell insulin content, which were equivalent in mouse islets expressing either TALK-1 Leu114Pro or TALK-1 WT (Fig. 3.9B).

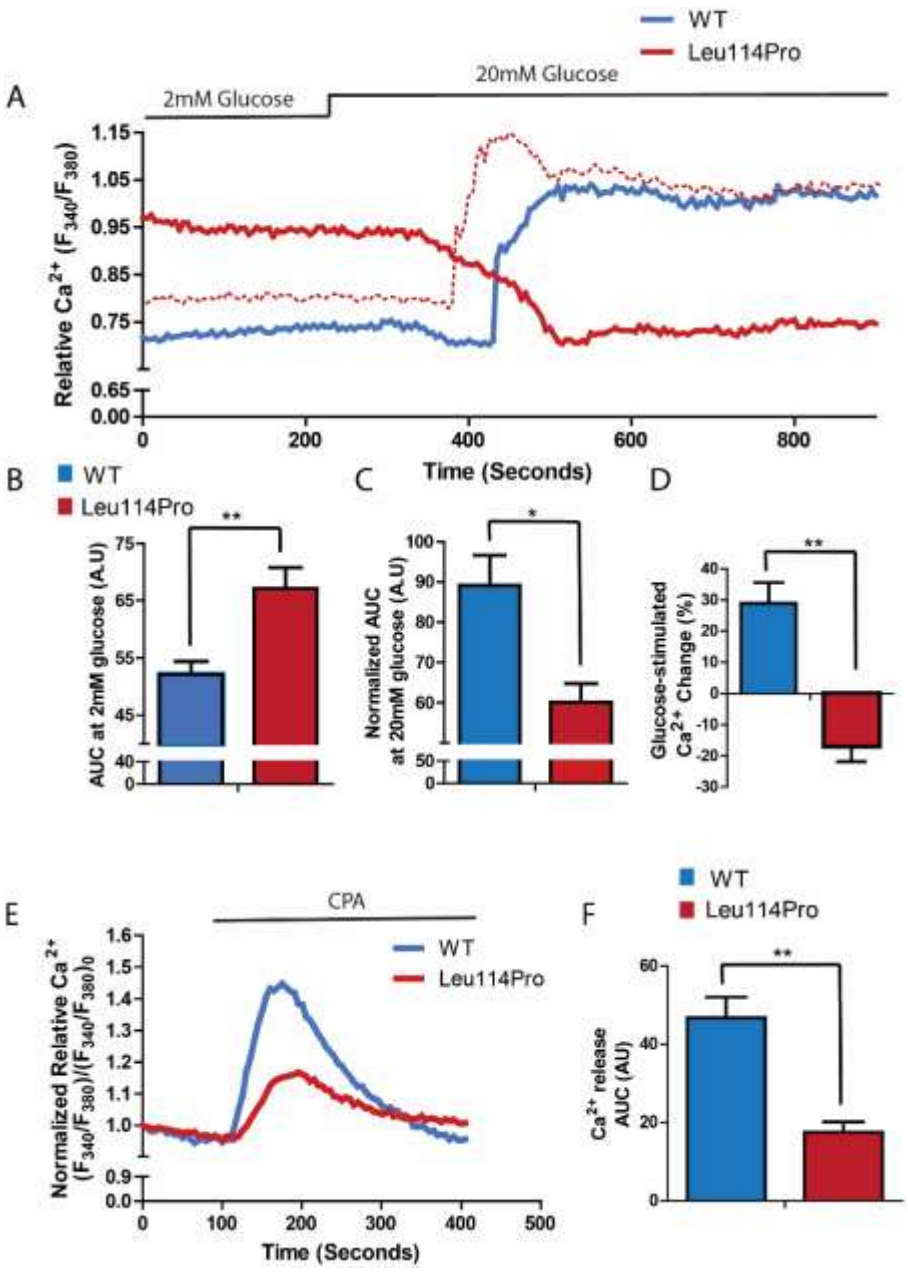

Figure 3.7: TALK-1 Leu114Pro modulates β-cell Ca^{2+} homeostasis.

Representative β-cell Ca^{2+} measurements in response to 2 mM and 20 mM glucose (Panel A). Area under the curve (AUC) analysis of β-cell Ca^{2+} under low (2 mM) glucose (Panel B) and high (20 mM) glucose conditions (Panel C). AUC percent change from low glucose to high glucose (Panel D). Representative β-cell Ca^{2+} measurements in response to [Ca^{2+}_{ER}] depletion by CPA (Panel E) and the AUC analysis of the CPA response (Panel F). mean ± SEM; N = 3 animals for TALK-1 WT and TALK-1 Leu114Pro Ca^{2+} experiments except the for the 2 mM condition that included N = 9 animals. **P* < 0.05, ***P* < 0.01, ****P* < 0.001.

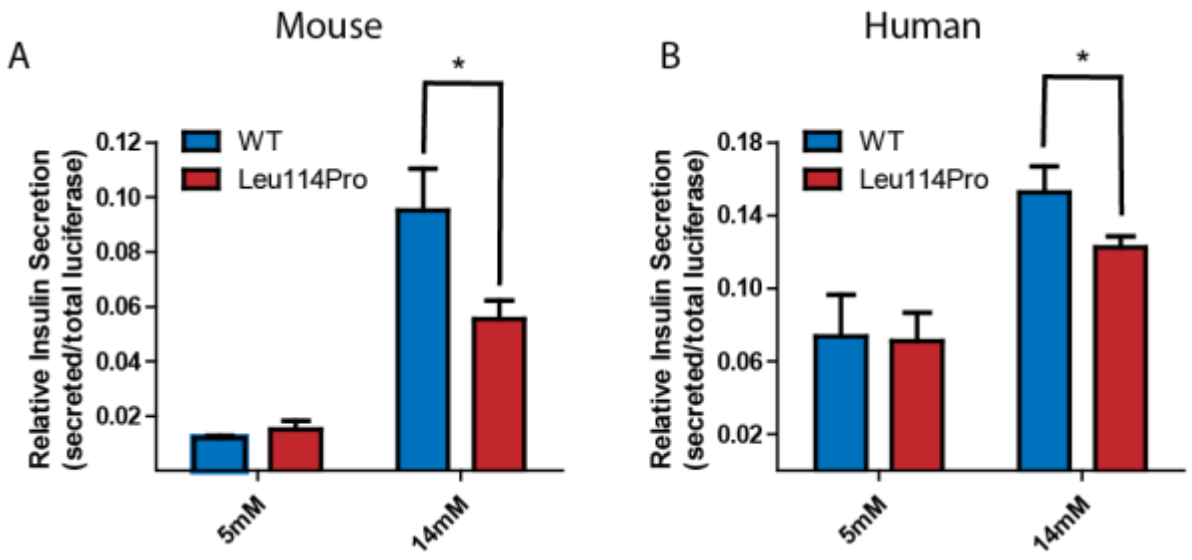

Figure 3.8: TALK-1 Leu114Pro reduces glucose-stimulated insulin secretion.

Mouse (Panel A) and human (Panel B) islets transduced with viruses selectively expressing either TALK-1 WT or TALK-1 Leu114Pro and the NanoLuc-proinsulin luciferase insulin reporter. Islets were monitored for total secreted luciferase following exposure to 5 mM or 14 mM glucose; mean ± SEM; N=6 animals (14 mM glucose, Panel A), N = 3 animals (5 mM glucose, Panel A); N = 8 Human Donors (14 mM glucose, Panel B), N = 5 Human Donors (5 mM glucose, Panel B). *$P < 0.05$

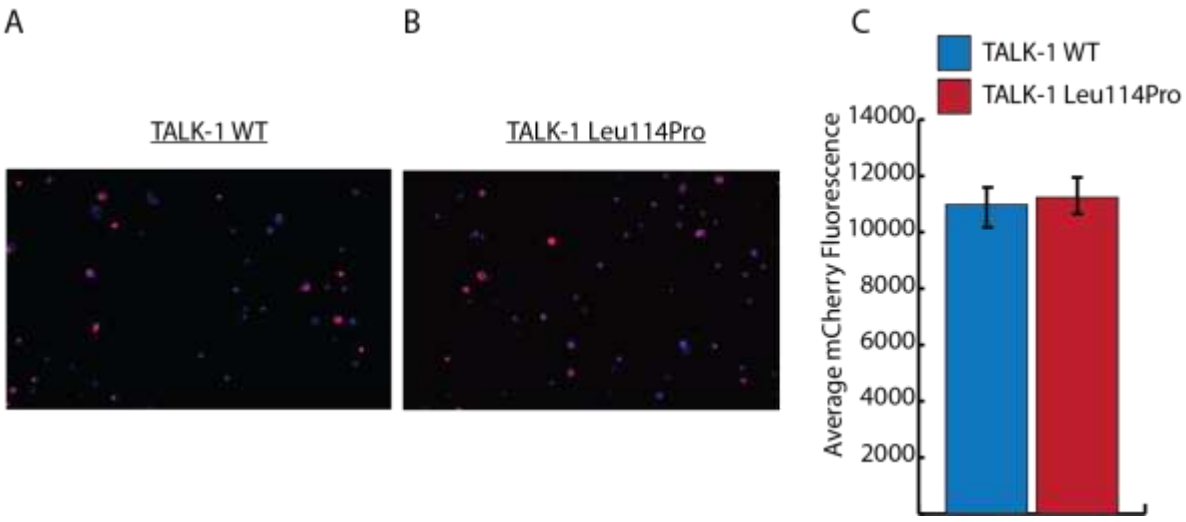

Figure 3.9. Expression of TALK-1 WT and TALK-1 Leu114Pro is similar in mouse β-cells.

Dispersed islet cells were transduced with the viruses containing a Rat-Insulin Promoter expressing TALK-1 followed by a P2A cleavage site and mCherry. TALK-1 expressing β-cells (shown in red) imaged with a 10X objective compared to total islet cells (nuclei stained with Hoescht (marked in blue)) for TALK-1 WT **(Panel A)** and TALK-1 Leu114Pro **(Panel B)**. Average mCherry fluorescence shows similar expression levels between TALK-1 WT and TALK-1 Leu114Pro **(Panel C)** (N = 48 cells expressing TALK-1 WT; N = 42 cells expressing TALK-1 Leu114Pro).

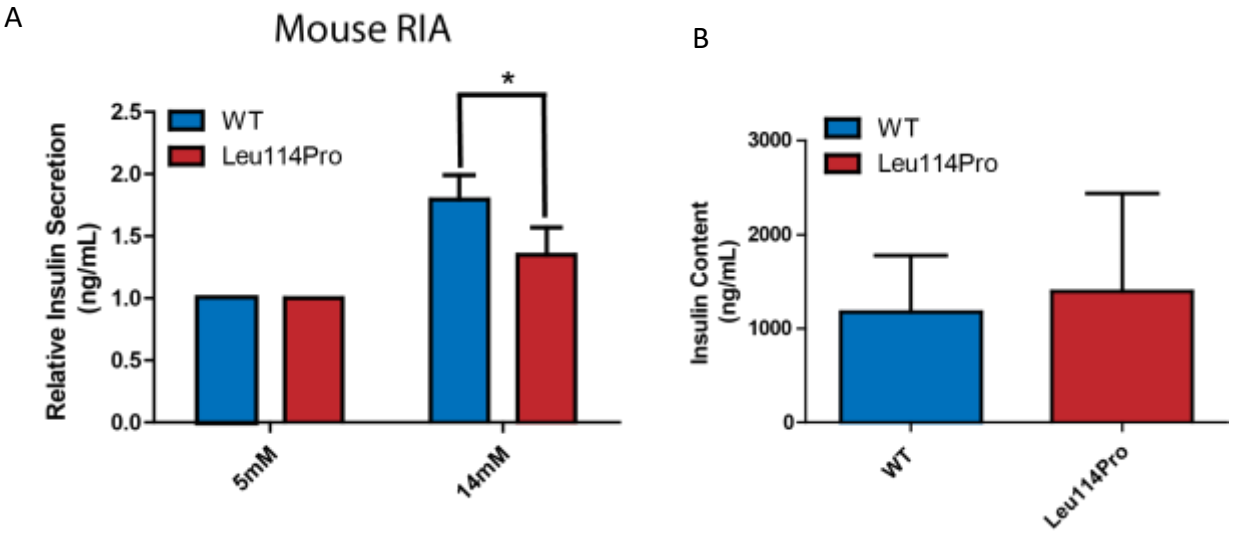

Figure 3.10 TALK-1 Leu114Pro reduces glucose-stimulated insulin secretion but does not change insulin content.

Total insulin secretion was measured via RIA following exposure to 5mM or 14mM glucose (A). Total insulin content was measured by RIA in islets expressing both TALk-1 WT and TALK-1 Leur114Pro (B); mean ± SEM; N = 3 animals *$P < 0.05$

Discussion

We have identified the first family with *KCNK16* associated MODY. The novel TALK-1 gain-of-function p.Leu114Pro mutation increases β-cell K^+ efflux resulting in membrane hyperpolarization, altering β-cell Ca^{2+} handling and decreasing GSIS. Unlike the only other MODY-associated K^+ channelopathy (i.e., K_{ATP} channel dysfunction), TALK-1 is unresponsive to sulfonylureas[79]. Thus, our data suggest not only a novel therapeutic target for *KCNK16*-associated MODY but for other forms of diabetes also.

TALK-1 belongs to the K2P channel family characterized by constitutive K^+ flux, which serve critical roles setting the V_m of electrically excitable cells. The *KCNK16* transcript encoding TALK-1 is the most abundant K^+ channel transcript in the human β-cell[182; 183]; and *KCNK16* shows the most islet-selective expression of all ion channel transcripts[92; 188]. Similar to other K^+ channels, such as K_{ATP}[189], TALK-1-mediated hyperpolarization of mouse and human β-cell membrane potential limits VDCC activity, Ca^{2+} entry and GSIS[79]. However, the K_{ATP} K^+ conductance is significantly greater than the small constitutive conductance of TALK-1[79; 92; 189; 190]. Thus, TALK-1 mainly regulates the β-cell membrane potential following glucose stimulation, when K_{ATP} channels close: their activity limits islet Ca^{2+} oscillation frequency and hence GSIS[79]. A gain-of-function TALK-1 mutation would be predicted to affect glucose tolerance adversely resulting in hyperglycemia, as demonstrated here.

The *KCNK16*-containing locus is strongly associated with T2DM, in multiple genome-wide association studies including populations with differing ethnicities[124; 126; 191-193], with strongest association ($p<2x10^{-8}$) observed with the common nonsynonymous polymorphism rs1535500 (minor allele frequency 0.41, ExAC database, non-Finnish European descent subjects). The protein change (p.Ala277Glu) affects the C-terminal tail of TALK-1 and causes a modest (1.4-fold) increase in TALK-1 channel current, with both enhanced open probability and increased cell surface localization[79]. The risk haplotype is also associated with increased expression of the adjacent gene *KCNK17* which encodes another K2P channel, TALK-2[194]. TALK-2 is also expressed in islet cells with high specificity, though lower than TALK-1 (islet expression specificity index for *KCNK16*=0.98 and for *KCNK17*=0.76)[194]. These data suggest that the association of this locus with T2DM is driven by more than one mechanism, with combined effects from overactive TALK-1 and overexpression of TALK-2, each of which potentially contributing to hyperpolarization of the β-cell membrane potential, reducing glucose-stimulated Ca^{2+} influx and GSIS. That association is seen in T2DM with a common variant in the same gene in which we are now reporting a novel mutation potentially causing MODY indicates that the encoded protein (i.e., TALK-1) is not functionally redundant; rather, that it is likely relevant to a high proportion of T2DM cases. These properties increase the potential of TALK-1 as a therapeutic target for T2DM.

Mutations in K2P channels causing significant changes in K^+ channel currents typically affect the pore domains of these channels[195-197]. For example, loss-of-function mutations in the first or second pore domains of *KCNK3* (respectively, p.Gly97Arg and p.Gly203Asp)

cause pulmonary hypertension[195]. Similarly, a loss-of-function mutation in the first pore domain of TASK-2 (p.Thr108Pro) causes Balkan Endemic Nephropathy[196]. A gain-of-function mutation (p.Gly88Arg) in the first pore domain of TALK-2, coded by *KCNK17*, causes a severe cardiac arrhythmia[197]; and is the only previously identified disease-associated mutation in TALK channels.

Gain-of-function mutations in K_{ATP} significantly increase β-cell K^+ flux, resulting in neonatal diabetes and MODY[179; 181]. In contrast, TALK-1 p.Leu114Pro results in a more modest diabetes phenotype despite the 300-fold increase in whole-cell TALK-1 activity. This may because TALK-1 activation shows voltage-dependence[79; 92]. Unlike K_{ATP}, which is active at all voltages, TALK-1 is an outward rectifying channel that shows increased activation during depolarization[79; 92]. Therefore, a gain-of-function in TALK-1 would be most active post-β-cell depolarization – limiting, but not abrogating, insulin secretion. The p.Leu114Pro mutation does increase TALK-1 current near the resting membrane potential (Fig. 3.2A, and Figure 3.3A, 3.3B); however, this current is still less than the total β-cell K_{ATP} conductance under euglycemic conditions. These data concord with the proband's clinical phenotype, with dramatic glucose elevation after an oral glucose load but only a modest increase in fasting plasma glucose.

TALK-1 is expressed on both the β-cell plasma membrane and the ER membrane[65]. Ca^{2+}_{ER} release is balanced by negative charge on the luminal ER membrane; this charge is dissipated by ER TALK-1 K^+ influx leading to enhanced Ca^{2+}_{ER} release[65]. Thus, overactive TALK-1 channels (e.g., TALK-1 Ala277Glu) increase Ca^{2+}_{ER} release, whereas

TALK-1 ablation reduces Ca^{2+}_{ER} release[65]. Importantly, enhanced β-cell Ca^{2+}_{ER} release under hyperglycemic conditions results in ER-stress, contributing to β-cell dysfunction[198]. TALK-1 Leu114Pro may contribute to β-cell dysfunction via ER-stress, as observed in some MODY subtypes (e.g., *INS* mutations in MODY-10[199]); however, this remains speculative. Additionally, although highly β-cell specific, TALK-1 is also expressed in human pancreatic δ-cells where it negatively regulates somatostatin release [171]. TALK-1 KO mice show increased somatostatin secretion under low and high glucose conditions, due to enhanced Ca^{2+}_{ER} release[171]; thus, a gain-of-function mutation in TALK-1 may reduce δ-cell somatostatin secretion. The glycemic effects of this would be complex given the inhibitory effect of somatostatin on both insulin and glucagon secretion[171]; and require future investigation.

Some MODY subtypes (e.g., *ABCC8*-, *KCNJ11*-, *HNF1α*- and *HNF4α*MODY) are manageable through K_{ATP} inhibition[179; 200; 201] – i.e., sulfonylurea use. Although β-cell membrane potential depolarization with sulfonylureas may allow greater VDCC activity, potentially increasing insulin secretion in affected individuals in this family, TALK-1 itself is not sensitive to sulfonylureas[79]. Further, and as detailed above, TALK-1 primarily modulates β-cell membrane potential during active insulin secretion when K_{ATP} is closed (i.e., during hyperglycemic conditions)[79]. Thus, K_{ATP} inhibition may not completely normalize β-cell membrane potential or insulin secretion in individuals with TALK-1 gain-of-function MODY. This raises the possibility of TALK-1 inhibition as a druggable target. Genetic evidence whether from rare (e.g., MODY) or common (e.g., T2DM[124; 126; 191-193]) human disease is a strong predictor of future successful drug development[202]. Thus, our

data have important therapeutic implications not only for TALK-1 MODY but also for the far more common form of diabetes T2DM.

In conclusion, we have identified a novel mutation in *KCNK16* causing a gain-of-function in TALK-1, reducing glucose-stimulated Ca^{2+} influx, Ca^{2+}_{ER} storage, and GSIS; which is associated with MODY. TALK-1 is the first ion channel linked to MODY after K_{ATP}; and is expressed more selectively in islet cells compared to K_{ATP}. The *KCNK16* locus is associated with T2DM risk in the general population. Our data suggest TALK-1 as an efficacious and islet-selective therapeutic target for both *KCNK16*-associated MODY and T2DM.

Chapter IV

A novel, neonatal diabetes-associated, mutation in *KCNK16* limits plasma membrane TALK-1 function and increases ER TALK-1 function, thereby ablating glucose-stimulated insulin secretion.

Abstract

Neonatal diabetes mellitus is a monogenic form of diabetes that results from impaired glucose-stimulated insulin secretion (GSIS). Genetic causes of neonatal diabetes include the genes encoding the ATP-activating K^+ channel subunits as well as the insulin gene. Not all neonatal diabetic cases have a known genetic etiology. TALK-1 is the most highly expressed β-cell K^+ channel transcript, it regulates both cytosolic Ca^{2+} ($[Ca^{2+}]_{cyto}$) influx as well as ER Ca^{2+} ($[Ca^{2+}]_{ER}$) handling, and has been associated with both T2DM and MODY. Here we identified a glutamine for arginine substitution mutation in TALK-1 (TALK-1 R13Q) associated with neonatal diabetes. Other neonatal diabetic K^+ channel mutations increase channel current at the plasma membrane; however, whole-cell K^+ channel currents from cells expressing TALK-1 R13Q show complete abolishment of plasmalemmal TALK-1 current. Interestingly, normal, single-channel TALK-1 current remained at the endoplasmic-reticulum (ER) membrane despite the mutation and $[Ca^{2+}]_{ER}$ was reduced, suggesting an increased number of TALK-1 channels on the ER membrane. TALK-1 contains two palmitoylation sites near the mutation that allows it to traffic from the ER membrane to the plasma membrane. When these palmitoylation sites are mutated (C7A, C9A), TALK-1 R13Q regains normal plasmalemmal TALK-1 current, suggesting that the mutation affects TALK-1 palmitoylation and therefore inhibits

trafficking to the plasma membrane. Interestingly, despite not displaying any current on the plasma membrane, TALK-1 R13Q completely abolishes glucose-stimulated $[Ca^{2+}]_{cyto}$ influx at the plasma membrane. TALK-1 R13Q completely inhibits glucose-stimulated insulin secretion (GSIS) suggesting that intracellular TALK-1 current can still affect β-cell membrane activity. This highlights a potential new intracellular role for TALK-1 and thus has implications for both β-cell function and dysfunction in diabetes.

Introduction

Neonatal diabetes mellitus is a rare form of monogenic diabetes that typically presents during the first 6-months of life[180]. Half of neonatal diabetic cases are transient, meaning they resolve later in life, but the other half are permanent, resulting in life-long complications[203]. The most common genetic causes of neonatal diabetes are mutations in the genes encoding the two subunits of K_{ATP}, *KCNJ11* and *ABCC8*, as well as mutations in the insulin gene (*INS*)[155; 156; 180; 204; 205]. These mutations result in impaired GSIS by impairing β-cell cytosolic Ca^{2+} ($[Ca^{2+}]_c$) influx or by causing ER-stress respectively.

Oscillations in β-cell $[Ca^{2+}]_c$ influx and endoplasmic reticulum (ER) Ca^{2+} ($[Ca^{2+}]_{ER}$) are essential for glucose-stimulated insulin secretion (GSIS) and become perturbed during the pathogenesis of diabetes[206]. Disruptions in β-cell $[Ca^{2+}]_c$ and $[Ca^{2+}]_{ER}$ also cause ER stress and β-cell failure under diabetic conditions[46; 207; 208]. K^+ channels regulate K^+ flux across the plasma membrane, which tunes Ca^{2+} influx by controlling the membrane potential (V_m) and therefore voltage-dependent Ca^{2+} channel activity (VDCC)[209]. K^+ channels also regulate K^+ flux across the ER membrane, which maintains ER electroneutrality and sustains the driving force for $[Ca^{2+}]_{ER}$ release[65; 70; 210-212]. The K2P

channel TALK-1, is an important K^+ channel that serves to modulate β-cell V_m at the plasma membrane and ER membrane[65; 79]. *KCNK16*, which encodes TALK-1, is the most highly expressed β-cell K^+ channel transcript and is almost exclusively expressed in pancreatic islets[79; 97; 190]. Importantly a nonsynonymous, coding sequence (cds) polymorphism (rs1535500) in *KCNK16* increases the risk for developing T2DM[98; 99] and a Leucine to Proline substitution near the K^+ selectivity filter potentially causes MODY (See chapter 3 of this dissertation). Altogether, this makes TALK-1 an interesting target for the treatment of diabetes.

Here, we have identified a novel mutation in *KCNK16* (TALK-1 R13Q) that has been associated with neonatal diabetes. This mutation ablations TALK-1 current at the plasma membrane but maintains current on the ER membrane. This is presumably due to altered palmitoylation-mediated TALK-1 trafficking. This results in abnormal β-cell Ca^{2+} handling and reduced GSIS.

Results

Novel KCNK16 mutation associated with neonatal diabetes ablates plasmalemmal TALK-1 current.

A novel, recessive, mutation in TALK-1 (TALK-1 R13Q) was identified in a neonatal diabetic patient from a consanguineous family. This mutation occurs in the N-terminal domain of TALK-1 and is conserved in both TALK-1 and TALK-2 (Figure 4.1A and 4.1B). K^+ currents were recorded using HEK293 cells transfected with either TALK-1 WT plus mCherry, TALK-1 R13Q plus mCherry, or mCherry alone. K^+ recordings in response to a

voltage ramp from -120mV to 0mV demonstrated that TALK-1 R13Q resulted in a complete abolishment of TALK-1 current at the plasma membrane (Figure 4.1C). This is highlighted by the fact that K^+ currents from cells expressing TALK-1 R13Q were identical to K^+ currents from cells expressing mCherry alone (Figure 4.1C).

TALK-1 R13Q maintains single-channel current on the ER membrane.

To investigate whether TALK-1 R13Q functions on the ER membrane, we used nuclear patch clamp electrophysiology[65; 213] to measure K^+ channel activity on the outer nuclear membrane, which is continuous with the ER membrane. In response to voltage stimulations between -100mV and +100mV, cells expressing TALK-1 R13Q showed similar single-channel ER TALK-1 currents compared to cells expressing TALK-1 WT (Figure 4.2A and 4.2B). ER TALK-1 R13Q currents were identical to TALK-1 WT currents in both amplitude and open probability (Figure 4.2C and 4.2D). Therefore, despite being a loss-of-function on the plasma membrane, TALK-1 R13Q maintained normal current on the ER membrane.

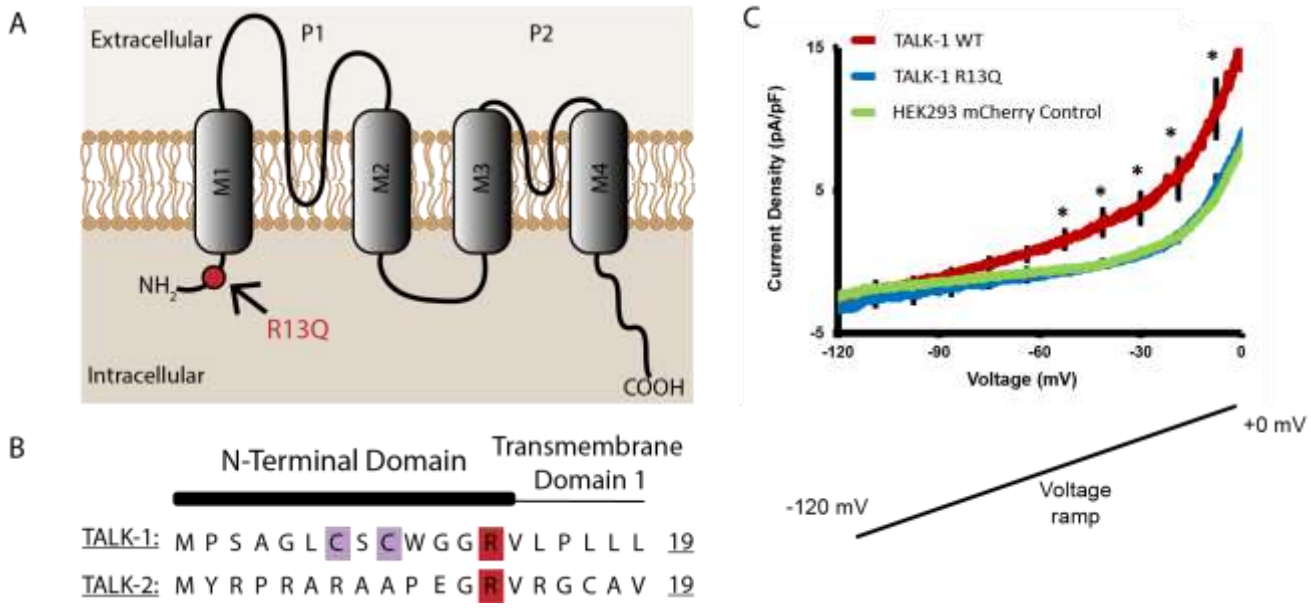

Figure 4.1: A novel *KCNK16* mutation found in an individual with neonatal diabetes ablates plasma membrane TALK-1 current.

A novel mutation in the C-terminus of TALK-1 **(A)** has been identified in a patient with neonatal diabetes. This mutation (red) is conserved in both TALK-1 and TALK-2 and is only 3 amino acids away from palmitoylation sites (purple) found in TALK-1 **(B)**. K^+ currents monitored from TALK-1 WT, TALK-1 R13Q, and HEK293 control cells with whole-cell voltage clamp recordings, in response to a voltage ramp from -120mV to 0mV. Mean ± SEM **(C)**

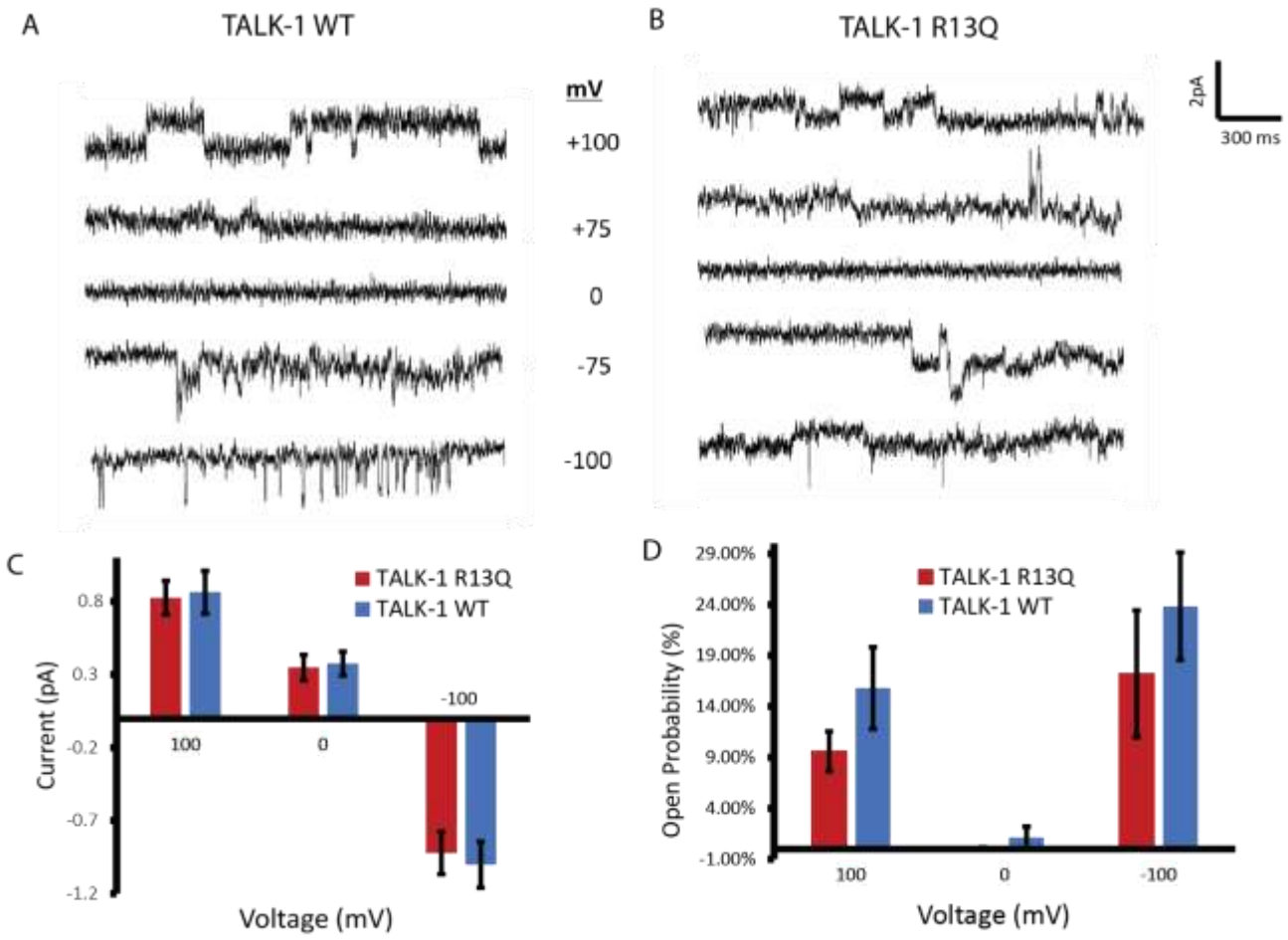

Figure 4.2: TALK-1 R13Q maintains current on the ER membrane.

Nuclear Patch clamp, single channel recordings of nuclei expressing TALK-1 WT and TALK-1 R13Q stimulated at either +100, +75, 0, -75, or -100mV **(A and B)** Single channel recordings were analyzed for average current and open probability of single channel, nuclear patch clamp currents **(C and D)**. Mean ± SEM.=; N=12 control cells; N=9 TALK-1 R13Q cells.

TALK-1 R13Q reduces $[Ca^{2+}]_{ER}$ stores

To assess whether TALK-1 R13Q current affects $[Ca^{2+}]_{ER}$ handling differently than TALK-1 WT, we transfected the MIN-6 β-cell line with either TALK-1 R13Q or TALK-1 WT, plus mCherry and measured $[Ca^{2+}]_{cyto}$ upon inhibition of SERCAs with cyclopiazonic acid (CPA) (Figure 4.3A and 4.3B). Inhibition of SERCA pumps prevents $[Ca^{2+}]_{ER}$ uptake, therefore dumping $[Ca^{2+}]_{ER}$ stores into the cytosol where it can then be measured with FURA2-AM[79]. MIN-6 cells expressing TALK-1 R13Q showed a reduction in $[Ca^{2+}]_{ER}$ stores compared to MIN-6 cells expressing TALK-1 WT (Figure 4.3A and 4.3B). Furthermore, we also utilized another β-cell line, INS-1, to directly measure $[Ca^{2+}]_{ER}$ with the $[Ca^{2+}]_{ER}$ indicator D4ER (Figure 4.3C and 4.3D). Cells transfected with D4ER plus either TALK-1 WT or TALK-1 R13Q showed that TALK-1 R13Q reduces $[Ca^{2+}]_{ER}$ compared to TALK1- WT (Figure 4.3C and 4.3D). This suggests that cells expressing TALK-1 R13Q have more K^+ current on the ER membrane, most likely due to an increased number of TALK-1 channels that have not been properly trafficked to the plasma membrane. This would increase the driving force for $[Ca^{2+}]_{ER}$ release and deplete $[Ca^{2+}]_{ER}$ storage.

TALK-1 is palmitoylated and preventing this palmitoylation recovers plasmalemmal TALK-1 R13Q currents.

Reduced $[Ca^{2+}]_{ER}$ storage in cells expressing TALK-1 R13Q suggests that there is more TALK-1 current on the ER of TALK-1 R13Q expressing cells than on the cells expressing TALK-1 WT. This, together with the fact that TALK-1 R13Q current is not on the plasma membrane led us to investigate possible mechanisms for the loss of plasma membrane

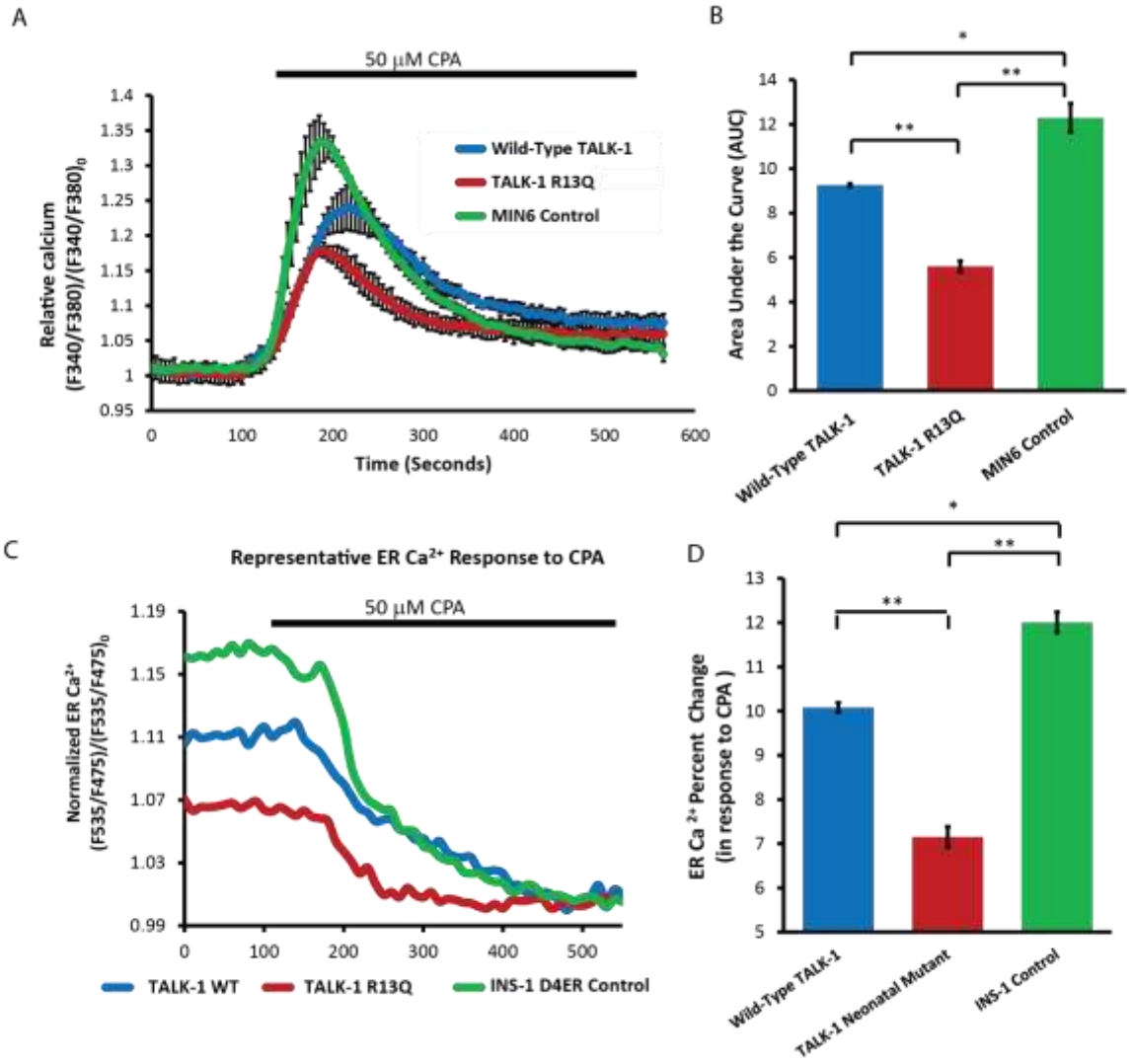

Figure 4.3: TALK-1 R13Q reduces $[Ca^{2+}]_{ER}$.

Cyclopiazonic Acid (CPA) was used to inhibit SERCA pumps on the ER membrane, resulting in $[Ca^{2+}]_{ER}$ depletion, was measured by the FURA-2AM Ca^{2+} indicator in MIN-6 cells **(A and B).** Rat insulinoma cells (INS-1) alone or expressing either wild-type TALK-1 or TALK-1 R13Q monitored for ER Ca^{2+} with the genetically encoded indicator, D4ER **(C and D)**. Mean ± SEM; N = 3 animals; *P < 0.05, **P < 0.01.

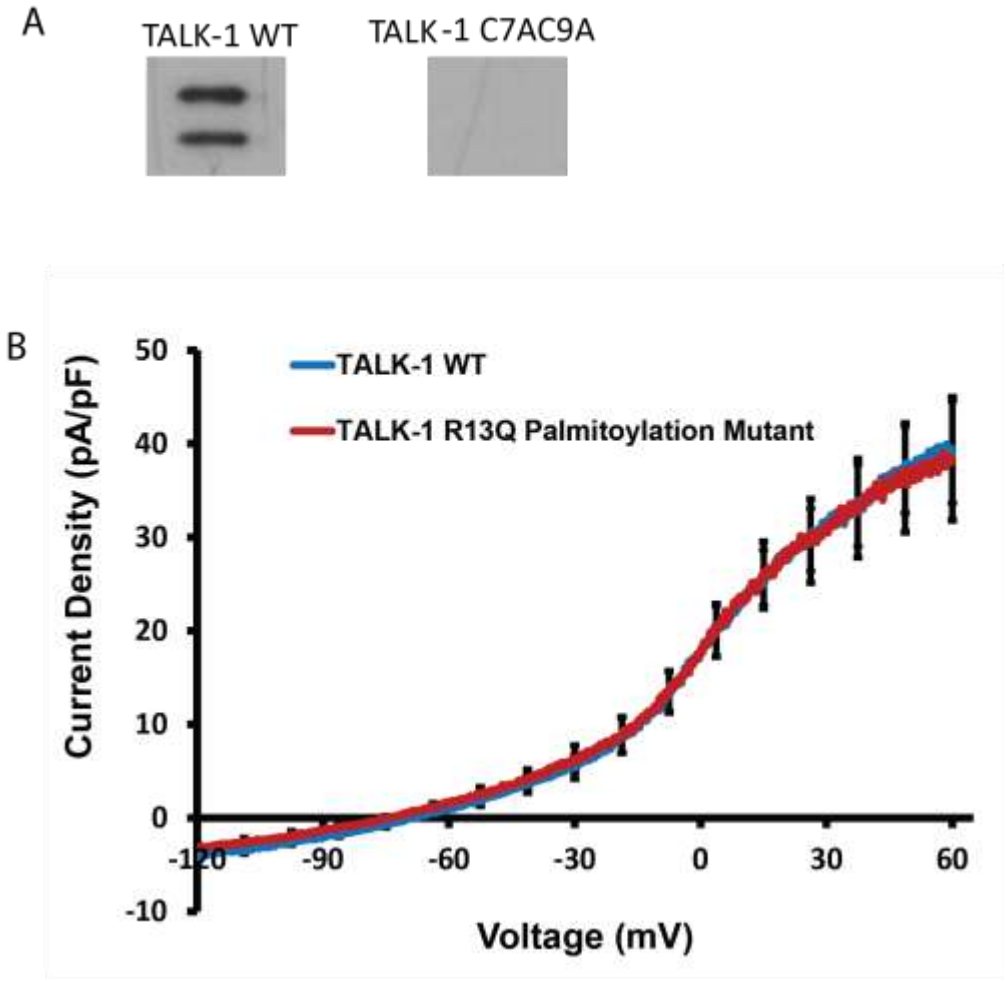

Figure 4.4: TALK-1 is palmitoylated on C7 and C9 and preventing this palmitoylation recovers TALK-1 R13Q currents.

A palmitoylation pull-down shows that TALK-1 is palmitoylated and mutating C7 and C9 to an alanine prevents this palmitoylation **(A)**. K^+ currents monitored from TALK-1 WT, TALK-1 R13Q Palmitoylation mutant in response to a voltage ramp from -120 mV to 60 mV **(B)**. Mean ± SEM

TALK-1. One mechanism that regulates trafficking of proteins such as ion channels is palmitoylation[214]. Indeed, with a palmitoylation pull-down, we found that TALK-1 is palmitoylated on Cysteine 7 (C7) and Cysteine 9 (C9) (Figure 4.4A -data generated by Dr. Matthew Dickerson), two residues in close proximity to the R13Q mutation. Palmitoylation of some proteins is known to facilitate protein trafficking away from the ER[215-218]; therefore, it is possible that palmitoylation on TALK-1 C7 and C9 regulates TALK-1 trafficking from the ER membrane to the plasma membrane. Mutating TALK-1 C7 and C9 to alanines (C7AC9A) prevents palmitoylation (Figure 4.4A), so we investigated whether TALK-1 C7AC9A affected the plasmalemmal current ablation seen with TALK-1 R13Q. To accomplish this, we transfected HEK293 Cells with either TALK-1 WT or TALK-1 R13Q C7AC9A. Interestingly, TALK-1 R13Q C7AC9A showed a recovery of plasmalemmal K^+ current up to the level of TALK-1 WT current (Figure 4.4B -data generated by Dr. Matthew Dickerson). This suggests that palmitoylation at C7 and C9 may be affected by R13Q and that, like other proteins[216-218], palmitoylation could prevent trafficking of TALK-1 from the ER membrane to the plasma membrane. This would result in an increased number of TALK-1 channels on the ER membrane and explain the reduction in $[Ca^{2+}]_{ER}$ storage we see with TALK-1 R13Q.

<u>TALK-1 R13Q completely abolishes glucose-stimulated insulin secretion.</u>

To see the affect that TALK-1 R13Q has on GSIS, islet clusters were transduced with lentiviral vectors hat contained a RIP promoter driving expression of either TALK-1 WT or TALK-1 Leu114Pro followed by a P2A cleavage site and the Nano-Luc Pro-insulin Luciferase reporter[219; 220]. Mouse islets expressing TALK-1 R13Q showed loss of GSIS

when compared to mouse islets expressing TALK-1 WT or TALK-1 R13Q Dominant Negative (Figure 4.5A). Furthermore, human islets expressing TALK-1 R13Q showed both loss of GSIS and reduced basal insulin secretion (Figure 4.5B).

The impact of TALK-1 R13Q on GSIS is not due to increased ER-stress or altered insulin granule processing.

As TALK-1 R13Q seems to only have functional current on the ER membrane and it reduces $[Ca^{2+}]_{ER}$ storage we were interested in whether the ablated GSIS was caused by increased ER-stress, which has been shown to cause beta-cell failure due to other mutations (e.g. in insulin and WFS1) that result in neonatal diabetes[157; 158; 221]. To investigate this, we utilized both an ATF-6 luciferase reporter assay[222] and a qRT-PCR to monitor ATF-6 cleavage and ER-stress marker expression levels respectively. Although TALK-1 R13Q reduced $[Ca^{2+}]_{ER}$ storage, we found no difference in ER-stress with either of these assays when comparing cells expressing TALK-1 R13Q and TALK-1 WT (Figure 4.6A and 4.6B).

As the loss of GSIS does not seem to be caused by ER-stress, we next investigated whether it could be due to improper ER insulin-processing and insulin granule formation. To test this, we transduced islet clusters with a lentivirus containing a RIP promoter expressing either TALK-1 WT or TALK-1 R13Q followed by a P2A cleavage site and the Nano-Luc Pro-insulin Luciferase reporter (Figure 4.7A). We then fixed the islets and stained for luciferase to visualize insulin production and trafficking into granules.

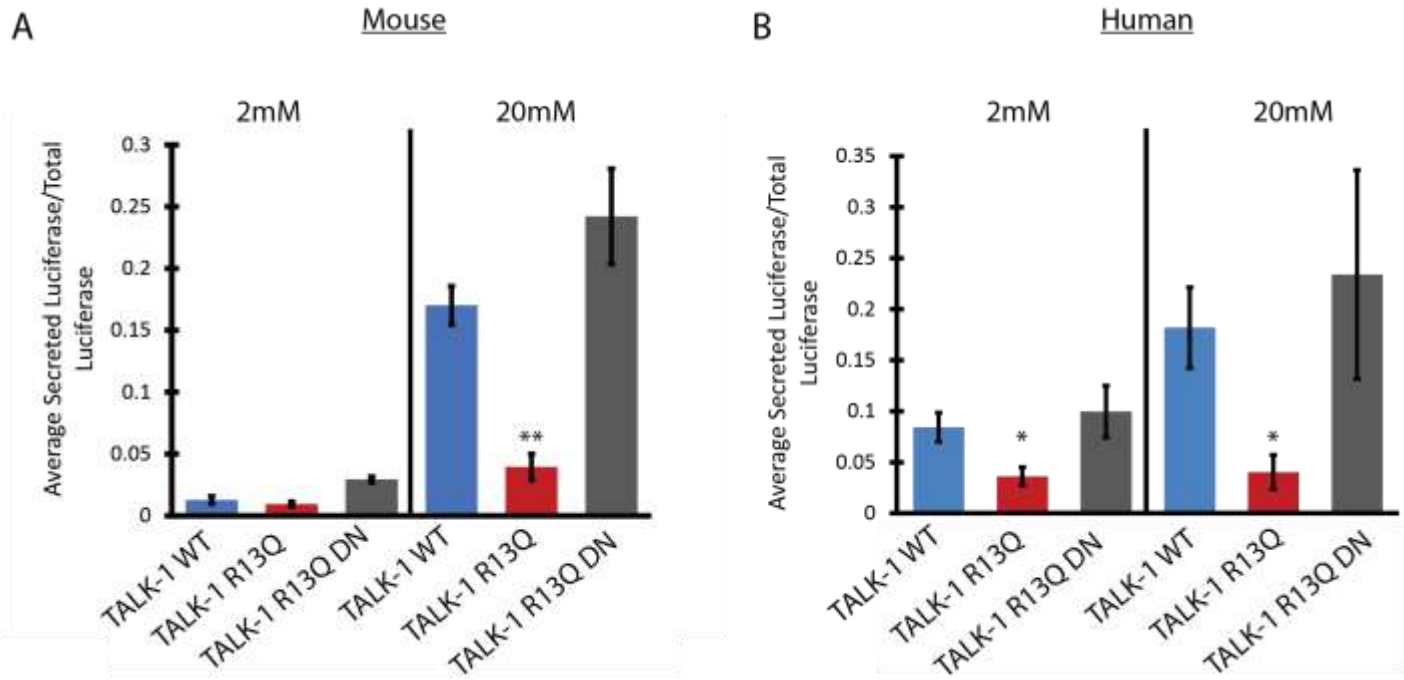

Figure 4.5: TALK-1 R13Q ablates glucose-stimulated insulin secretion.

Mouse and Human islets were transduced with viruses containing the RIP promoter expressing either wild-type TALK-1, TALK-1 R13Q, or TALK-1 R13Q Dominant Negative (DN) followed by a P2A cleavage site and the NanoLuc-proinsulin luciferase. Average secreted luciferase at 2 mM and 20 mM glucose from mouse **(A)** and human **(B)** islets; Mean ± SEM, N = 3 mice, N = 6 humans.

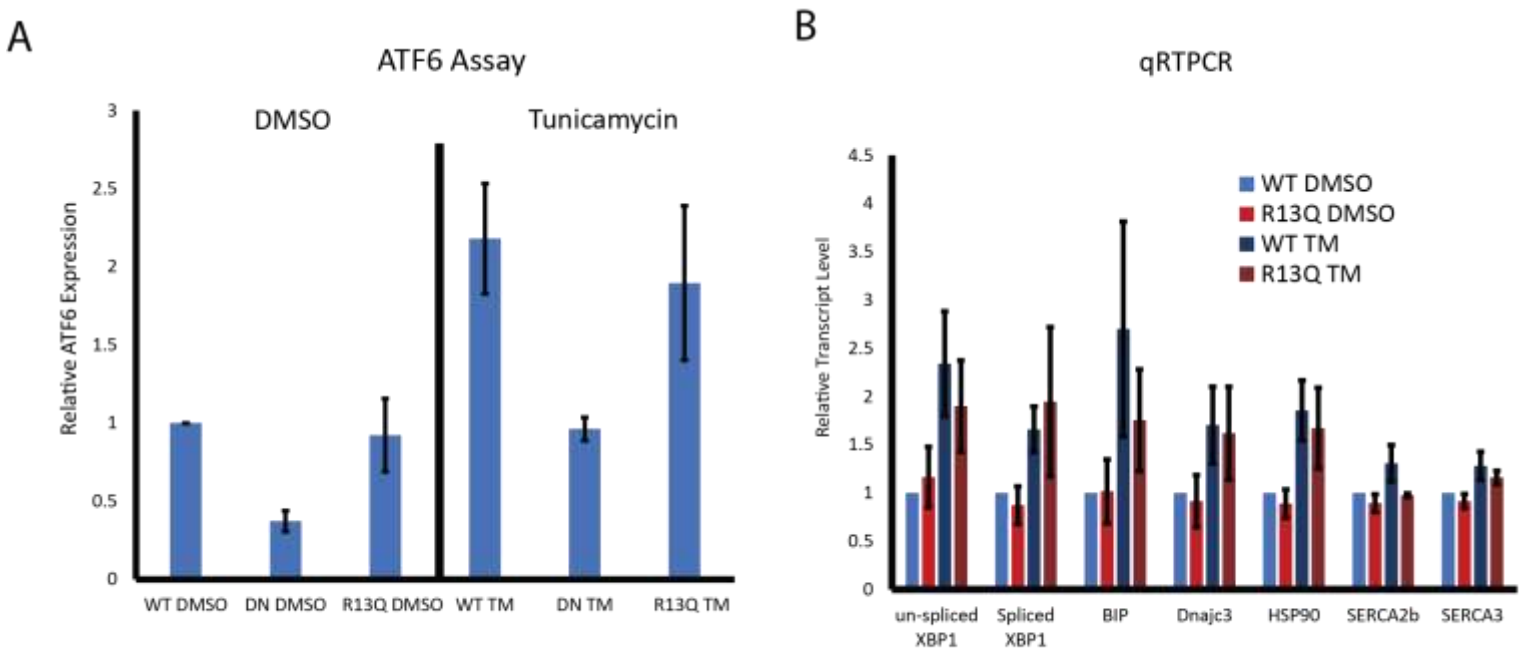

Figure 4.6: TALK-1 R13Q does not increase ER-stress.

Cells expressing an ATF6 reporter construct (contains an ATF6 DNA binding domain upstream of a luciferase) plus either TALK-1 WT, TALK-1 DN, or TALK-1 R13Q were exposed to either tunicamycin (TM) or vehicle for 16-20 hours and then a luciferase assay was run **(A)**. INS-1 cells expressing either TALK-1 R13Q or TALK-1 WT were treated with either TM or vehicle for 16-20 hours and RNA was isolated and a qRT-PCR was run **(B)**; mean ± SEM; N = 3

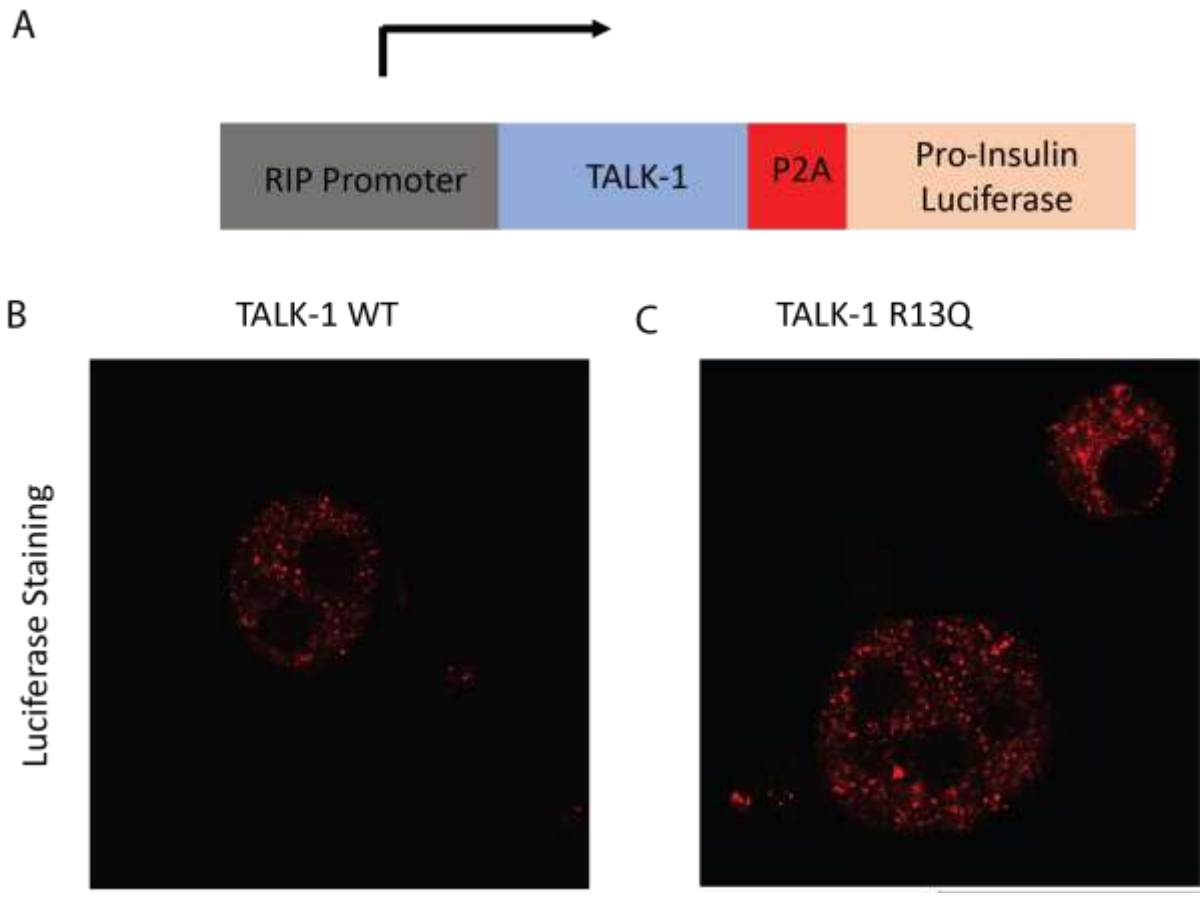

Figure 4.7: TALK-1 R13Q does not overtly affect insulin staining patterns.

Islet clusters were transduced with a virus containing a RIP promoter expressing either TALK-1 WT or TALK1- R13Q followed by a P2A cleavage site and the Nanoluc-proinsulin luciferase **(A)**. Transduced islet clusters were fixed and stained for luciferase **(B and C)**.

Islets expressing TALK-1 R13Q did not show any obvious or immediate differences in insulin granule staining compared to islets expressing TALK-1 WT, which suggests that insulin production in the presence of TALK-1 R13Q is packaged into granules and properly trafficked (Figure 4.7)

TALK-1 R13Q abolishes glucose-stimulated Ca^{2+} influx.

As TALK-1 R13Q did not show any obvious ER function defects, we next assessed $[Ca^{2+}]_{cyto}$ handling. To accomplish this, we utilized β-cells that were transduced with a virus containing the RIP promoter expressing either TALK-1 R13Q or TALK-1 R13Q Dominant Negative (DN) followed by a P2A cleavage site and mCherry (Figure 4.8A) and measured glucose-stimulated $[Ca^{2+}]_{cyto}$ influx with the $[Ca^{2+}]_{cyto}$ indicator, Fura2-AM. The DN was designed by mutating the K^+ selectivity filter of TALK-1 (TALK-1 G110E)[79]. TALK-1 with this G110E point mutation prevents channel activity by dimerizing with endogenous TALK-1 subunits and disrupting the channel's K^+ selectivity filter to abolish K^+ flux[79; 223]. Remarkably, β-cells expressing TALK-1 R13Q had a complete loss of glucose-stimulated $[Ca^{2+}]_{cyto}$ influx (Figure 4.8B). Whereas β-cells expressing the control TALK-1 R13Q DN displayed normal glucose-stimulated $[Ca^{2+}]_{cyto}$ influx (Figure 4.8B). This suggests that while TALK-1 R13Q does not have functional current on the plasma membrane, it can still greatly affect plasma membrane ion channel activity and may indicate a novel role for intracellular TALK-1 current.

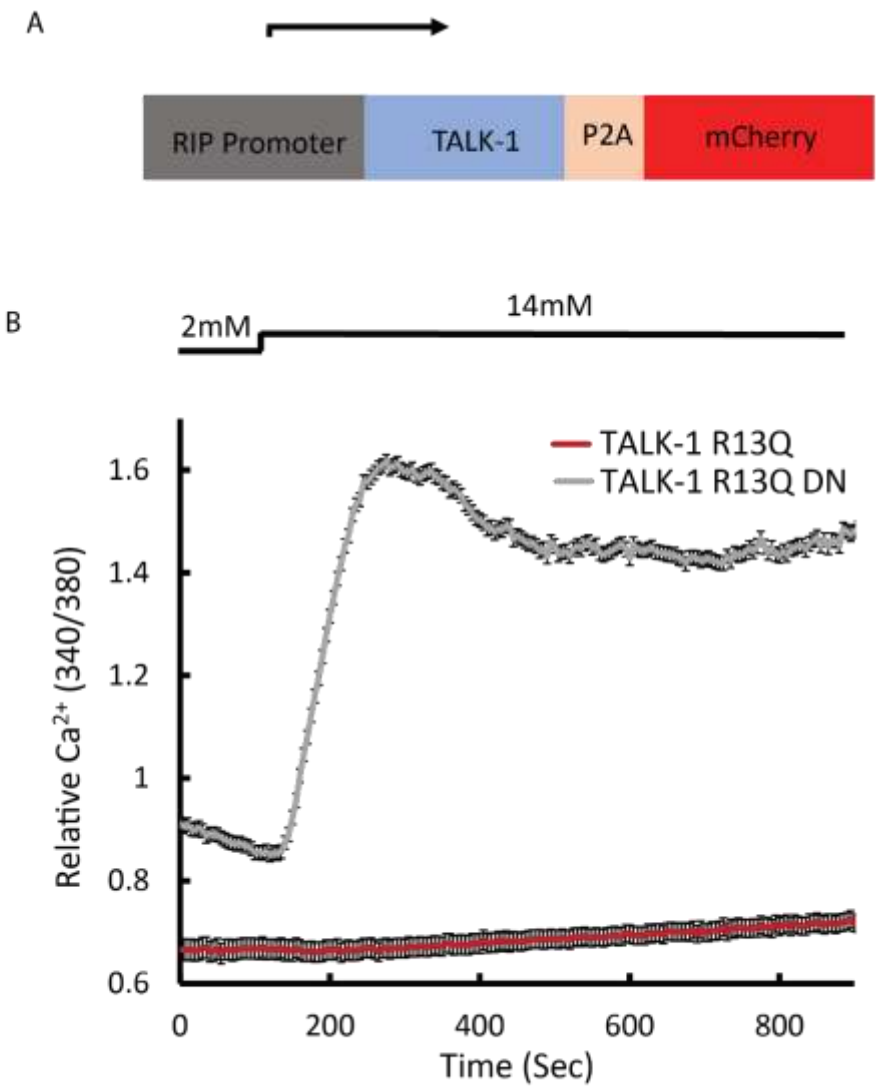

Figure 4.8: TALK-1 R13Q ablates glucose-stimulated Ca^{2+} influx.

β-cells were transduced with a virus containing the RIP promoter expressing either TALK-1 R13Q or TALK-1 R13Q DN followed by a P2A cleavage site and mCherry **(A)**. Transduced cells were then monitored for $[Ca^{2+}]_{cyto}$ upon stimulation from 2 mM to 14 mM glucose. Mean ± SEM; N = 97 R13Q DN cells; N = 121 R13Q cells.

Discussion

We have identified the first case of neonatal diabetes that is likely due to a mutation in *KCNK16*. The novel TALK-1 R13Q mutation results in a loss of K^+ efflux at the plasma membrane, but maintains current on the ER-membrane, presumably due to a loss of proper TALK-1 trafficking from the ER to the plasma membrane. While, TALK-1 R13Q is only functional intracellularly, it still results in abolished β-cell $[Ca^{2+}]_{cyto}$ influx and therefore, abolished GSIS. This highlights a critical role of intracellular TALK-1 function in β-cell physiology. Unlike other neonatal diabetes-associated K^+ channelopathies, TALK-1 is unresponsive to sulfonylureas[79]. Thus, our data suggest not only a novel therapeutic target for *KCNK16*-associated neonatal diabetes but for other forms of diabetes as well.

TALK-1 belongs to the "leak" K2P channel family characterized by constitutive K^+ flux. TALK-1-mediated hyperpolarization of β-cell membrane potential limits VDCC activity, Ca^{2+} entry and GSIS[79]. Neonatal diabetic mutations in K_{ATP} result in neonatal diabetes by activating the channel thereby hyperpolarizing the β-cell membrane and preventing insulin secretion[181; 205]. We predicted that this would also be the case for TALK-1 R13Q; however, we find that TALK-1 R13Q is a loss-of-function mutation at the plasma membrane. This would be predicted to increase β-cell insulin-secretion, however, that is not what we see with TALK-1 R13Q. Instead, the TALK-1 R13Q plasmalemmal loss-of-function shows complete abolishment of GSIS.

This made us turn to a possible intracellular role for TALK-1 R13Q. Indeed, while TALK-1 R13Q is a loss-of-function at the plasma membrane, it maintains potassium permeable channel function on the ER-membrane. This suggests that TALK-1 is not efficiently trafficked to the plasma membrane. Although the exact mechanisms that regulate TALK-

1 trafficking have not been conclusively defined, palmitoylation has been shown to play an important role in regulating other potassium channels trafficking to the membrane. Interestingly, TALK-1 has a strong palmitoylation motif near R13Q with two cysteine residues separated by a serine. Interestingly, arginine residues that reside near palmitoylation motifs have been implicated in the ability of enzymes to palmitoylate their targets[224; 225]. Here, we show that preventing that palmitoylation rescues TALK-1 R13Q current on the plasma membrane, indicating the R13Q mutation could be preventing de-palmitoylation and trafficking to the plasma membrane. Preventing this trafficking would result in an increased number of TALK-1 R13Q channels on the ER membrane and therefore reduced $[Ca^{2+}]_{ER}$ stores. Indeed, we show that compared to cells expressing TALK-1 WT, cells expressing TALK-1 R13Q have reduced $[Ca^{2+}]_{ER}$ stores.

Other neonatal-diabetic mutations, such as mutations in *INS-1* and *WFS-1*, cause β-cell ER-stress[157; 221]. Mutations in INS-1 result in ER stress by prohibiting proper insulin processing thereby initiating the unfolded-protein response[157]. Specifically, mutations in *WFS-1*, a transmembrane protein, deplete $[Ca^{2+}]_{ER}$ stores leading to β-cell apoptosis[226]. This apoptosis can be prevented by overexpressing SERCA to restore $[Ca^{2+}]_{ER}$ stores[226]. Furthermore, SERCA activity has been shown to control proinsulin processing and secretion[53]. Based on this, we predicted that the reduction in $[Ca^{2+}]_{ER}$ stores seen with TALK-1 R13Q would cause ER-stress, thereby causing the un-folded protein response, improper insulin processing, and β-cell failure. However, expression of TALK-1 R13Q in β-cells did not result in ER-stress or alterations of insulin granule staining. Therefore, we had to consider other possible explanations.

We found that while there are no functional TALK-1 R13Q channels on the plasma membrane, TALK-1 R13Q still completely abolished β-cell glucose-stimulated $[Ca^{2+}]_{cyto}$ influx. This loss of glucose-stimulated $[Ca^{2+}]_{cyto}$ influx explains the complete loss of GSIS we see with TALK-1 R13Q. Future studies are needed to clarify how a K^+ channel that is not functional on the plasma membrane could affect plasma membrane Ca^{2+} influx.

As described in chapter II of this dissertation, TALK-1 activity controls mitochondrial function. Specifically, we showed that a β-cell specific TALK-1 KO has increased mitochondrial Ca^{2+} ($[Ca^{2+}]_{mito}$) and increased mitochondrial respiration. Therefore, it is possible that the TALK-1 R13Q mutation resulting in an increased number of TALK-1 channels on the ER-membrane is depleting $[Ca^{2+}]_{ER}$ stores to the point that it is limiting Ca^{2+} transfer from the ER to the mitochondria at the mitochondrial-associated membrane (MAM). This would reduce $[Ca^{2+}]_{mito}$ and therefore reduce ATP production , ATP-mediated closure of K_{ATP} channels, and eventually GSIS. Pyruvate kinase activity is also affected by cellular Ca^{2+} signaling, and Dr. Merrins group recently developed a model in which pyruvate kinase generates the ATP/ADP ratio required for GSIS[227]. Interestingly TALK-1 has already been shown to interact with a protein found at the MAM, TMX2[104]. TMX2 shows increased MAM expression upon palmitoylation[228] suggesting that changes to TALK-1 R13Q palmitoylation could alter TALK-1 localization to the MAM. This highlights an exciting new possibility that intracellular TALK-1 function is linked to neonatal diabetes.

In conclusion, we have identified a novel mutation in *KCNK16* causing a plasmalemmal loss-of-function in TALK-1, improper TALK-1 palmitoylation, possible alterations in TALK-1 cellular trafficking, which result in reduced $[Ca^{2+}]_{ER}$ stores, loss of glucose-stimulated Ca^{2+} influx and inhibition of GSIS. Our data suggest that the role of TALK-1 in regulating

ER function, as well as possibly mitochondrial function, can result in reduced VDCC channel activation, limit GSIS, and control β-cell function independently from its role on the plasma membrane.

Chapter V
Summary and Future Directions

Diabetes affects 422 million people worldwide, including almost 10% of the American population, and is caused by pancreatic β-cell failure[117]. Islet cell K^+ channels are contributors to β-cell dysfunction. Furthermore, targeting K^+ channels has proved to be an effective treatment for diabetes. Indeed, inhibition of β-cell K_{ATP} insulin secretion lowers blood glucose levels. GWAS studies have identified four K^+ channel loci possibly associated with T2DM susceptibility, including *KCNJ11*[118-121], *KCNJ15*[122], *KCNQ1*[123], and the TALK-1 locus, *KCNK16*[98; 99; 124; 125]. Specifically, the studies on *KCNK16* established that *KCNK16* contains a single nucleotide, non-synonymous, polymorphism (rs1535500) associated with an increased risk for T2DM in Pima-American Indians as well as individuals of East Asian ancestry[98; 124; 126]. The observations described in this dissertation suggest the exciting possibility that TALK-1 could be targeted as a diabetic therapy.

During β-cell glucose stimulation, the outward rectifying, non-inactivating K^+ current of TALK hyperpolarizes the β-cell membrane, thereby limiting VDCC channel activation and subsequent insulin secretion[79]. Global TALK-1 KO causes the β-cell membrane potential to depolarize thereby increasing action-potential firing frequency[79]. This increased action potential frequency results in increased Ca^{2+} oscillations, and therefore increased first-phase pulsatile-insulin secretion[79]. At the ER membrane, TALK-1 allows K^+ to move down its concentration gradient and into the ER thereby providing a counter-current for $[Ca^{2+}]_{ER}$ release[65]. This was established with studies that showed increased $[Ca^{2+}]_{ER}$ in global TALK-1 KO cells and reduced $[Ca^{2+}]_{ER}$ in cells expressing TALK-1 with a gain-of-function polymorphism[65; 79]. Reduced $[Ca^{2+}]_{ER}$ results in ER stress and reduced insulin secretion[49;

[65]. While these studies elucidated that TALK-1 modulates glucose homeostasis, the exact role(s) that TALK-1 plays in modulating β-cell function remained unknown. Therefore, in this dissertation, we generated a β-cell specific TALK-1 KO mouse model (β-TALK1-KO).

TALK-1 Control of Mitochondrial Function.

Similar to the global TALK-1 KO mouse model, the β-TALK1-KO showed increased β-cell $[Ca^{2+}]_c$ oscillation frequency (Figure 2.2). Both $[Ca^{2+}]_c$ and $[Ca^{2+}]_{ER}$ are known to be tightly associated with mitochondrial function. Indeed, β-TALK1-KO islets also showed increased $[Ca^{2+}]_{mito}$ (Figures 2.3 and 2.4). These changes to β-cell Ca^{2+} handling resulted in β-TALK1-KO islets also having increased mitochondrial ATP production (Figure 2.6). Our data indicates that TALK-1 regulates β-cell $[Ca^{2+}]_{mito}$ thereby modulating mitochondrial function and islet ATP synthesis.

It has also been shown that cytosolic ATP levels drop during β-cell activation, possibly due to increased ATP hydrolysis by SERCA and PMCA[58]. As β-TALK1-KO islets have increased $[Ca^{2+}]_c$ oscillations, it is possible that they also have increased PMCA and SERCA activity thereby requiring more ATP production. To test this in future studies, we could first measure PMCA and SERCA mRNA expression in both β-TALK1-KO and control islets. We can then utilize a microplate technique that concurrently measures $[Ca^{2+}]_{ER}$ and SERCA ATP hydrolysis[229] to test whether SERCA activity does indeed utilize more ATP in β-TALK1-KO islets compared to control. Furthermore, we could utilize a SERCA inhibitor to see if ATP levels become similar between β-TALK1-KO and control islets upon SERCA inhibition.

ATP is required for β-cell K_{ATP} channel closure and GSIS. Therefore, it would be interesting to measure K_{ATP} current in β-TALK1-KO mice to see if the increased ATP production increases K_{ATP} currents.

TALK-1 Regulation of Insulin Resistance

We next tested how β-TALK1-KO mice respond to diabetic conditions. β-TALK1-KO mice have improved glucose tolerance on a high-fat diet (Figure 2.7) but interestingly show reduced GSIS compared to controls (Figure 2.8). Interestingly, the mass of the insulin pulse that signals at the liver can determine the amount of hepatic insulin clearance that occurs[175]. specifically, hepatic IRS-1 and IRS-2 signaling becomes delayed when the pulsatile pattern of insulin secretion is disrupted[172]. Dr. Peter Butler's group showed thatTALK-1 affects β-cell pulsatility, TALK-1 inhibitors could improve insulin efficacy and thus prevent β-cell dysfunction under diabetic conditions.

β-TALK1-KO mice show increased (Figure 2.2)we decided to look at liver insulin sensitivity with TALK-1 ablation. We showed that global TALK-1 KO islets had increased levels of pAKT in response to insulin compared to control (Figure 2.8), indicating that pancreatic TALK-1 channels are somehow regulating hepatic insulin sensitivity.

An adequate insulin pulse frequency is also required for inhibition of endogenous glucose production[176]. Therefore, it is possible that TALK-1 regulation of pulsatile insulin secretion results in β-TALK1-KO mice having reduced hepatic glucose production. This will be accomplished by measuring mRNA expression of gluconeogenic enzymes such as PEPCK and glucose-6-phosphatase[230] or by using labeled glucose[231].

If neither of these hypotheses are able to explain the interesting glucose handling in β-TALK1-KO mice, we could also test the possibility that there is diminished glucose reabsorption by the kidney and glucose is lost in the urine. To test this a simple urine glucose test on β-TALK1-KO and control mice could be performed. Alternatively, it could be insulin resistance in another tissue, such as muscle tissue, that is being affected by the β-TALK1-KO. Indeed, preliminary studies by Arya Nakhe in the Jacobson lab indicate higher basal insulin sensitivity in β-TALK1-KO skeletal muscle when compared to control.

These studies will verify whether or not β-cell TALK-1 channels regulate peripheral insulin sensitivity under diabetic conditions. If this is indeed true, these findings will have implications for how the GOF single nucleotide polymorphism in *KCNK16* (rs1535500) results in an increased risk for developing T2DM. This could be tested by using CRISPR to generate the rs1535500 cds change in a mouse model.

TALK-1 and Monogenic Diabetes

These findings, along with the currently known T2DM associated polymorphism (rs1535500) described above, highlight TALK-1 as a viable candidate for diabetic therapies. Therefore, in this dissertation we next sought to describe the role of TALK-1 in the pathogenesis of diabetes. To accomplish this, we studied a mutation in *KCNK16* that potentially causes MODY (Leu114Pro) and a mutation in *KCNK16* that is associated with neonatal diabetes (R13Q).

Mature-Onset Diabetes of the Young

We first demonstrated that whole-cell K^+ currents were drastically increased with TALK-1 Leu114Pro expression vs. TALK-1 WT expression, due to greater single channel activity (Figure 3.4). This is due to the location of the proline substitution. This substitution occurs in the pore domain right near the selectivity filter. Homology modeling indicated that the proline substitution results in a kink that could hold the pore in an open state (Figure 3.1). This would result in both the increased amplitude and frequency of channel openings we see in Leu114Pro when compared to the small, fast, openings of normal K2P channels.

This increased hyperpolarizing current resulted in an inhibition of glucose-stimulated $[Ca^{2+}]_c$ influx and less $[Ca^{2+}]_{ER}$ storage (Figure 3.6). Together, these alterations to β-cell Ca^{2+} handling resulted in TALK-1 Leu114Pro significantly blunting GSIS compared to TALK-1 WT in both mouse and human islets (Figures 3.7 and 3.9). Complete GSIS inhibition most likely does not occur due to TALK-1 Leu114Pro activity in δ-cells. Global TALK-1 KO results in increased somatostatin secretion[171]; therefore, the gain-of-function seen with TALK-1 Leu114Pro would be expected to reduce somatostatin secretion. This would lower somatostatin inhibition of insulin secretion thereby mitigating the effects that β-cell TALK-1 Leu114Pro has on insulin secretion.

Further studies are required to determine the in-vivo effects of this mutation; on parameters such as insulin sensitivity, ER stress, and β-cell destruction. Arya Nakhe in the Jacobson lab is developing a TALK-1 Leu114Pro mouse model with which she will investigate the effects of TALK-1 in the pathogenesis of diabetes.

Neonatal Diabetes

In contrast to TALK-1 Leu114Pro, whole-cell K^+ channel currents from cells expressing TALK-1 R13Q show complete abolishment of plasmalemmal TALK-1 current (Figures 4.1). Interestingly, despite not displaying any current on the plasma membrane, TALK-1 R13Q completely abolishes glucose-stimulated $[Ca^{2+}]_{cyto}$ influx at the plasma membrane (Figure 4.8). TALK-1 R13Q also completely inhibits GSIS (Figure 4.5) suggesting that intracellular TALK-1 current can still affect β-cell membrane activity. This could be due to effects on store operated Ca^{2+} entry (SOCE). When $[Ca^{2+}]_{ER}$ is low, stromal interaction molecule (STIM1) localizes to the ER-plasma membrane junction where it activates the Ca^{2+} channel, Orai1, thereby initiating SOCE. Studies have shown that STIM1 can inhibit L-type Ca^{2+} channels[232]; therefore, as TALK-1 R13Q reduces $[Ca^{2+}]_{ER}$, it is possible that it upregulates STIM1 localization to the ER-plasma membrane junction and therefore reduces L-type Ca^{2+} channel current.

Additionally, normal, single-channel TALK-1 current remained at the ER membrane despite the loss of function at the plasma membrane (Figure 4.2), and $[Ca^{2+}]_{ER}$ was reduced (Figure 4.3), suggesting increased TALK-1 ER current. This suggests improper trafficking of the TALK-1 protein. While the exact mechanisms that regulate TALK-1 trafficking have not been conclusively defined, palmitoylation has been shown to play an important role in regulating other potassium channels trafficking, such as TMX and calnexin trafficking to the MAM[228]. Interestingly, TALK-1 has a strong palmitoylation motif near R13Q with two cysteine residues separated by a serine. When these palmitoylation sites are mutated TALK-1 R13Q regains normal plasmalemmal TALK-1 current (Figure 4.4), suggesting that the mutation affects TALK-1 palmitoylation and therefore inhibits trafficking to the plasma membrane. In this dissertation we show that preventing

palmitoylation at these sites rescues TALK-1 R13Q current on the plasma membrane, indicating the R13Q mutation could be preventing de-palmitoylation and trafficking to the plasma membrane. This is the first indication that improper TALK-1 trafficking can lead diabetes.

Future studies need to be completed to investigate whether insulin secretion can be rescued with TALK-1 R13Q palmitoylation mutants. If so, this would provide a novel new therapeutic target for treating loss of insulin secretion in diabetes. Furthermore, studies on the exact mechanism of TALK-1 palmitoylation will provide invaluable insights into β-cell K^+ channel regulation. Perhaps TALK-1 palmitoylation localizes it to the MAM where it can modulate $[Ca^{2+}]_{mito}$ and ATP synthesis. To test this, seahorse measurements could be done to compare respiration in TALK-1 R13Q islets and control islets.

Elucidating the δ-cell specific role of TALK-1

In this dissertation we focus on the role of TALK-1 in pancreatic β-cells. However, we also created a δ-cell specific TALK-1 KO mouse model (δ-TALK1-KO) to investigate the role of TALK-1 in regulating δ-cell function (Figure 5.1). We found that in, contrast to β-TALK1-KO mice, δ-TALK1-KO mice show no difference in glucose tolerance but interestingly show improved fasting blood glucose under a HFD (Figure 5.1). This is presumably due to increased somatostatin secretion and reduced glucagon secretion[171] and suggests that δ-cell TALK-1 regulation of somatostatin secretion has a larger effect on α-cell glucagon secretion than it does on β-cell insulin secretion. These effects explain why global TALK-1 KO mice had improved fasting blood glucose by no changes to GTT. However,

extensive studies on δ-TALK1-KO islets are required to understand the mechanism of δ-cell TALK-1 glucose regulation. Arya Nakhe in the Jacobson Lab will continue these studies.

Furthermore, the GOF TALK-1 Leu114Pro mutation described in this dissertation would also be affecting TALK-1 in δ-cells and may reduce δ-cell somatostatin secretion. The glycemic effects of this could be very complex given the paracrine inhibitory effect of somatostatin on both insulin and glucagon secretion[171]; however, elucidating this mechanism will provide great insight into potential MODY caused by TALK-1 Leu114Pro. Arya Nakhe in the Jacobson Lab will continue these studies.

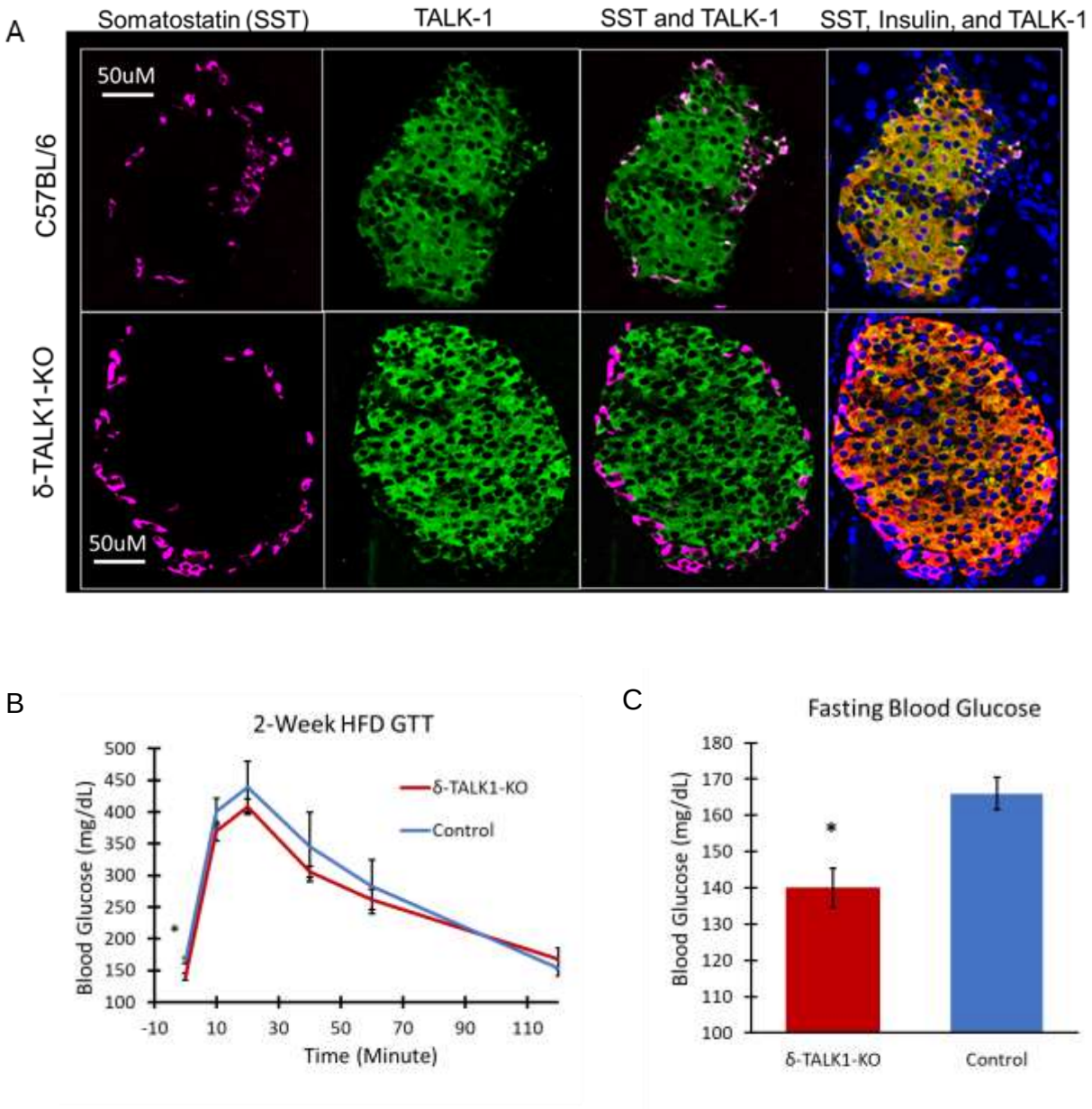

Figure 5.1. δ-TALK-1-KO pancreata show improved fasting blood glucose.

Representative immunofluorescent staining of control and δ-TALK-1-KO islets for insulin, somatostatin, and TALK-1 (nuclei in blue labeled with Hoechst) **(A)**. δ-TALK1-KO mice and control mice (fl/fl) were given an IP GTT (2mg of glucose per gram of body weight) post 2-weeks HFD. Glucose tolerance **(B)** and fasting blood glucose **(A and B)** were measured. Mean ± SEM, N = 4 control and 5 δ-TALK-1-KO. $P < 0.05$.

Chapter VI: Research Design and Methods

Islet and β-Cell Isolation

Islets were isolated from mouse pancreata as previously described[79]. Some islets were dispersed into cell clusters or single cells and then cultured for 12–18 hours[79]. Cells were maintained in RPMI 1640 with 15% FBS, 100 IU/mL penicillin, and 100 mg/mL streptomycin in a humidified incubator at 37°C with an atmosphere of 95% air and 5% CO_2.

TALK-1 Whole-Cell Currents

Voltage-clamp mode on an Axopatch 200B amplifier (Molecular Devices) was used to measure whole-cell TALK-1 currents. A Digidata 1440 was used to digitize currents that were low-pass–filtered at 1 kHz. To record only whole cell TALK-1 currents in β-cells, Ca^{2+} was removed from the extracellular buffer and TEA, a general K^+ channel inhibitor that does not affect TALK-1, was also added. A giga-ohm seal was first created between the electrode pipette and the cell, followed by the addition of more pressure to rupture the membrane and the pipette tip and gain access to the cell. The β-cell V_m was then ramped from 0mV to 60mV and the corresponding currents were measured. The whole cell currents were analyzed using ClampFit and Excel.

Cytosolic Calcium Handling Measurements

Islets were incubated for 25 min in RPMI supplemented with 2 μM Fura-2, AM (Molecular Probes), followed by incubation in Krebs-Ringer–HEPES buffer with 2mmol/L glucose for 20min[79]. Cells were then imaged every 5 second using a Nikon Eclipse Ti2 microscope equipped with a Photometrics Prime 95B 25 mm sCMOS Camera. The 535 nm emission ratios of Fura-2AM fluorescence excited at 340 and 380 nm (F340/F380) were measured. The cells were perifused at a flow rate of 2 mL/min at 37°C. For glucose stimulated measurements, perfusion was switched from 2 mM glucose to 11 mM glucose.

Lentivirus Production

To measure [$Ca^{2+}]_{mito}$ specifically in the β-cell, Cepia2mt[162] and MitoFret[164] were cloned into a lentiviral plasmid and expressed by a RIP promoter. To turn these plasmids into working lentiviruses, HEK293FT cells were cultured in DMEM GlutaMax with 10% FBS, 100IU/mL penicillin, and 100mg/mL streptomycin to 50-70% confluency in 100mm dishes. The media was then switched to DMEM GlutaMax with 10% Heat-Inactivated FBS for transfection. Chloroquine was added to the cells and allowed to sit for 10 minutes. The following DNA mixture (46.7 μl of 2.5M $CaCl_2$, 18.65 μg lentiviral plasmid, 13.9 μg packaging plasmid (pCMV-dR7.74psPAX2), and 5.56 μg envelope plasmid (pMD2.G) brought up to 470 μl with water) was added to 470ul of 2X HBS and then added dropwise onto the cells. Cells were incubated with DNA mixture for 5-7 hours and then the transfection media was aspirated off and replaced with fresh DMEM GlutaMax with 10% FBS, 100 IU/mL penicillin, and 100 mg/mL streptomycin. Media containing lentivirus was harvested 72 hours later and frozen at −80°C before use in mouse and human islet cells.

Lentivirus Expression

To transduce β-cells with the lentiviruses, islets were isolated from mouse pancreata and dispersed into clusters through trituration in 0.005% trypsin. After overnight recovery, the islet clusters were transduced using polybrene with 3rd-generation lentiviruses containing the appropriate lentiviral plasmids. The virus was left on the cells for 5-7 hours and then replaced with fresh media. The virus was then allowed to express for 2-3 days.

Mitochondrial Calcium Measurements

$[Ca^{2+}]_{mito}$ was measured using the Cepia2mt and MitoFret lentiviruses described above. After transduction, β-cells expressing Cepia2mt or MitoFret were incubated in 1 mM glucose Krebs-Ringer–HEPES buffer for 20 minutes and then imaged. β-cells expressing Cepia2mt were imaged on a Zeiss LSM780 with a 20X objective at either 0.5X or 1X magnification and excited with with a wavelength of 488 nm with an emission of 535 nm every 5 seconds. β-cells expressing MitoFret were imaged on a Nikon Eclipse Ti2 microscope equipped with a Photometrics Prime 95B 25mm sCMOS Camera with a 20x objective excited at 410nm. The ratio of the emissions for CFP (480 nm) and YFP (535 nm) were measured. For both Cepia2mt and Mitofret measurements, the cells were perifused at a flow rate of 2 mL/min at 37°C and glucose stimulation was achieved by switching from 1 mM glucose to 11 mM glucose. Only β-cells expressing Cepia2mt or MitoFret were analyzed.

Seahorse Assays

Seahorse Assays were run using a Seahorse XFE96 with an Agilent Seahorse XFe96 Spheroid Microplate and Agilent Seahorse XFe96 Spheroid Flux Pak (102960-000) as previously described[170]. Whole islets were isolated from either control or β-TALK1-KO mice that had either been on a standard chow diet or a high-fat diet (HFD) (D12492; 60% kcal% fat; Research Diets, Inc.) and allowed to rest over-night in RPMI supplemented with 0.5% BSA. 15 mouse islets were seeded into wells of a CellTak coated XF96 spheroid plate containing 170 µl/well of warm assay medium (Seahorse XF base medium minimal DMEM, supplemented with 2 mM glucose and 0.1% FBS). To seed the islets, 15 islets were collected in 5 µl of RPMI. The pipette containing the 5 µl RPMI was inserted to the bottom of the spheroid well and held steady to allow the islets in the pipette to drift down towards the tip of the pipette. The pipette was then lifted straight up, allowing the islets to be pulled out of the pipette and settle directly into the bottom of the well. The plate was then allowed to incubate for 1 hour in a 37°C incubator with no CO_2. The sensor cartridge was prepped according to the protocol (Agilent 102960-000) and the assay was run with the Agilent Seahorse XF Cell Mito Stress Test Kit (103015-100).

Glucose Tolerance and Insulin Tolerance Tests

Mice were placed on either a standard chow diet or a high-fat diet (HFD) (D12492; 60% kcal% fat; Research Diets, Inc.). Glucose tolerance testing (GTT) and insulin tolerance testing (ITT) were performed as previously described[233-235]. Briefly, mice were fasted for 5-6 hours and then intraperitoneally injected with either 2mg/g body weight of dextrose in

PBS or 0.75 units/kg body weight of human regular insulin. Tail glucose measurements were then taken at the indicated time points.

Serum Insulin Measurements

Mice were fasted for 5-6 hours and then intraperitoneally injected with either 2mg/g body weight of dextrose in PBS. Tail blood samples were collected in Sarstedt EDTA coated Microvette CB 300 K2E (16.444.100) tubes at the indicated time points. Serum insulin was then measured by the Vanderbilt University Hormone Core through radioimmunoassay.

Clinical Recruitment for MODY

A four-generation family with six affected family members with autosomal dominant diabetes was identified through a non-obese proband who presented aged 15 years (Fig.1A) with elevated fasting plasma glucose (7.8 mmol/L) and an abnormal oral glucose tolerance test (glucose 19.6 mmol/L two hours after 75 g glucose). Antibody testing (islet cell, islet antigen 2, and glutamic acid decarboxylase-65) was negative. Over two decades, the proband required minimal insulin to maintain HbA1c of 5.7-6.5%; and she did not experience ketosis or other diabetes-related complications. Sanger sequencing for mutations in *GCK*, *HNF1A* and *HNF4A* (the commonest MODY genes) was negative. Other family members manifest diabetes similarly. The study protocol was approved by the relevant human research ethics committee (approval HREC/12/QPAH/109). All living family members gave written informed consent.

Exome sequencing

DNA was extracted from blood or saliva and sequencing libraries constructed according to each manufacturer's instructions. Exome capture was performed using either Nimblegen SeqCap EZ Human v3.0 Exome Enrichment Kit for the proband (Roche, Basel, Switzerland) or NexteraTM Rapid Capture Exome kit for subsequent family members (Illumina, San Diego, CA, USA). Pre- and post-capture quality and yield were assessed by Agilent High Sensitivity DNA assay (Agilent, Santa Clare, CA) using Bioanalyzer 2100 (Agilent, Santa Clare, CA) and by qPCR using the KAPA Library Quantification Kit (Kapa Biosystems, Wilmington, MA).

Multiplexed massively parallel sequencing (six samples per flowcell lane) was performed on an Illumina HiSeq 2000 for the proband or HiSeq 2500 for additional family members (Illumina, San Diego, CA, USA), generating 100-base pair paired-end reads.

Data were demultiplexed using Illumina Data Analysis Pipeline software (Bcl2fastq v1.8.4) and aligned to the current reference human genome (hg19, released February 2009) using the Novoalign alignment tool (V3.00.02). Sequence alignment files were converted using Picard tools (v1.124). Variants were called using the Genome Analysis Toolkit (GATK v2.7-2) and annotated using ANNOVAR. Further analysis of sequence data was performed using custom scripts employing R and Bioconductor.

Exome data from the proband was analyzed for good-quality likely damaging rare variants in known MODY genes[147], using a conservative minor allele frequency (MAF) threshold of <0.001, based on: (a) prevalence of pediatrics diabetes of 0.2%[236]; and (b) prevalence of MODY mutations in 2% of a pediatric diabetes population[151]; further, most MODY

mutations are private. After quality control and exclusion of artifact, good quality variants with minor allele frequency (MAF) <0.05 (assessed against internal and external databases, including ExAC1, 1000 Genomes2, and dbSNP1373) were retained for analysis.

Plasmids for TALK-1 Leu114Pro studies

Lentiviral plasmids expressing TALK-1 WT and TALK-1 Leu114Pro were designed for HEK cell and β-cell studies. A cartoon representation of the different lentiviral constructs that were utilized in these experiments is presented in Figure 3.2. For whole-cell current recordings, a lentiviral plasmid was created that contains the CMV enhancer and CMV promoter placed immediately upstream of either TALK-1 WT or TALK-1 Leu114Pro followed by a P2A cleavage site and mCherry. For the β-cell Ca^{2+} experiments, a lentiviral plasmid was created that contains the β-cell specific RIP1-mini-CMV promoter placed immediately upstream of either TALK-1 WT or TALK-1 Leu114Pro. To utilize the Nano Luc Pro-insulin Luciferase as a read-out of insulin secretion we developed lentiviral plasmids that contained the same RIP1-mini-CMV Promoter mentioned above expressing either TALK-1 WT or TALK-1 Leu114Pro followed by a P2A cleavage site and the Nano-Luc Pro-insulin Luciferase. A CMV promoter expressing GFP was also inserted into the plasmid to enable visualization of plasmid expression. The sequences for TALK-1 are those corresponding to transcript variant 3 (NM_001135105). Transcript Variant 3 was used for these experiments because it is the most highly expressed ion channel producing variant of *KCNK16* in human β-cells. Expression levels were identical between the TALK-1 WT and TALK-1 Leu114Pro constructs (Figure 3.8). Transduction efficiency was also

similar between the two constructs, approxixmately 55% for TALK-1 WT and 61% for TALK1 Leu114Pro.

TALK-1 Single Channel Currents

Single Channel currents were measured in HEK cells using attached-patch voltage-clamp technique. Electrodes were pulled to a resistance of 8 to 10 megaohms and then coated with Sigmacote. Extracellular solution contained 135 mM NaCl, 5 mM KCl, 1 mM MgCl2, 1 mM $CaCl_2$, and 10 mM Hepes (pH 7.3 with NaOH). Intracellular pipette solution contained 150 mM KCl, 1 mM MgCl2, 5 mM EGTA, and 10 mM HEPES (pH 7.3 with KOH). Single channel current openings were analyzed for open probability and current amplitude during a 5-second period of stimulation with 100 mV, 50 mV, and 0 mV. A threshold of 0.75 pA was set to determine channel openings. Only mCherry positive cells were recorded. Our reported amplitude and open probability for TALK-1 WT is similar to that previously published for TALK-1[92; 190].

β-cell V_m recordings

Mouse islet clusters transduced with TALK-1 WT-P2A-mCherry or TALK-1 Leu114Pro-P2A-mCherry were washed twice with Krebs-Ringer–HEPES buffer (KRHB) with (in mmol/L) 119.0 NaCl, 2.0 $CaCl_2$, 4.7 KCl, 25.0 HEPES, 1.2 $MgSO_4$, 1.2 KH_2PO_4 (adjusted to pH 7.4 with NaOH) supplemented with either 2 or 14 mM glucose and cultured in KRHB for 20 min at 37°C, 5% CO_2. Patch electrodes (4–6 MΩ) were filled with V_m IC with (in mmol/L) 140.0 KCl, 1.0 $MgCl_2$, and 5.0 HEPES (adjusted to pH 7.2 with KOH) supplemented with 20 μg/mL amphotericin B. The V_m of individual mCherry positive β-

cells within islet clusters (10–20 cells) was recorded in current clamp mode using an Axopatch 200B amplifier with pCLAMP10 software. The electrical activity of patched β-cells was recorded in response to treatments indicated in figure legends. Cells were identified as β-cells if electrical activity ceased with 2 mM glucose.

Insulin Secretion Measurements

Islet clusters were cultured in a 96-well plate at 20 islet equivalents per well. Islet clusters were transduced as described above with lentiviral plasmids that contained the RIP1-mini-CMV Promoter[17] expressing either TALK-1 WT or TALK-1 Leu114Pro (Chapter III) or TALK-1 R13Q (Chapter IV) followed by a P2A cleavage site and the Nano-Luc Pro-insulin Luciferase[219; 220]. The islet clusters were starved for one hour in 100ul media (DMEM) containing 5 mM glucose before running the assay. The assay was then run using the protocol for Promega Nano-Glo® Luciferase Assay System. In short, the starvation media is replaced with fresh media containing 5mM glucose and the islet clusters are allowed to secrete for one hour. The media is then collected and replaced with media containing 14 mM glucose and the islet clusters are again allowed to secrete for one hour. After the secretion the cells are lysed and collected. The total lysate, the 5 mM glucose secretion media, and 14 mM glucose secretion media are mixed with the Promega Nano-Glo® substrate and imaged for luminescence using a BioTek Synergy™ H4 Hybrid Microplate Reader. Luminescence from the low and high glucose secretion media were divided by total luminescence from the lysate.

Human Islet Cells

Human islets were obtained for the Nano-Luc Pro-insulin Luciferase studies from the Integrated Islet Distribution Program (IIDP). Human donors were both male and female as well as from multiple ethnic backgrounds. Information on each human donor is presented in Table 6.1.

Plasmids for TALK1-R13Q studies

Plasmids expressing TALK-1 WT and TALK-1 R13Q were designed for HEK cell and β-cell studies. For whole-cell current recordings, a plasmid was created that contains the CMV enhancer and CMV promoter placed immediately upstream of either TALK-1 WT or TALK-1 R13Q. For the β-cell Ca^{2+} experiments, a lentiviral plasmid was created that contains the β-cell specific RIP1-mini-CMV promoter[237] placed immediately upstream of either TALK-1 WT or TALK-1 Leu114Pro. To utilize the Nano Luc Pro-insulin Luciferase as a read-out of insulin secretion we developed lentiviral plasmids that contained the same RIP1-mini-CMV Promoter mentioned above expressing either TALK-1 WT or TALK-1 Leu114Pro followed by a P2A cleavage site and the Nano-Luc Pro-insulin Luciferase. A CMV promoter expressing GFP was also inserted into the plasmid to enable visualization of plasmid expression. The sequences for TALK-1 are those corresponding to transcript variant 3 (NM_001135105).

Table 6.1. Human islet donor information.

Human islets received for human insulin secretion studies from the Integrated Islet Distribution Program.

Islet Isolation Center	Age	Gender	Ethnicity	Weight (kg)	Height (cm)	BMI	Cause of Death	Purity (%)	Average blood glucose in mmol/L
Southern California	53	Male	White	83.9	182.9	25.1	Stroke	96	6.2
Southern California	51	Male	White	76	177.8	24.0	Head Trauma	96	7.8
Miami	57	Female	Black	79.5	165.0	29.2	Stroke	95	9.6
Scharp/Lacy	50	Male	Hispanic	83.9	160.0	32.8	Anoxia	90	7.5
Scharp/Lacy	57	Male	Hispanic	72.6	167.6	25.8	Stroke	95	7.8
Wisconsin	53	Female	White	38.1	145.0	40.0	Stroke	92	7.0
Scharp/Lacy	45	Male	Black	106.1	180.3	32.6	Anoxia	95	7.3
Southern California	33	Male	White	106.4	179.0	33.2	Anoxia	80	7.8

*1 mg/dL = 0.0555 mmol/L

TALK-1 Nuclear Patch Clamp Single Channel Currents

Nuclear patch clamp experiments were performed using the approach described by Mak and colleagues[213]. Briefly, HEK293 cells were transfected as described above, lifted from the cell culture plate, and then disturbed with a pestle to pop out the nuclei. The isolated nuclei were patched in a solution containing 150 mM KCl, 10 mM Hepes, 0.5 mM EGTA, and 0.36 mM $CaCl_2$ (pH 7.3 with KOH). Patch electrodes were pulled to a resistance of 8 to 10 megaohms, loaded with recording solution, and coated with Sigmacote. Single-channel currents were low-pass–filtered at 1 kHz and sampled at 50 kHz. Our reported amplitude and open probability for TALK-1 WT on the ER-membrane is similar to that previously published for TALK-1[65].

Real-time quantitative polymerase chain reaction

qRT-PCR of mouse islet cDNA was performed according to previous described methods[53].

ATF6 ER-stress luciferase assay

INS-1 (832/13) cells were cultured in RPMI 1640 supplemented with 15% fetal bovine serum and penicillin-streptomycin and then transfected (as described above) with p5xATF6-GL3[222] (#11976, Addgene) and plasmids encoding TALK-1 WT, TALK-1 R13Q, or TALK-1 DN. Cells were incubated overnight with vehicle (DMSO) or tunicamycin (0.25 µg/ml) for 16 to 20 hours before performing a luciferase assay using the Steady-Glo Luciferase Assay System (Promega) according to the manufacturer's instructions.

Immunofluorescence Staining

Islet clusters were transduced (as described above) with a virus containing a RIP promoter expressing either TALK-1 WT or TALK1- R13Q followed by a P2A cleavage site and the Nanoluc-proinsulin luciferase. The clusters were then fixed with 4% paraformaldehyde and stained with a primary antibody against NanoLuc® Luciferase (R&D Systems MAB100261).

Statistical Analyses

Functional data were analyzed using Clampfit, GraphPad Prism, or Microsoft Excel and presented as mean ± SEM. Statistical significance was determined using Student's *t*-test; a two-sided *P*-value ≤0.05 was considered statistically significant.

References

1. Gerich, J.E. (2000). Physiology of glucose homeostasis. Diabetes Obes Metab 2, 345-350.
2. Vlassara, H., and Striker, G.E. (2013). Advanced glycation endproducts in diabetes and diabetic complications. Endocrinol Metab Clin North Am 42, 697-719.
3. Wolff, S.P., Jiang, Z.Y., and Hunt, J.V. (1991). Protein glycation and oxidative stress in diabetes mellitus and ageing. Free Radic Biol Med 10, 339-352.
4. Xia, L., Wang, H., Munk, S., Frecker, H., Goldberg, H.J., Fantus, I.G., and Whiteside, C.I. (2007). Reactive oxygen species, PKC-beta1, and PKC-zeta mediate high-glucose-induced vascular endothelial growth factor expression in mesangial cells. Am J Physiol Endocrinol Metab 293, E1280-1288.
5. Xia, L., Wang, H., Munk, S., Kwan, J., Goldberg, H.J., Fantus, I.G., and Whiteside, C.I. (2008). High glucose activates PKC-zeta and NADPH oxidase through autocrine TGF-beta1 signaling in mesangial cells. Am J Physiol Renal Physiol 295, F1705-1714.
6. Nishikawa, T., Edelstein, D., Du, X.L., Yamagishi, S., Matsumura, T., Kaneda, Y., Yorek, M.A., Beebe, D., Oates, P.J., Hammes, H.P., et al. (2000). Normalizing mitochondrial superoxide production blocks three pathways of hyperglycaemic damage. Nature 404, 787-790.
7. Du, X.L., Edelstein, D., Rossetti, L., Fantus, I.G., Goldberg, H., Ziyadeh, F., Wu, J., and Brownlee, M. (2000). Hyperglycemia-induced mitochondrial superoxide overproduction activates the hexosamine pathway and induces plasminogen activator inhibitor-1 expression by increasing Sp1 glycosylation. Proc Natl Acad Sci U S A 97, 12222-12226.
8. Brownlee, M. (2005). The pathobiology of diabetic complications: a unifying mechanism. Diabetes 54, 1615-1625.
9. Sakula, A. (1988). Paul Langerhans (1847-1888): a centenary tribute. J R Soc Med 81, 414-415.
10. Edgerton, D.S., Lautz, M., Scott, M., Everett, C.A., Stettler, K.M., Neal, D.W., Chu, C.A., and Cherrington, A.D. (2006). Insulin's direct effects on the liver dominate the control of hepatic glucose production. J Clin Invest 116, 521-527.
11. Ramnanan, C.J., Edgerton, D.S., Kraft, G., and Cherrington, A.D. (2011). Physiologic action of glucagon on liver glucose metabolism. Diabetes Obes Metab 13 Suppl 1, 118-125.
12. Hausler, N., Browning, J., Merritt, M., Storey, C., Milde, A., Jeffrey, F.M., Sherry, A.D., Malloy, C.R., and Burgess, S.C. (2006). Effects of insulin and cytosolic redox state on glucose production pathways in the isolated perfused mouse liver measured by integrated 2H and 13C NMR. Biochem J 394, 465-473.
13. Kido, Y., Nakae, J., and Accili, D. (2001). Clinical review 125: The insulin receptor and its cellular targets. J Clin Endocrinol Metab 86, 972-979.
14. Cunha, V.N., de Paula Lima, M., Motta-Santos, D., Pesquero, J.L., de Andrade, R.V., de Almeida, J.A., Araujo, R.C., Grubert Campbell, C.S., Lewis, J.E., and Simoes, H.G. (2015). Role of exercise intensity on GLUT4 content, aerobic fitness and fasting plasma glucose in type 2 diabetic mice. Cell Biochem Funct 33, 435-442.
15. Kawamori, D., Kurpad, A.J., Hu, J., Liew, C.W., Shih, J.L., Ford, E.L., Herrera, P.L., Polonsky, K.S., McGuinness, O.P., and Kulkarni, R.N. (2009). Insulin signaling in alpha cells modulates glucagon secretion in vivo. Cell Metab 9, 350-361.
16. Agius, L. (2015). Role of glycogen phosphorylase in liver glycogen metabolism. Mol Aspects Med 46, 34-45.
17. Gelling, R.W., Du, X.Q., Dichmann, D.S., Romer, J., Huang, H., Cui, L., Obici, S., Tang, B., Holst, J.J., Fledelius, C., et al. (2003). Lower blood glucose, hyperglucagonemia, and pancreatic alpha cell hyperplasia in glucagon receptor knockout mice. Proc Natl Acad Sci U S A 100, 1438-1443.

18. Svendsen, B., Larsen, O., Gabe, M.B.N., Christiansen, C.B., Rosenkilde, M.M., Drucker, D.J., and Holst, J.J. (2018). Insulin Secretion Depends on Intra-islet Glucagon Signaling. Cell Rep 25, 1127-1134 e1122.
19. Zhu, L., Dattaroy, D., Pham, J., Wang, L., Barella, L.F., Cui, Y., Wilkins, K.J., Roth, B.L., Hochgeschwender, U., Matschinsky, F.M., et al. (2019). Intra-islet glucagon signaling is critical for maintaining glucose homeostasis. JCI Insight 5.
20. Svendsen, B., and Holst, J.J. (2021). Paracrine regulation of somatostatin secretion by insulin and glucagon in mouse pancreatic islets. Diabetologia 64, 142-151.
21. Vergari, E., Knudsen, J.G., Ramracheya, R., Salehi, A., Zhang, Q., Adam, J., Asterholm, I.W., Benrick, A., Briant, L.J.B., Chibalina, M.V., et al. (2019). Insulin inhibits glucagon release by SGLT2-induced stimulation of somatostatin secretion. Nat Commun 10, 139.
22. Smith, P.A., Sellers, L.A., and Humphrey, P.P. (2001). Somatostatin activates two types of inwardly rectifying K+ channels in MIN-6 cells. J Physiol 532, 127-142.
23. Kailey, B., van de Bunt, M., Cheley, S., Johnson, P.R., MacDonald, P.E., Gloyn, A.L., Rorsman, P., and Braun, M. (2012). SSTR2 is the functionally dominant somatostatin receptor in human pancreatic beta- and alpha-cells. Am J Physiol Endocrinol Metab 303, E1107-1116.
24. Elliott, A.D., Ustione, A., and Piston, D.W. (2015). Somatostatin and insulin mediate glucose-inhibited glucagon secretion in the pancreatic alpha-cell by lowering cAMP. Am J Physiol Endocrinol Metab 308, E130-143.
25. Gromada, J., Hoy, M., Buschard, K., Salehi, A., and Rorsman, P. (2001). Somatostatin inhibits exocytosis in rat pancreatic alpha-cells by G(i2)-dependent activation of calcineurin and depriming of secretory granules. J Physiol 535, 519-532.
26. Yoshimoto, Y., Fukuyama, Y., Horio, Y., Inanobe, A., Gotoh, M., and Kurachi, Y. (1999). Somatostatin induces hyperpolarization in pancreatic islet alpha cells by activating a G protein-gated K+ channel. FEBS Lett 444, 265-269.
27. Rorsman, P., and Ashcroft, F.M. (2018). Pancreatic beta-Cell Electrical Activity and Insulin Secretion: Of Mice and Men. Physiol Rev 98, 117-214.
28. Brissova, M., Fowler, M.J., Nicholson, W.E., Chu, A., Hirshberg, B., Harlan, D.M., and Powers, A.C. (2005). Assessment of human pancreatic islet architecture and composition by laser scanning confocal microscopy. J Histochem Cytochem 53, 1087-1097.
29. Hart, N.J., and Powers, A.C. (2019). Use of human islets to understand islet biology and diabetes: progress, challenges and suggestions. Diabetologia 62, 212-222.
30. Osipovich, A.B., Stancill, J.S., Cartailler, J.P., Dudek, K.D., and Magnuson, M.A. (2020). Excitotoxicity and Overnutrition Additively Impair Metabolic Function and Identity of Pancreatic beta-Cells. Diabetes 69, 1476-1491.
31. Taborsky, G.J., Jr. (2011). Islets have a lot of nerve! Or do they? Cell Metab 14, 5-6.
32. Rodriguez-Diaz, R., Abdulreda, M.H., Formoso, A.L., Gans, I., Ricordi, C., Berggren, P.O., and Caicedo, A. (2011). Innervation patterns of autonomic axons in the human endocrine pancreas. Cell Metab 14, 45-54.
33. Ahren, B. (2000). Autonomic regulation of islet hormone secretion--implications for health and disease. Diabetologia 43, 393-410.
34. Rosengren, A.H., Jokubka, R., Tojjar, D., Granhall, C., Hansson, O., Li, D.Q., Nagaraj, V., Reinbothe, T.M., Tuncel, J., Eliasson, L., et al. (2010). Overexpression of alpha2A-adrenergic receptors contributes to type 2 diabetes. Science 327, 217-220.
35. Henderson, J.R., and Moss, M.C. (1985). A morphometric study of the endocrine and exocrine capillaries of the pancreas. Q J Exp Physiol 70, 347-356.
36. Saito, K., Yaginuma, N., and Takahashi, T. (1979). Differential volumetry of A, B and D cells in the pancreatic islets of diabetic and nondiabetic subjects. Tohoku J Exp Med 129, 273-283.

37. Saunders, D., and Powers, A.C. (2016). Replicative capacity of beta-cells and type 1 diabetes. J Autoimmun 71, 59-68.
38. Nichols, C.G. (2006). KATP channels as molecular sensors of cellular metabolism. Nature 440, 470-476.
39. Yang, S.N., and Berggren, P.O. (2006). The role of voltage-gated calcium channels in pancreatic beta-cell physiology and pathophysiology. Endocr Rev 27, 621-676.
40. Rorsman, P., Braun, M., and Zhang, Q. (2012). Regulation of calcium in pancreatic alpha- and beta-cells in health and disease. Cell Calcium 51, 300-308.
41. Wiser, O., Trus, M., Hernandez, A., Renstrom, E., Barg, S., Rorsman, P., and Atlas, D. (1999). The voltage sensitive Lc-type Ca2+ channel is functionally coupled to the exocytotic machinery. Proc Natl Acad Sci U S A 96, 248-253.
42. Wheeler, M.B., Sheu, L., Ghai, M., Bouquillon, A., Grondin, G., Weller, U., Beaudoin, A.R., Bennett, M.K., Trimble, W.S., and Gaisano, H.Y. (1996). Characterization of SNARE protein expression in beta cell lines and pancreatic islets. Endocrinology 137, 1340-1348.
43. Nagamatsu, S., Nakamichi, Y., Yamamura, C., Matsushima, S., Watanabe, T., Ozawa, S., Furukawa, H., and Ishida, H. (1999). Decreased expression of t-SNARE, syntaxin 1, and SNAP-25 in pancreatic beta-cells is involved in impaired insulin secretion from diabetic GK rat islets: restoration of decreased t-SNARE proteins improves impaired insulin secretion. Diabetes 48, 2367-2373.
44. Jahn, R., and Fasshauer, D. (2012). Molecular machines governing exocytosis of synaptic vesicles. Nature 490, 201-207.
45. Trexler, A.J., and Taraska, J.W. (2017). Regulation of insulin exocytosis by calcium-dependent protein kinase C in beta cells. Cell Calcium 67, 1-10.
46. Gilon, P., Chae, H.Y., Rutter, G.A., and Ravier, M.A. (2014). Calcium signaling in pancreatic beta-cells in health and in Type 2 diabetes. Cell Calcium 56, 340-361.
47. Dickerson, M.T., Bogart, A.M., Altman, M.K., Milian, S.C., Jordan, K.L., Dadi, P.K., and Jacobson, D.A. (2018). Cytokine-mediated changes in K(+) channel activity promotes an adaptive Ca(2+) response that sustains beta-cell insulin secretion during inflammation. Sci Rep 8, 1158.
48. Van Coppenolle, F., Vanden Abeele, F., Slomianny, C., Flourakis, M., Hesketh, J., Dewailly, E., and Prevarskaya, N. (2004). Ribosome-translocon complex mediates calcium leakage from endoplasmic reticulum stores. J Cell Sci 117, 4135-4142.
49. Luciani, D.S., Gwiazda, K.S., Yang, T.L., Kalynyak, T.B., Bychkivska, Y., Frey, M.H., Jeffrey, K.D., Sampaio, A.V., Underhill, T.M., and Johnson, J.D. (2009). Roles of IP3R and RyR Ca2+ channels in endoplasmic reticulum stress and beta-cell death. Diabetes 58, 422-432.
50. Kono, T., Tong, X., Taleb, S., Bone, R.N., Iida, H., Lee, C.C., Sohn, P., Gilon, P., Roe, M.W., and Evans-Molina, C. (2018). Impaired Store-Operated Calcium Entry and STIM1 Loss Lead to Reduced Insulin Secretion and Increased Endoplasmic Reticulum Stress in the Diabetic beta-Cell. Diabetes 67, 2293-2304.
51. Ravier, M.A., Daro, D., Roma, L.P., Jonas, J.C., Cheng-Xue, R., Schuit, F.C., and Gilon, P. (2011). Mechanisms of control of the free Ca2+ concentration in the endoplasmic reticulum of mouse pancreatic beta-cells: interplay with cell metabolism and [Ca2+]c and role of SERCA2b and SERCA3. Diabetes 60, 2533-2545.
52. Fridlyand, L.E., Tamarina, N., and Philipson, L.H. (2010). Bursting and calcium oscillations in pancreatic beta-cells: specific pacemakers for specific mechanisms. Am J Physiol Endocrinol Metab 299, E517-532.
53. Tong, X., Kono, T., Anderson-Baucum, E.K., Yamamoto, W., Gilon, P., Lebeche, D., Day, R.N., Shull, G.E., and Evans-Molina, C. (2016). SERCA2 Deficiency Impairs Pancreatic beta-Cell Function in Response to Diet-Induced Obesity. Diabetes 65, 3039-3052.

54. Yamamoto, W.R., Bone, R.N., Sohn, P., Syed, F., Reissaus, C.A., Mosley, A.L., Wijeratne, A.B., True, J.D., Tong, X., Kono, T., et al. (2019). Endoplasmic reticulum stress alters ryanodine receptor function in the murine pancreatic beta cell. J Biol Chem 294, 168-181.
55. McBride, H.M., Neuspiel, M., and Wasiak, S. (2006). Mitochondria: more than just a powerhouse. Curr Biol 16, R551-560.
56. Tarasov, A.I., Semplici, F., Li, D., Rizzuto, R., Ravier, M.A., Gilon, P., and Rutter, G.A. (2013). Frequency-dependent mitochondrial Ca(2+) accumulation regulates ATP synthesis in pancreatic beta cells. Pflugers Arch 465, 543-554.
57. Merrins, M.J., Fendler, B., Zhang, M., Sherman, A., Bertram, R., and Satin, L.S. (2010). Metabolic oscillations in pancreatic islets depend on the intracellular Ca2+ level but not Ca2+ oscillations. Biophys J 99, 76-84.
58. Merrins, M.J., Poudel, C., McKenna, J.P., Ha, J., Sherman, A., Bertram, R., and Satin, L.S. (2016). Phase Analysis of Metabolic Oscillations and Membrane Potential in Pancreatic Islet beta-Cells. Biophys J 110, 691-699.
59. Giacomello, M., Drago, I., Bortolozzi, M., Scorzeto, M., Gianelle, A., Pizzo, P., and Pozzan, T. (2010). Ca2+ hot spots on the mitochondrial surface are generated by Ca2+ mobilization from stores, but not by activation of store-operated Ca2+ channels. Mol Cell 38, 280-290.
60. Tamarina, N.A., Wang, Y., Mariotto, L., Kuznetsov, A., Bond, C., Adelman, J., and Philipson, L.H. (2003). Small-conductance calcium-activated K+ channels are expressed in pancreatic islets and regulate glucose responses. Diabetes 52, 2000-2006.
61. Gopel, S.O., Kanno, T., Barg, S., Eliasson, L., Galvanovskis, J., Renstrom, E., and Rorsman, P. (1999). Activation of Ca(2+)-dependent K(+) channels contributes to rhythmic firing of action potentials in mouse pancreatic beta cells. J Gen Physiol 114, 759-770.
62. Zhang, M., Houamed, K., Kupershmidt, S., Roden, D., and Satin, L.S. (2005). Pharmacological properties and functional role of Kslow current in mouse pancreatic beta-cells: SK channels contribute to Kslow tail current and modulate insulin secretion. J Gen Physiol 126, 353-363.
63. Houamed, K.M., Sweet, I.R., and Satin, L.S. (2010). BK channels mediate a novel ionic mechanism that regulates glucose-dependent electrical activity and insulin secretion in mouse pancreatic beta-cells. J Physiol 588, 3511-3523.
64. Jacobson, D.A., Mendez, F., Thompson, M., Torres, J., Cochet, O., and Philipson, L.H. (2010). Calcium-activated and voltage-gated potassium channels of the pancreatic islet impart distinct and complementary roles during secretagogue induced electrical responses. J Physiol 588, 3525-3537.
65. Vierra, N.C., Dadi, P.K., Milian, S.C., Dickerson, M.T., Jordan, K.L., Gilon, P., and Jacobson, D.A. (2017). TALK-1 channels control beta cell endoplasmic reticulum Ca(2+) homeostasis. Science signaling 10.
66. MacDonald, P.E., Ha, X.F., Wang, J., Smukler, S.R., Sun, A.M., Gaisano, H.Y., Salapatek, A.M., Backx, P.H., and Wheeler, M.B. (2001). Members of the Kv1 and Kv2 voltage-dependent K(+) channel families regulate insulin secretion. Mol Endocrinol 15, 1423-1435.
67. MacDonald, P.E., Sewing, S., Wang, J., Joseph, J.W., Smukler, S.R., Sakellaropoulos, G., Wang, J., Saleh, M.C., Chan, C.B., Tsushima, R.G., et al. (2002). Inhibition of Kv2.1 voltage-dependent K+ channels in pancreatic beta-cells enhances glucose-dependent insulin secretion. J Biol Chem 277, 44938-44945.
68. Kelly, R.P., Sutton, R., and Ashcroft, F.M. (1991). Voltage-activated calcium and potassium currents in human pancreatic beta-cells. J Physiol 443, 175-192.
69. Li, Y., Um, S.Y., and McDonald, T.V. (2006). Voltage-gated potassium channels: regulation by accessory subunits. Neuroscientist 12, 199-210.

70. Yazawa, M., Ferrante, C., Feng, J., Mio, K., Ogura, T., Zhang, M., Lin, P.H., Pan, Z., Komazaki, S., Kato, K., et al. (2007). TRIC channels are essential for Ca2+ handling in intracellular stores. Nature 448, 78-82.
71. Yamazaki, D., Komazaki, S., Nakanishi, H., Mishima, A., Nishi, M., Yazawa, M., Yamazaki, T., Taguchi, R., and Takeshima, H. (2009). Essential role of the TRIC-B channel in Ca2+ handling of alveolar epithelial cells and in perinatal lung maturation. Development 136, 2355-2361.
72. Kuum, M., Veksler, V., Liiv, J., Ventura-Clapier, R., and Kaasik, A. (2012). Endoplasmic reticulum potassium-hydrogen exchanger and small conductance calcium-activated potassium channel activities are essential for ER calcium uptake in neurons and cardiomyocytes. J Cell Sci 125, 625-633.
73. Goldstein, S.A., Bockenhauer, D., O'Kelly, I., and Zilberberg, N. (2001). Potassium leak channels and the KCNK family of two-P-domain subunits. Nat Rev Neurosci 2, 175-184.
74. Feliciangeli, S., Chatelain, F.C., Bichet, D., and Lesage, F. (2015). The family of K2P channels: salient structural and functional properties. J Physiol 593, 2587-2603.
75. Schewe, M., Nematian-Ardestani, E., Sun, H., Musinszki, M., Cordeiro, S., Bucci, G., de Groot, B.L., Tucker, S.J., Rapedius, M., and Baukrowitz, T. (2016). A Non-canonical Voltage-Sensing Mechanism Controls Gating in K2P K(+) Channels. Cell 164, 937-949.
76. Czirjak, G., Toth, Z.E., and Enyedi, P. (2004). The two-pore domain K+ channel, TRESK, is activated by the cytoplasmic calcium signal through calcineurin. J Biol Chem 279, 18550-18558.
77. Lesage, F., and Lazdunski, M. (2000). Molecular and functional properties of two-pore-domain potassium channels. Am J Physiol Renal Physiol 279, F793-801.
78. Patel, A.J., and Honore, E. (2001). Properties and modulation of mammalian 2P domain K+ channels. Trends Neurosci 24, 339-346.
79. Vierra, N.C., Dadi, P.K., Jeong, I., Dickerson, M., Powell, D.R., and Jacobson, D.A. (2015). Type 2 Diabetes-Associated K+ Channel TALK-1 Modulates beta-Cell Electrical Excitability, Second-Phase Insulin Secretion, and Glucose Homeostasis. Diabetes 64, 3818-3828.
80. Niemeyer, M.I., Cid, L.P., Gonzalez, W., and Sepulveda, F.V. (2016). Gating, Regulation, and Structure in K2P K+ Channels: In Varietate Concordia? Mol Pharmacol 90, 309-317.
81. Cohen, A., Ben-Abu, Y., Hen, S., and Zilberberg, N. (2008). A novel mechanism for human K2P2.1 channel gating. Facilitation of C-type gating by protonation of extracellular histidine residues. J Biol Chem 283, 19448-19455.
82. Zilberberg, N., Ilan, N., and Goldstein, S.A. (2001). KCNKO: opening and closing the 2-P-domain potassium leak channel entails "C-type" gating of the outer pore. Neuron 32, 635-648.
83. Yellen, G. (1998). The moving parts of voltage-gated ion channels. Q Rev Biophys 31, 239-295.
84. Lesage, F., Guillemare, E., Fink, M., Duprat, F., Lazdunski, M., Romey, G., and Barhanin, J. (1996). TWIK-1, a ubiquitous human weakly inward rectifying K+ channel with a novel structure. EMBO J 15, 1004-1011.
85. Arrighi, I., Lesage, F., Scimeca, J.C., Carle, G.F., and Barhanin, J. (1998). Structure, chromosome localization, and tissue distribution of the mouse twik K+ channel gene. FEBS Lett 425, 310-316.
86. Chatelain, F.C., Bichet, D., Douguet, D., Feliciangeli, S., Bendahhou, S., Reichold, M., Warth, R., Barhanin, J., and Lesage, F. (2012). TWIK1, a unique background channel with variable ion selectivity. Proc Natl Acad Sci U S A 109, 5499-5504.
87. Duprat, F., Lesage, F., Fink, M., Reyes, R., Heurteaux, C., and Lazdunski, M. (1997). TASK, a human background K+ channel to sense external pH variations near physiological pH. EMBO J 16, 5464-5471.
88. Dadi, P.K., Vierra, N.C., and Jacobson, D.A. (2014). Pancreatic beta-cell-specific ablation of TASK-1 channels augments glucose-stimulated calcium entry and insulin secretion, improving glucose tolerance. Endocrinology 155, 3757-3768.

89. Dadi, P.K., Luo, B., Vierra, N.C., and Jacobson, D.A. (2015). TASK-1 Potassium Channels Limit Pancreatic alpha-Cell Calcium Influx and Glucagon Secretion. Mol Endocrinol 29, 777-787.
90. Renigunta, V., Yuan, H., Zuzarte, M., Rinne, S., Koch, A., Wischmeyer, E., Schlichthorl, G., Gao, Y., Karschin, A., Jacob, R., et al. (2006). The retention factor p11 confers an endoplasmic reticulum-localization signal to the potassium channel TASK-1. Traffic 7, 168-181.
91. Kilisch, M., Lytovchenko, O., Schwappach, B., Renigunta, V., and Daut, J. (2015). The role of protein-protein interactions in the intracellular traffic of the potassium channels TASK-1 and TASK-3. Pflugers Arch 467, 1105-1120.
92. Girard, C., Duprat, F., Terrenoire, C., Tinel, N., Fosset, M., Romey, G., Lazdunski, M., and Lesage, F. (2001). Genomic and functional characteristics of novel human pancreatic 2P domain K(+) channels. Biochem Biophys Res Commun 282, 249-256.
93. Lawlor, N., George, J., Bolisetty, M., Kursawe, R., Sun, L., Sivakamasundari, V., Kycia, I., Robson, P., and Stitzel, M.L. (2017). Single-cell transcriptomes identify human islet cell signatures and reveal cell-type-specific expression changes in type 2 diabetes. Genome Res 27, 208-222.
94. Ku, G.M., Kim, H., Vaughn, I.W., Hangauer, M.J., Myung Oh, C., German, M.S., and McManus, M.T. (2012). Research resource: RNA-Seq reveals unique features of the pancreatic beta-cell transcriptome. Mol Endocrinol 26, 1783-1792.
95. Benner, C., van der Meulen, T., Caceres, E., Tigyi, K., Donaldson, C.J., and Huising, M.O. (2014). The transcriptional landscape of mouse beta cells compared to human beta cells reveals notable species differences in long non-coding RNA and protein-coding gene expression. BMC Genomics 15, 620.
96. Stitzel, M.L., Sethupathy, P., Pearson, D.S., Chines, P.S., Song, L., Erdos, M.R., Welch, R., Parker, S.C., Boyle, A.P., Scott, L.J., et al. (2010). Global epigenomic analysis of primary human pancreatic islets provides insights into type 2 diabetes susceptibility loci. Cell Metab 12, 443-455.
97. Han, J., Kang, D., and Kim, D. (2003). Functional properties of four splice variants of a human pancreatic tandem-pore K+ channel, TALK-1. Am J Physiol Cell Physiol 285, C529-538.
98. Cho, Y.S., Chen, C.H., Hu, C., Long, J., Ong, R.T., Sim, X., Takeuchi, F., Wu, Y., Go, M.J., Yamauchi, T., et al. (2011). Meta-analysis of genome-wide association studies identifies eight new loci for type 2 diabetes in east Asians. Nat Genet 44, 67-72.
99. Replication, D.I.G., Meta-analysis, C., Asian Genetic Epidemiology Network Type 2 Diabetes, C., South Asian Type 2 Diabetes, C., Mexican American Type 2 Diabetes, C., Type 2 Diabetes Genetic Exploration by Nex-generation sequencing in muylti-Ethnic Samples, C., Mahajan, A., Go, M.J., Zhang, W., Below, J.E., et al. (2014). Genome-wide trans-ancestry meta-analysis provides insight into the genetic architecture of type 2 diabetes susceptibility. Nat Genet 46, 234-244.
100. Scharfmann, R., Pechberty, S., Hazhouz, Y., von Bulow, M., Bricout-Neveu, E., Grenier-Godard, M., Guez, F., Rachdi, L., Lohmann, M., Czernichow, P., et al. (2014). Development of a conditionally immortalized human pancreatic beta cell line. J Clin Invest 124, 2087-2098.
101. Ravassard, P., Hazhouz, Y., Pechberty, S., Bricout-Neveu, E., Armanet, M., Czernichow, P., and Scharfmann, R. (2011). A genetically engineered human pancreatic beta cell line exhibiting glucose-inducible insulin secretion. J Clin Invest 121, 3589-3597.
102. Hastoy, B., Godazgar, M., Clark, A., Nylander, V., Spiliotis, I., van de Bunt, M., Chibalina, M.V., Barrett, A., Burrows, C., Tarasov, A.I., et al. (2018). Electrophysiological properties of human beta-cell lines EndoC-betaH1 and -betaH2 conform with human beta-cells. Sci Rep 8, 16994.
103. Ndiaye, F.K., Ortalli, A., Canouil, M., Huyvaert, M., Salazar-Cardozo, C., Lecoeur, C., Verbanck, M., Pawlowski, V., Boutry, R., Durand, E., et al. (2017). Expression and functional assessment of candidate type 2 diabetes susceptibility genes identify four new genes contributing to human insulin secretion. Mol Metab 6, 459-470.

104. Dickerson, M.T., Vierra, N.C., Milian, S.C., Dadi, P.K., and Jacobson, D.A. (2017). Osteopontin activates the diabetes-associated potassium channel TALK-1 in pancreatic beta-cells. PLoS One 12, e0175069.
105. Huttlin, E.L., Ting, L., Bruckner, R.J., Gebreab, F., Gygi, M.P., Szpyt, J., Tam, S., Zarraga, G., Colby, G., Baltier, K., et al. (2015). The BioPlex Network: A Systematic Exploration of the Human Interactome. Cell 162, 425-440.
106. Adriaenssens, A.E., Svendsen, B., Lam, B.Y., Yeo, G.S., Holst, J.J., Reimann, F., and Gribble, F.M. (2016). Transcriptomic profiling of pancreatic alpha, beta and delta cell populations identifies delta cells as a principal target for ghrelin in mouse islets. Diabetologia 59, 2156-2165.
107. Zhang, Q., Bengtsson, M., Partridge, C., Salehi, A., Braun, M., Cox, R., Eliasson, L., Johnson, P.R., Renstrom, E., Schneider, T., et al. (2007). R-type Ca(2+)-channel-evoked CICR regulates glucose-induced somatostatin secretion. Nat Cell Biol 9, 453-460.
108. Vierra, N.C., Dickerson, M.T., Jordan, K.L., Dadi, P.K., Katdare, K.A., Altman, M.K., Milian, S.C., and Jacobson, D.A. (2018). TALK-1 reduces delta-cell endoplasmic reticulum and cytoplasmic calcium levels limiting somatostatin secretion. Mol Metab 9, 84-97.
109. Guthrie, R.A., and Guthrie, D.W. (2004). Pathophysiology of diabetes mellitus. Crit Care Nurs Q 27, 113-125.
110. Cheung, N., Mitchell, P., and Wong, T.Y. (2010). Diabetic retinopathy. Lancet 376, 124-136.
111. Nyenwe, E.A., and Kitabchi, A.E. (2016). The evolution of diabetic ketoacidosis: An update of its etiology, pathogenesis and management. Metabolism 65, 507-521.
112. Deli, G., Bosnyak, E., Pusch, G., Komoly, S., and Feher, G. (2013). Diabetic neuropathies: diagnosis and management. Neuroendocrinology 98, 267-280.
113. American Diabetes, A. (2013). Diagnosis and classification of diabetes mellitus. Diabetes Care 36 Suppl 1, S67-74.
114. Henning, R.J. (2018). Type-2 diabetes mellitus and cardiovascular disease. Future Cardiol 14, 491-509.
115. Maqbool, M., Cooper, M.E., and Jandeleit-Dahm, K.A.M. (2018). Cardiovascular Disease and Diabetic Kidney Disease. Semin Nephrol 38, 217-232.
116. Thomas, M.C., Brownlee, M., Susztak, K., Sharma, K., Jandeleit-Dahm, K.A., Zoungas, S., Rossing, P., Groop, P.H., and Cooper, M.E. (2015). Diabetic kidney disease. Nat Rev Dis Primers 1, 15018.
117. World Health Organization. (2020). Diabetes. In. (
118. Feng, Y., Liu, J., Wang, M., Liu, M., Shi, L., Yuan, W., Ye, J., Hu, D., and Wan, J. (2017). The E23K variant of the Kir6.2 subunit of the ATP-sensitive potassium channel increases susceptibility to ventricular arrhythmia in response to ischemia in rats. Int J Cardiol 232, 192-198.
119. Villareal, D.T., Koster, J.C., Robertson, H., Akrouh, A., Miyake, K., Bell, G.I., Patterson, B.W., Nichols, C.G., and Polonsky, K.S. (2009). Kir6.2 variant E23K increases ATP-sensitive K+ channel activity and is associated with impaired insulin release and enhanced insulin sensitivity in adults with normal glucose tolerance. Diabetes 58, 1869-1878.
120. Haghvirdizadeh, P., Mohamed, Z., Abdullah, N.A., Haghvirdizadeh, P., Haerian, M.S., and Haerian, B.S. (2015). KCNJ11: Genetic Polymorphisms and Risk of Diabetes Mellitus. J Diabetes Res 2015, 908152.
121. Rizvi, S., Raza, S.T., Mahdi, F., Singh, S.P., Rajput, M., and Rahman, Q. (2018). Genetic polymorphisms in KCNJ11 (E23K, rs5219) and SDF-1beta (G801A, rs1801157) genes are associated with the risk of type 2 diabetes mellitus. Br J Biomed Sci 75, 139-144.
122. Okamoto, K., Iwasaki, N., Doi, K., Noiri, E., Iwamoto, Y., Uchigata, Y., Fujita, T., and Tokunaga, K. (2012). Inhibition of glucose-stimulated insulin secretion by KCNJ15, a newly identified susceptibility gene for type 2 diabetes. Diabetes 61, 1734-1741.

123. Rosengren, A.H., Braun, M., Mahdi, T., Andersson, S.A., Travers, M.E., Shigeto, M., Zhang, E., Almgren, P., Ladenvall, C., Axelsson, A.S., et al. (2012). Reduced insulin exocytosis in human pancreatic beta-cells with gene variants linked to type 2 diabetes. Diabetes 61, 1726-1733.
124. Muller, Y.L., Piaggi, P., Chen, P., Wiessner, G., Okani, C., Kobes, S., Knowler, W.C., Bogardus, C., Hanson, R.L., and Baier, L.J. (2017). Assessing variation across 8 established East Asian loci for type 2 diabetes mellitus in American Indians: Suggestive evidence for new sex-specific diabetes signals in GLIS3 and ZFAND3. Diabetes/metabolism research and reviews 33.
125. Wood, A.R., Jonsson, A., Jackson, A.U., Wang, N., van Leewen, N., Palmer, N.D., Kobes, S., Deelen, J., Boquete-Vilarino, L., Paananen, J., et al. (2017). A Genome-Wide Association Study of IVGTT-Based Measures of First-Phase Insulin Secretion Refines the Underlying Physiology of Type 2 Diabetes Variants. Diabetes 66, 2296-2309.
126. Zhang, S., Jamaspishvili, E., Tong, H., Chen, Y., Zhou, Z., Sun, L., Kazakova, E., and Hong, Q. (2019). East Asian Genome-wide association study derived loci in relation to type 2 diabetes in the Han Chinese population. Acta biochimica Polonica 66, 159-165.
127. Whitelaw, D.C., and Gilbey, S.G. (1998). Insulin resistance. Ann Clin Biochem 35 (Pt 5), 567-583.
128. Wilcox, G. (2005). Insulin and insulin resistance. Clin Biochem Rev 26, 19-39.
129. Bajaj, M., and Defronzo, R.A. (2003). Metabolic and molecular basis of insulin resistance. J Nucl Cardiol 10, 311-323.
130. Karlsson, H.K., and Zierath, J.R. (2007). Insulin signaling and glucose transport in insulin resistant human skeletal muscle. Cell Biochem Biophys 48, 103-113.
131. Bouzakri, K., Roques, M., Gual, P., Espinosa, S., Guebre-Egziabher, F., Riou, J.P., Laville, M., Le Marchand-Brustel, Y., Tanti, J.F., and Vidal, H. (2003). Reduced activation of phosphatidylinositol-3 kinase and increased serine 636 phosphorylation of insulin receptor substrate-1 in primary culture of skeletal muscle cells from patients with type 2 diabetes. Diabetes 52, 1319-1325.
132. Krook, A., Bjornholm, M., Galuska, D., Jiang, X.J., Fahlman, R., Myers, M.G., Jr., Wallberg-Henriksson, H., and Zierath, J.R. (2000). Characterization of signal transduction and glucose transport in skeletal muscle from type 2 diabetic patients. Diabetes 49, 284-292.
133. Kim, Y.B., Kotani, K., Ciaraldi, T.P., Henry, R.R., and Kahn, B.B. (2003). Insulin-stimulated protein kinase C lambda/zeta activity is reduced in skeletal muscle of humans with obesity and type 2 diabetes: reversal with weight reduction. Diabetes 52, 1935-1942.
134. Aguirre, V., Uchida, T., Yenush, L., Davis, R., and White, M.F. (2000). The c-Jun NH(2)-terminal kinase promotes insulin resistance during association with insulin receptor substrate-1 and phosphorylation of Ser(307). J Biol Chem 275, 9047-9054.
135. Yung, J.H.M., and Giacca, A. (2020). Role of c-Jun N-terminal Kinase (JNK) in Obesity and Type 2 Diabetes. Cells 9.
136. Petersen, M.C., and Shulman, G.I. (2018). Mechanisms of Insulin Action and Insulin Resistance. Physiol Rev 98, 2133-2223.
137. Lee, Y.S., Li, P., Huh, J.Y., Hwang, I.J., Lu, M., Kim, J.I., Ham, M., Talukdar, S., Chen, A., Lu, W.J., et al. (2011). Inflammation is necessary for long-term but not short-term high-fat diet-induced insulin resistance. Diabetes 60, 2474-2483.
138. de Luca, C., and Olefsky, J.M. (2008). Inflammation and insulin resistance. FEBS Lett 582, 97-105.
139. Olefsky, J.M., and Glass, C.K. (2010). Macrophages, inflammation, and insulin resistance. Annu Rev Physiol 72, 219-246.
140. Hill, A.A., Anderson-Baucum, E.K., Kennedy, A.J., Webb, C.D., Yull, F.E., and Hasty, A.H. (2015). Activation of NF-kappaB drives the enhanced survival of adipose tissue macrophages in an obesogenic environment. Mol Metab 4, 665-677.
141. Gassaway, B.M., Petersen, M.C., Surovtseva, Y.V., Barber, K.W., Sheetz, J.B., Aerni, H.R., Merkel, J.S., Samuel, V.T., Shulman, G.I., and Rinehart, J. (2018). PKCepsilon contributes to lipid-induced insulin

resistance through cross talk with p70S6K and through previously unknown regulators of insulin signaling. Proc Natl Acad Sci U S A 115, E8996-E9005.
142. Leem, J., and Koh, E.H. (2012). Interaction between mitochondria and the endoplasmic reticulum: implications for the pathogenesis of type 2 diabetes mellitus. Exp Diabetes Res 2012, 242984.
143. Tubbs, E., Theurey, P., Vial, G., Bendridi, N., Bravard, A., Chauvin, M.A., Ji-Cao, J., Zoulim, F., Bartosch, B., Ovize, M., et al. (2014). Mitochondria-associated endoplasmic reticulum membrane (MAM) integrity is required for insulin signaling and is implicated in hepatic insulin resistance. Diabetes 63, 3279-3294.
144. Al-Shukaili, A., Al-Ghafri, S., Al-Marhoobi, S., Al-Abri, S., Al-Lawati, J., and Al-Maskari, M. (2013). Analysis of inflammatory mediators in type 2 diabetes patients. Int J Endocrinol 2013, 976810.
145. Spranger, J., Kroke, A., Mohlig, M., Hoffmann, K., Bergmann, M.M., Ristow, M., Boeing, H., and Pfeiffer, A.F. (2003). Inflammatory cytokines and the risk to develop type 2 diabetes: results of the prospective population-based European Prospective Investigation into Cancer and Nutrition (EPIC)-Potsdam Study. Diabetes 52, 812-817.
146. Dula, S.B., Jecmenica, M., Wu, R., Jahanshahi, P., Verrilli, G.M., Carter, J.D., Brayman, K.L., and Nunemaker, C.S. (2010). Evidence that low-grade systemic inflammation can induce islet dysfunction as measured by impaired calcium handling. Cell Calcium 48, 133-142.
147. Thanabalasingham, G., and Owen, K.R. (2011). Diagnosis and management of maturity onset diabetes of the young (MODY). BMJ 343, d6044.
148. Malikova, J., Kaci, A., Dusatkova, P., Aukrust, I., Torsvik, J., Vesela, K., Kankova, P.D., Njolstad, P.R., Pruhova, S., and Bjorkhaug, L. (2020). Functional Analyses of HNF1A-MODY Variants Refine the Interpretation of Identified Sequence Variants. J Clin Endocrinol Metab 105.
149. Negahdar, M., Aukrust, I., Molnes, J., Solheim, M.H., Johansson, B.B., Sagen, J.V., Dahl-Jorgensen, K., Kulkarni, R.N., Sovik, O., Flatmark, T., et al. (2014). GCK-MODY diabetes as a protein misfolding disease: the mutation R275C promotes protein misfolding, self-association and cellular degradation. Mol Cell Endocrinol 382, 55-65.
150. Bonnycastle, L.L., Chines, P.S., Hara, T., Huyghe, J.R., Swift, A.J., Heikinheimo, P., Mahadevan, J., Peltonen, S., Huopio, H., Nuutila, P., et al. (2013). Autosomal dominant diabetes arising from a Wolfram syndrome 1 mutation. Diabetes 62, 3943-3950.
151. Johnson, S.R., Ellis, J.J., Leo, P.J., Anderson, L.K., Ganti, U., Harris, J.E., Curran, J.A., McInerney-Leo, A.M., Paramalingam, N., Song, X., et al. (2019). Comprehensive genetic screening: The prevalence of maturity-onset diabetes of the young gene variants in a population-based childhood diabetes cohort. Pediatric diabetes 20, 57-64.
152. Shepherd, M., Shields, B., Hammersley, S., Hudson, M., McDonald, T.J., Colclough, K., Oram, R.A., Knight, B., Hyde, C., Cox, J., et al. (2016). Systematic Population Screening, Using Biomarkers and Genetic Testing, Identifies 2.5% of the U.K. Pediatric Diabetes Population With Monogenic Diabetes. Diabetes Care 39, 1879-1888.
153. Shields, B.M., Hicks, S., Shepherd, M.H., Colclough, K., Hattersley, A.T., and Ellard, S. (2010). Maturity-onset diabetes of the young (MODY): how many cases are we missing? Diabetologia 53, 2504-2508.
154. De Franco, E., Flanagan, S.E., Houghton, J.A., Lango Allen, H., Mackay, D.J., Temple, I.K., Ellard, S., and Hattersley, A.T. (2015). The effect of early, comprehensive genomic testing on clinical care in neonatal diabetes: an international cohort study. Lancet 386, 957-963.
155. Flanagan, S.E., Dung, V.C., Houghton, J.A.L., De Franco, E., Ngoc, C.T.B., Damhuis, A., Ashcroft, F.M., Harries, L.W., and Ellard, S. (2017). An ABCC8 Nonsense Mutation Causing Neonatal Diabetes Through Altered Transcript Expression. J Clin Res Pediatr Endocrinol 9, 260-264.
156. Edghill, E.L., Flanagan, S.E., and Ellard, S. (2010). Permanent neonatal diabetes due to activating mutations in ABCC8 and KCNJ11. Rev Endocr Metab Disord 11, 193-198.

157. De Franco, E., Flanagan, S.E., Yagi, T., Abreu, D., Mahadevan, J., Johnson, M.B., Jones, G., Acosta, F., Mulaudzi, M., Lek, N., et al. (2017). Dominant ER Stress-Inducing WFS1 Mutations Underlie a Genetic Syndrome of Neonatal/Infancy-Onset Diabetes, Congenital Sensorineural Deafness, and Congenital Cataracts. Diabetes 66, 2044-2053.
158. Stoy, J., Steiner, D.F., Park, S.Y., Ye, H., Philipson, L.H., and Bell, G.I. (2010). Clinical and molecular genetics of neonatal diabetes due to mutations in the insulin gene. Rev Endocr Metab Disord 11, 205-215.
159. Bermont, F., Hermant, A., Benninga, R., Chabert, C., Jacot, G., Santo-Domingo, J., Kraus, M.R., Feige, J.N., and De Marchi, U. (2020). Targeting Mitochondrial Calcium Uptake with the Natural Flavonol Kaempferol, to Promote Metabolism/Secretion Coupling in Pancreatic beta-cells. Nutrients 12.
160. Jiang, L., Allagnat, F., Nguidjoe, E., Kamagate, A., Pachera, N., Vanderwinden, J.M., Brini, M., Carafoli, E., Eizirik, D.L., Cardozo, A.K., et al. (2010). Plasma membrane Ca2+-ATPase overexpression depletes both mitochondrial and endoplasmic reticulum Ca2+ stores and triggers apoptosis in insulin-secreting BRIN-BD11 cells. J Biol Chem 285, 30634-30643.
161. Thorens, B., Tarussio, D., Maestro, M.A., Rovira, M., Heikkila, E., and Ferrer, J. (2015). Ins1(Cre) knock-in mice for beta cell-specific gene recombination. Diabetologia 58, 558-565.
162. Suzuki, J., Kanemaru, K., Ishii, K., Ohkura, M., Okubo, Y., and Iino, M. (2014). Imaging intraorganellar Ca2+ at subcellular resolution using CEPIA. Nat Commun 5, 4153.
163. Nita, II, Hershfinkel, M., Fishman, D., Ozeri, E., Rutter, G.A., Sensi, S.L., Khananshvili, D., Lewis, E.C., and Sekler, I. (2012). The mitochondrial Na+/Ca2+ exchanger upregulates glucose dependent Ca2+ signalling linked to insulin secretion. PLoS One 7, e46649.
164. Greotti, E., Fortunati, I., Pendin, D., Ferrante, C., Galla, L., Zentilin, L., Giacca, M., Kaludercic, N., Di Sante, M., Mariotti, L., et al. (2019). mCerulean3-Based Cameleon Sensor to Explore Mitochondrial Ca(2+) Dynamics In Vivo. iScience 16, 340-355.
165. Gerencser, A.A. (2018). Metabolic activation-driven mitochondrial hyperpolarization predicts insulin secretion in human pancreatic beta-cells. Biochim Biophys Acta Bioenerg 1859, 817-828.
166. Rutter, G.A. (1990). Ca2(+)-binding to citrate cycle dehydrogenases. Int J Biochem 22, 1081-1088.
167. Rutter, G.A., Burnett, P., Rizzuto, R., Brini, M., Murgia, M., Pozzan, T., Tavare, J.M., and Denton, R.M. (1996). Subcellular imaging of intramitochondrial Ca2+ with recombinant targeted aequorin: significance for the regulation of pyruvate dehydrogenase activity. Proc Natl Acad Sci U S A 93, 5489-5494.
168. Rutter, G.A. (2001). Nutrient-secretion coupling in the pancreatic islet beta-cell: recent advances. Mol Aspects Med 22, 247-284.
169. De Marchi, U., Thevenet, J., Hermant, A., Dioum, E., and Wiederkehr, A. (2014). Calcium co-regulates oxidative metabolism and ATP synthase-dependent respiration in pancreatic beta cells. J Biol Chem 289, 9182-9194.
170. Taddeo, E.P., Stiles, L., Sereda, S., Ritou, E., Wolf, D.M., Abdullah, M., Swanson, Z., Wilhelm, J., Bellin, M., McDonald, P., et al. (2018). Individual islet respirometry reveals functional diversity within the islet population of mice and human donors. Mol Metab 16, 150-159.
171. Vierra, N.C., Dickerson, M.T., Jordan, K.L., Dadi, P.K., Kadare, K.A., Altman, M.K., Milian, S.C., and Jacobson, D.A. (2018). TALK-1 reduces delta-cell endoplasmic reticulum and cytoplasmic calcium levels limiting somatostatin secretion. Mol Metab.
172. Matveyenko, A.V., Liuwantara, D., Gurlo, T., Kirakossian, D., Dalla Man, C., Cobelli, C., White, M.F., Copps, K.D., Volpi, E., Fujita, S., et al. (2012). Pulsatile portal vein insulin delivery enhances hepatic insulin action and signaling. Diabetes 61, 2269-2279.
173. Bergsten, P., Grapengiesser, E., Gylfe, E., Tengholm, A., and Hellman, B. (1994). Synchronous oscillations of cytoplasmic Ca2+ and insulin release in glucose-stimulated pancreatic islets. J Biol Chem 269, 8749-8753.

174. Eaton, R.P., Allen, R.C., and Schade, D.S. (1983). Hepatic removal of insulin in normal man: dose response to endogenous insulin secretion. J Clin Endocrinol Metab 56, 1294-1300.
175. Meier, J.J., Veldhuis, J.D., and Butler, P.C. (2005). Pulsatile insulin secretion dictates systemic insulin delivery by regulating hepatic insulin extraction in humans. Diabetes 54, 1649-1656.
176. Paolisso, G., Scheen, A.J., Giugliano, D., Sgambato, S., Albert, A., Varricchio, M., D'Onofrio, F., and Lefebvre, P.J. (1991). Pulsatile insulin delivery has greater metabolic effects than continuous hormone administration in man: importance of pulse frequency. J Clin Endocrinol Metab 72, 607-615.
177. Misler, S., Barnett, D.W., Pressel, D.M., Gillis, K.D., Scharp, D.W., and Falke, L.C. (1992). Stimulus-secretion coupling in beta-cells of transplantable human islets of Langerhans. Evidence for a critical role for Ca2+ entry. Diabetes 41, 662-670.
178. Frankel, B.J., Atwater, I., and Grodsky, G.M. (1981). Calcium affects insulin release and membrane potential in islet beta-cells. Am J Physiol 240, C64-72.
179. Bowman, P., Flanagan, S.E., Edghill, E.L., Damhuis, A., Shepherd, M.H., Paisey, R., Hattersley, A.T., and Ellard, S. (2012). Heterozygous ABCC8 mutations are a cause of MODY. Diabetologia 55, 123-127.
180. Flanagan, S.E., Edghill, E.L., Gloyn, A.L., Ellard, S., and Hattersley, A.T. (2006). Mutations in KCNJ11, which encodes Kir6.2, are a common cause of diabetes diagnosed in the first 6 months of life, with the phenotype determined by genotype. Diabetologia 49, 1190-1197.
181. Gloyn, A.L., Pearson, E.R., Antcliff, J.F., Proks, P., Bruining, G.J., Slingerland, A.S., Howard, N., Srinivasan, S., Silva, J.M., Molnes, J., et al. (2004). Activating mutations in the gene encoding the ATP-sensitive potassium-channel subunit Kir6.2 and permanent neonatal diabetes. N Engl J Med 350, 1838-1849.
182. Bramswig, N.C., Everett, L.J., Schug, J., Dorrell, C., Liu, C., Luo, Y., Streeter, P.R., Naji, A., Grompe, M., and Kaestner, K.H. (2013). Epigenomic plasticity enables human pancreatic alpha to beta cell reprogramming. The Journal of clinical investigation 123, 1275-1284.
183. Blodgett, D.M., Nowosielska, A., Afik, S., Pechhold, S., Cura, A.J., Kennedy, N.J., Kim, S., Kucukural, A., Davis, R.J., Kent, S.C., et al. (2015). Novel Observations From Next-Generation RNA Sequencing of Highly Purified Human Adult and Fetal Islet Cell Subsets. Diabetes 64, 3172-3181.
184. Desmet, F.O., Hamroun, D., Lalande, M., Collod-Beroud, G., Claustres, M., and Beroud, C. (2009). Human Splicing Finder: an online bioinformatics tool to predict splicing signals. Nucleic Acids Res 37, e67.
185. Kim, Y.K., Kim, Y.S., Yoo, K.J., Lee, H.J., Lee, D.R., Yeo, C.Y., and Baek, K.H. (2007). The expression of Usp42 during embryogenesis and spermatogenesis in mouse. Gene Expr Patterns 7, 143-148.
186. Schwarz, J.M., Cooper, D.N., Schuelke, M., and Seelow, D. (2014). MutationTaster2: mutation prediction for the deep-sequencing age. Nature methods 11, 361-362.
187. Adzhubei, I.A., Schmidt, S., Peshkin, L., Ramensky, V.E., Gerasimova, A., Bork, P., Kondrashov, A.S., and Sunyaev, S.R. (2010). A method and server for predicting damaging missense mutations. Nature methods 7, 248-249.
188. Stitzel, M.L., Sethupathy, P., Pearson, D.S., Chines, P.S., Song, L., Erdos, M.R., Welch, R., Parker, S.C., Boyle, A.P., Scott, L.J., et al. (2010). Global epigenomic analysis of primary human pancreatic islets provides insights into type 2 diabetes susceptibility loci. Cell metabolism 12, 443-455.
189. Smith, P.A., Ashcroft, F.M., and Rorsman, P. (1990). Simultaneous recordings of glucose dependent electrical activity and ATP-regulated K(+)-currents in isolated mouse pancreatic beta-cells. FEBS Lett 261, 187-190.
190. Kang, D., and Kim, D. (2004). Single-channel properties and pH sensitivity of two-pore domain K+ channels of the TALK family. Biochem Biophys Res Commun 315, 836-844.

191. Cho, Y.S., Chen, C.H., Hu, C., Long, J., Hee Ong, R.T., Sim, X., Takeuchi, F., Wu, Y., Go, M.J., Yamauchi, T., et al. (2011). Meta-analysis of genome-wide association studies identifies eight new loci for type 2 diabetes in east Asians. Nature genetics 44, 67-72.
192. Sakai, K., Imamura, M., Tanaka, Y., Iwata, M., Hirose, H., Kaku, K., Maegawa, H., Watada, H., Tobe, K., Kashiwagi, A., et al. (2013). Replication study for the association of 9 East Asian GWAS-derived loci with susceptibility to type 2 diabetes in a Japanese population. PloS one 8, e76317.
193. Wood, A.R., Jonsson, A., Jackson, A.U., Wang, N., van Leewen, N., Palmer, N.D., Kobes, S., Deelen, J., Boquete-Vilarino, L., Paananen, J., et al. (2017). A Genome-Wide Association Study of IVGTT-Based Measures of First-Phase Insulin Secretion Refines the Underlying Physiology of Type 2 Diabetes Variants. Diabetes 66, 2296-2309.
194. Varshney, A., Scott, L.J., Welch, R.P., Erdos, M.R., Chines, P.S., Narisu, N., Albanus, R.D., Orchard, P., Wolford, B.N., Kursawe, R., et al. (2017). Genetic regulatory signatures underlying islet gene expression and type 2 diabetes. Proceedings of the National Academy of Sciences of the United States of America 114, 2301-2306.
195. Ma, L., Roman-Campos, D., Austin, E.D., Eyries, M., Sampson, K.S., Soubrier, F., Germain, M., Tregouet, D.A., Borczuk, A., Rosenzweig, E.B., et al. (2013). A novel channelopathy in pulmonary arterial hypertension. N Engl J Med 369, 351-361.
196. Reed, A.P., Bucci, G., Abd-Wahab, F., and Tucker, S.J. (2016). Dominant-Negative Effect of a Missense Variant in the TASK-2 (KCNK5) K+ Channel Associated with Balkan Endemic Nephropathy. PloS one 11, e0156456.
197. Friedrich, C., Rinne, S., Zumhagen, S., Kiper, A.K., Silbernagel, N., Netter, M.F., Stallmeyer, B., Schulze-Bahr, E., and Decher, N. (2014). Gain-of-function mutation in TASK-4 channels and severe cardiac conduction disorder. EMBO molecular medicine 6, 937-951.
198. Eizirik, D.L., Cardozo, A.K., and Cnop, M. (2008). The role for endoplasmic reticulum stress in diabetes mellitus. Endocrine reviews 29, 42-61.
199. Meur, G., Simon, A., Harun, N., Virally, M., Dechaume, A., Bonnefond, A., Fetita, S., Tarasov, A.I., Guillausseau, P.J., Boesgaard, T.W., et al. (2010). Insulin gene mutations resulting in early-onset diabetes: marked differences in clinical presentation, metabolic status, and pathogenic effect through endoplasmic reticulum retention. Diabetes 59, 653-661.
200. Gupta, R.K., Vatamaniuk, M.Z., Lee, C.S., Flaschen, R.C., Fulmer, J.T., Matschinsky, F.M., Duncan, S.A., and Kaestner, K.H. (2005). The MODY1 gene HNF-4alpha regulates selected genes involved in insulin secretion. The Journal of clinical investigation 115, 1006-1015.
201. Bonnefond, A., Philippe, J., Durand, E., Dechaume, A., Huyvaert, M., Montagne, L., Marre, M., Balkau, B., Fajardy, I., Vambergue, A., et al. (2012). Whole-exome sequencing and high throughput genotyping identified KCNJ11 as the thirteenth MODY gene. PloS one 7, e37423.
202. Nelson, M.R., Tipney, H., Painter, J.L., Shen, J., Nicoletti, P., Shen, Y., Floratos, A., Sham, P.C., Li, M.J., Wang, J., et al. (2015). The support of human genetic evidence for approved drug indications. Nature genetics 47, 856-860.
203. von Muhlendahl, K.E., and Herkenhoff, H. (1995). Long-term course of neonatal diabetes. N Engl J Med 333, 704-708.
204. Greeley, S.A., Naylor, R.N., Philipson, L.H., and Bell, G.I. (2011). Neonatal diabetes: an expanding list of genes allows for improved diagnosis and treatment. Curr Diab Rep 11, 519-532.
205. Gloyn, A.L., Cummings, E.A., Edghill, E.L., Harries, L.W., Scott, R., Costa, T., Temple, I.K., Hattersley, A.T., and Ellard, S. (2004). Permanent neonatal diabetes due to paternal germline mosaicism for an activating mutation of the KCNJ11 Gene encoding the Kir6.2 subunit of the beta-cell potassium adenosine triphosphate channel. J Clin Endocrinol Metab 89, 3932-3935.
206. Satin, L.S. (2000). Localized calcium influx in pancreatic beta-cells: its significance for Ca2+-dependent insulin secretion from the islets of Langerhans. Endocrine 13, 251-262.

207. Khaldi, M.Z., Guiot, Y., Gilon, P., Henquin, J.C., and Jonas, J.C. (2004). Increased glucose sensitivity of both triggering and amplifying pathways of insulin secretion in rat islets cultured for 1 wk in high glucose. Am J Physiol Endocrinol Metab 287, E207-217.
208. Collins, S.C., Hoppa, M.B., Walker, J.N., Amisten, S., Abdulkader, F., Bengtsson, M., Fearnside, J., Ramracheya, R., Toye, A.A., Zhang, Q., et al. (2010). Progression of diet-induced diabetes in C57BL6J mice involves functional dissociation of Ca2(+) channels from secretory vesicles. Diabetes 59, 1192-1201.
209. Islam, M.S. (2010). The islets of Langerhans. Preface. Adv Exp Med Biol 654, vii-viii.
210. Kuum, M., Veksler, V., and Kaasik, A. (2015). Potassium fluxes across the endoplasmic reticulum and their role in endoplasmic reticulum calcium homeostasis. Cell Calcium 58, 79-85.
211. Abramcheck, C.W., and Best, P.M. (1989). Physiological role and selectivity of the in situ potassium channel of the sarcoplasmic reticulum in skinned frog skeletal muscle fibers. J Gen Physiol 93, 1-21.
212. Gillespie, D., and Fill, M. (2008). Intracellular calcium release channels mediate their own countercurrent: the ryanodine receptor case study. Biophys J 95, 3706-3714.
213. Mak, D.O., Vais, H., Cheung, K.H., and Foskett, J.K. (2013). Nuclear patch-clamp electrophysiology of Ca2+ channels. Cold Spring Harb Protoc 2013, 885-891.
214. Shipston, M.J. (2011). Ion channel regulation by protein palmitoylation. J Biol Chem 286, 8709-8716.
215. Linder, M., and Deschenes, R. (2006). Protein palmitoylation. Methods 40, 125-126.
216. Coleman, D.T., Gray, A.L., Kridel, S.J., and Cardelli, J.A. (2016). Palmitoylation regulates the intracellular trafficking and stability of c-Met. Oncotarget 7, 32664-32677.
217. Hayashi, T., Thomas, G.M., and Huganir, R.L. (2009). Dual palmitoylation of NR2 subunits regulates NMDA receptor trafficking. Neuron 64, 213-226.
218. Hayashi, T., Rumbaugh, G., and Huganir, R.L. (2005). Differential regulation of AMPA receptor subunit trafficking by palmitoylation of two distinct sites. Neuron 47, 709-723.
219. Burns, S.M., Vetere, A., Walpita, D., Dancik, V., Khodier, C., Perez, J., Clemons, P.A., Wagner, B.K., and Altshuler, D. (2015). High-throughput luminescent reporter of insulin secretion for discovering regulators of pancreatic Beta-cell function. Cell metabolism 21, 126-137.
220. Ling, Y., Jiang, P., Li, N., Yan, Q., and Wang, X. (2018). A luciferase immunoprecipitation assay for the detection of proinsulin/insulin autoantibodies. Clin Biochem 54, 51-55.
221. Stoy, J., Edghill, E.L., Flanagan, S.E., Ye, H., Paz, V.P., Pluzhnikov, A., Below, J.E., Hayes, M.G., Cox, N.J., Lipkind, G.M., et al. (2007). Insulin gene mutations as a cause of permanent neonatal diabetes. Proc Natl Acad Sci U S A 104, 15040-15044.
222. Wang, Y., Shen, J., Arenzana, N., Tirasophon, W., Kaufman, R.J., and Prywes, R. (2000). Activation of ATF6 and an ATF6 DNA binding site by the endoplasmic reticulum stress response. J Biol Chem 275, 27013-27020.
223. Pei, L., Wiser, O., Slavin, A., Mu, D., Powers, S., Jan, L.Y., and Hoey, T. (2003). Oncogenic potential of TASK3 (Kcnk9) depends on K+ channel function. Proc Natl Acad Sci U S A 100, 7803-7807.
224. Belanger, C., Ansanay, H., Qanbar, R., and Bouvier, M. (2001). Primary sequence requirements for S-acylation of beta(2)-adrenergic receptor peptides. FEBS Lett 499, 59-64.
225. Bizzozero, O.A., Bixler, H.A., and Pastuszyn, A. (2001). Structural determinants influencing the reaction of cysteine-containing peptides with palmitoyl-coenzyme A and other thioesters. Biochim Biophys Acta 1545, 278-288.
226. Hara, T., Mahadevan, J., Kanekura, K., Hara, M., Lu, S., and Urano, F. (2014). Calcium efflux from the endoplasmic reticulum leads to beta-cell death. Endocrinology 155, 758-768.
227. Lewandowski, S.L., Cardone, R.L., Foster, H.R., Ho, T., Potapenko, E., Poudel, C., VanDeusen, H.R., Sdao, S.M., Alves, T.C., Zhao, X., et al. (2020). Pyruvate Kinase Controls Signal Strength in the Insulin Secretory Pathway. Cell Metab 32, 736-750 e735.

228. Lynes, E.M., Bui, M., Yap, M.C., Benson, M.D., Schneider, B., Ellgaard, L., Berthiaume, L.G., and Simmen, T. (2012). Palmitoylated TMX and calnexin target to the mitochondria-associated membrane. EMBO J 31, 457-470.
229. McMullen, D.C., Kean, W.S., Verma, A., Cole, J.T., and Watson, W.D. (2012). A microplate technique to simultaneously assay calcium accumulation in endoplasmic reticulum and SERCA release of inorganic phosphate. Biol Proced Online 14, 4.
230. Lin, H.V., and Accili, D. (2011). Hormonal regulation of hepatic glucose production in health and disease. Cell Metab 14, 9-19.
231. Kalderon, B., Gopher, A., and Lapidot, A. (1986). Metabolic pathways leading to liver glycogen repletion in vivo, studied by GC-MS and NMR. FEBS Lett 204, 29-32.
232. Park, C.Y., Shcheglovitov, A., and Dolmetsch, R. (2010). The CRAC channel activator STIM1 binds and inhibits L-type voltage-gated calcium channels. Science 330, 101-105.
233. Dadi, P.K., Vierra, N.C., Ustione, A., Piston, D.W., Colbran, R.J., and Jacobson, D.A. (2014). Inhibition of pancreatic beta-cell Ca2+/calmodulin-dependent protein kinase II reduces glucose-stimulated calcium influx and insulin secretion, impairing glucose tolerance. J Biol Chem 289, 12435-12445.
234. Jacobson, D.A., Kuznetsov, A., Lopez, J.P., Kash, S., Ammala, C.E., and Philipson, L.H. (2007). Kv2.1 ablation alters glucose-induced islet electrical activity, enhancing insulin secretion. Cell Metab 6, 229-235.
235. Bao, S., Jacobson, D.A., Wohltmann, M., Bohrer, A., Jin, W., Philipson, L.H., and Turk, J. (2008). Glucose homeostasis, insulin secretion, and islet phospholipids in mice that overexpress iPLA2beta in pancreatic beta-cells and in iPLA2beta-null mice. Am J Physiol Endocrinol Metab 294, E217-229.
236. Dabelea, D., Mayer-Davis, E.J., Saydah, S., Imperatore, G., Linder, B., Divers, J., Bell, R., Badaru, A., Talton, J.W., Crume, T., et al. (2014). Prevalence of type 1 and type 2 diabetes among children and adolescents from 2001 to 2009. Jama 311, 1778-1786.
237. Wang, H., Bender, A., Wang, P., Karakose, E., Inabnet, W.B., Libutti, S.K., Arnold, A., Lambertini, L., Stang, M., Chen, H., et al. (2017). Insights into beta cell regeneration for diabetes via integration of molecular landscapes in human insulinomas. Nat Commun 8, 767.